

Chapter 4

Geology of the Project Sites

4.1. Introduction

In this chapter, the geological characteristics of the Asmari Formation at the following dam sites are discussed:

1. *Karun-3 Dam*, in Khuzestan Province,
2. *Karun-4 Dam* in Chaharmahal Bakhtyari Province,
3. *Marun Dam* in Khuzestan Province,
4. *Seymareh Dam (Hini Mini)* in Ilam Province and
5. *Salman Farsi Dam (Ghir)* in Fars Province

The Asmari Formation limestone is the main foundation rock mass at all investigated dam sites (Figure 4.1) and generally consists of cream to light gray limestone, marly limestone, dolomitic limestone and marlstone with sporadically thin layers of shale. Karstification of limestone due to aggressive water and warm springs are well developed especially at the dam sites which are located on the northern flank of anticlines (Seymareh, Marun and Salman Farsi). The direction of shortening at the region due to tectonic movements are indicated by white arrows. Shortening directions are derived from all axial planar orientation.



Figure 4.1. The topographical map of Zagros folded belt and locations of five dam sites. Seymareh (4), Karun-3 (1), Karun-4 (2), Marun (3) and Salman Farsi (5). The direction of shortening at the region due to tectonic movements are indicated by white arrows. (Lexicorient base map, 2001).

The petrographic characteristics have been determined from thin section studies from the systematic sampling of outcrops and boreholes (Appendix 1 to 5). It should be noted that the lithology shown in lithological columns are according to borehole loggings and surface investigations of outcrops. The detailed petrographical studies have been carried out based on Folk (1959) and Dunham (1962) the two most widely used methods of carbonate rock classification. These classifications are used based on the concept of textural (fabric) maturity, where the fabric is believed to relate to the energy level during the deposition of limestone.

The porosity values and porosity types are defined according to Choquette and Pray (1970) who divided carbonate rocks into three groups of fabric-selective type, non-fabric-selective porosity type and the third group may display a fabric control or not. The detailed petrographical descriptions with related photomicrographs are introduced for all index layers/ subunits of the Asmari succession. Finally, the lithological columns in each locality of the research area were introduced based on the above investigations and the engineering properties of the rock units.

Attention was paid to the lithological distribution of the various rock types, their engineering properties, the compilation of stratigraphic sections, and to structural geology including bedding, folds, faults and major joints. Also the extent of rock outcrops was delineated, fault exposures were inspected and logged to assess the likelihood of current fault activity.

Discontinuity surveys were performed during different stages with more than 2000 discontinuities such as joints and bedding planes measured and plotted to establish statistical trends (contour plot, rosette plot, and pole plot of joints on equal area projection Schmidt net). These data were used to define the stability analysis of rock wedges in excavated tunnels including the diversion and hydropower tunnels, as well as rock slope stability analysis especially around the dam structure.

Finally, the direction of shortening (major principal stresses) at each dam site (anticlines) due to active tectonic movements in the Zagros Mountains was derived from all axial planar orientations.

4.2. Geology of the Karun-3 Dam and Power plant

The Karun-3 dam project is located 28 km east of the town of Izeh in northeast Khuzestan Province. Its crest elevation is 850 m and the average reservoir elevation is 840 m. This is a double curvature concrete arch dam, symmetrical in shape about a plane running approximately parallel to the valley direction. The location and alignment of the dam is limited by geological and topographical features on both abutments. The subsurface powerhouse is located downstream from the dam and power tunnels.

The service spillway is a chute spillway located on the right flank. Gated orifices in the dam wall serve as auxiliary spillways and there is also a crest overflow for emergency conditions. Other structures consist of upstream and downstream cofferdams and a diversion tunnel under the right flank. The cofferdams are earth and rock fill structures. The diversion tunnel is a 350 m long and 15 m diameter excavation. The powerhouse contains eight units with a total capacity of 2 000 MW (Figures 4.2.1 and 4.2.2).



Figure 4.2.1. The satellite image of Karun-3 dam project and surrounding area before reservoir impoundment. This project located at 28 km east of Izeh town in Khuzestan Province. Access road of Dehdez – Izeh can be seen on middle part of picture (Google Earth, European Technology, 2009).

The reservoir is 60 km long with storage volume of $3 \times 10^9 \text{ m}^3$ (Table 4.2.1).

4.2.1. Objectives and benefits of the project

- Generating annually 4 137 million kWh hydroelectric energy through a 2 000 MW power plant that can be extended to 3 000 MW (MG co. geological report, 1993).
- Controlling floods and supplying approximately one billion m^3 water for irrigation.
- Increasing hydroelectric energy of the country by 60% and 2.7% of the total electricity generated in the country.
- Approximately 200 million dollars of annual benefit.



Figure 4.2.2. Karun-3 dam a double curvature concrete arch dam constructed on the Karun River.

Table 4.2.1. The technical specifications of the Karun-3 dam and power plant project.

Dam Type	Double curvature concrete arch dam
Height from the foundation	205.0 m
Length of the crest	388.0 m
Width of the dam at foundation	29.0 m
Width of the crest	5.50 m
Total volume of the reservoir	2750 million m ³
Useful volume of the reservoir	1500 million m ³
Power plant type	underground
Spillway	Chute, gated orifice types and free
Discharge capacity of the spillway	21730 m ³ /s
Water diversion system	U/S dike with the height of 43 m small D/S dike with the height of 32 m/ two diversion tunnels with the completed diameter of 13 m and the length of 613 m for the first one and the length of 536 m for the second one.
Power of the power plant	2000 MW (8 units of 250 MW)

4.2.2. Bedrock Geology of Project Area

A summary of the principal bedrock formations present in the project area is given in Table 4.2.2. A continuous sequence of sediments from the late Cretaceous period to the Pliocene stage is represented (Figure 4.2.3 to 4.2.5).

The Lower Asmari Formation is made up of interbedded limestone and marly limestone. The limestone is generally light grey to light brownish grey, fine to medium grained, strong to very strong. In general the porosity values are between 1% to 15.7% that imply medium to extremely porous rocks and has been subdivided into four subunits 4a1, 4a2, 4a3, 4a4.

The measured weighted mean RQD is between 50% to 85% which indicates fair to good quality rock mass.

Table 4.2.2. Bedrock formations present at the Karun-3 dam (after James and Wynd, 1965).

Rock Formation/ Group	General Description	Age
Bakhtyari Formation	Chert and limestone conglomerate, Sandstone and gritstone	Late Pliocene
Agha Jari Formation	Alternating brownish-grey, calcareous, fossiliferous sandstone, red marlstone and siltstone	Late Miocene to Early Pliocene
Gachsaran Formation	Alternating reddish brown and grey salt, anhydrite, marlstone, marly limestone, sandstone, siltstone and shale	Early Miocene
Asmari Formation	Alternating grey limestone, marly limestone and marlstone, overlying thick bedded fossiliferous limestone	Oligocene to Early Miocene
Pabdeh Formation	Alternating marly limestone, shale and marlstone, overlying shale with minor marly limestone	Paleocene to Eocene
Gurpi Formation	Purple shale with marly limestone and marl	Late Cretaceous
Bangestan Group	Grey, thick bedded marly limestone with shale partings, overlying bituminous shale(Kazhdumi)	Middle Cretaceous
KhamiGroup	Grey brown fossiliferous, thick bedded limestone	Early Cretaceous

The Upper Asmari Formation consists thin to medium bedded marly limestone, marlstone and shale. The limestone and marly limestone are strong to very strong. The porosity values are generally between 1% to 13.8% which indicate medium to extremely high values. The rock quality is variable with the weighted mean RQD of unit 4b between 31% to 81%, which indicates poor to good quality rock mass (MG co., Koleini, 2009).

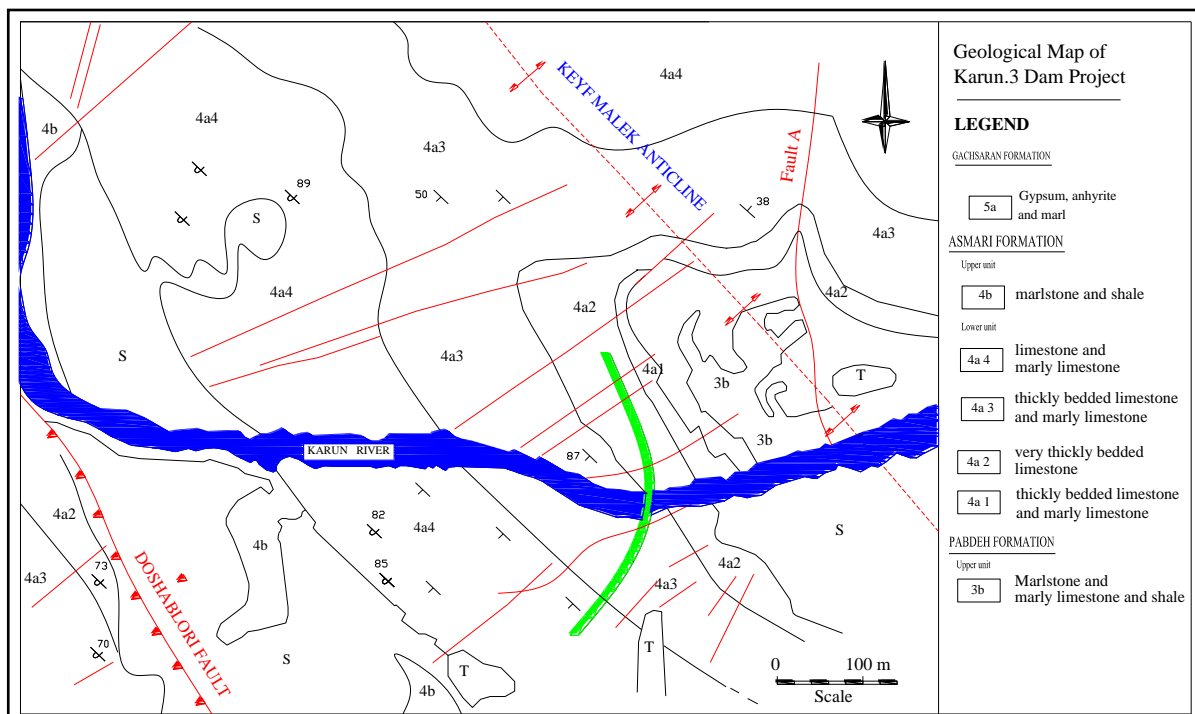


Figure 4.2.3. Geological map of the Karun-3 Dam and power plant site (after MG co., 2009).

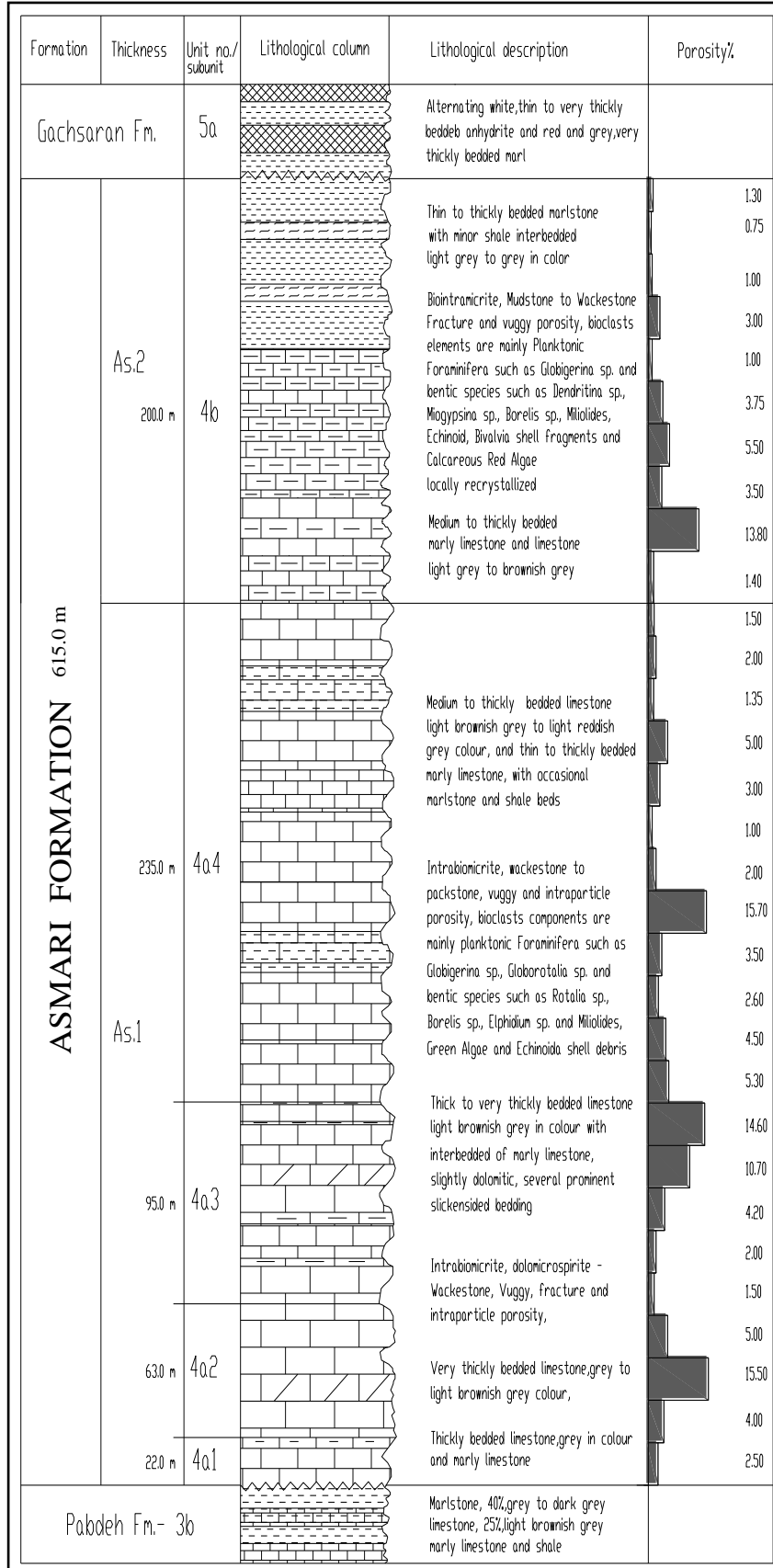


Figure 4.2.4. Lithological column of the Asmari Formation in the Karun-3 dam site.

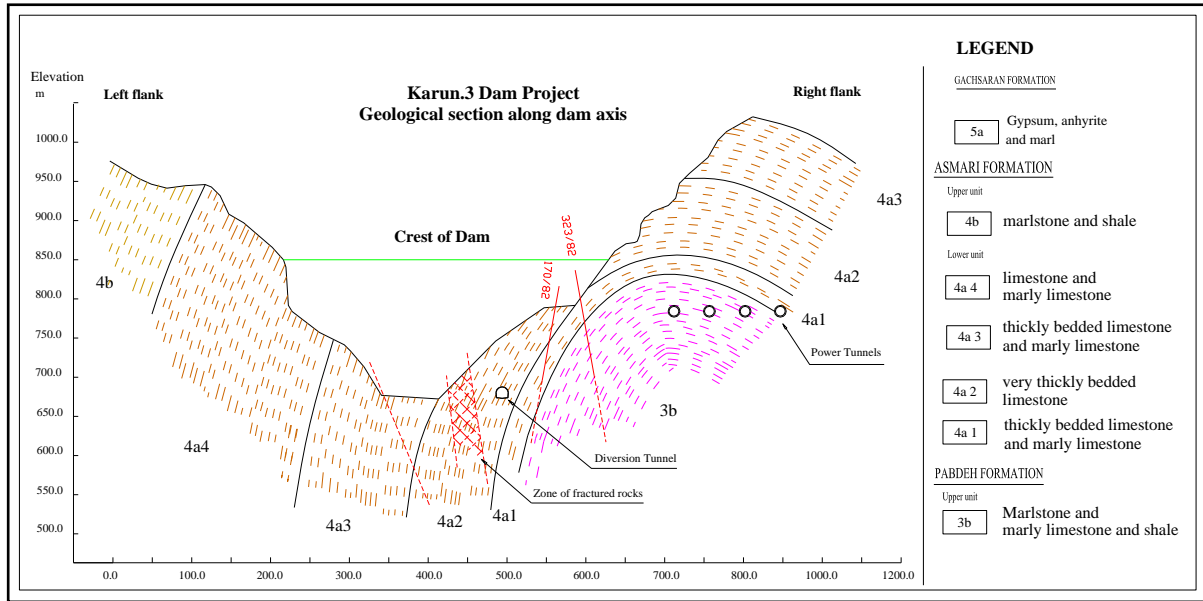


Figure 4.2.5. Geological section along Karun-3 Dam axes. The hydropower tunnels (4 circular 15 m, 10 m in diameter) and the diversion tunnel (15 m in diameter) located on right abutment (after MG co., 2009).

4.2.3. Structural Geology

The dam and powerhouse sites are located on the south-western flank of the north-west-southeast striking Keyf Malek Anticline (Figures 4.2.2 and 4.2.5). This feature controls the topography and dominant bedrock structure of the project area. The bedding, which is well developed, has shallow dip at the crown of the anticline but on the south-western limb, the dip is steep to the southwest. Regular joint sets are developed and these have consistent orientations across the project area. The Doshablari Fault strikes in a north-west-southeast direction and passes within 500 m to the southwest of the damsite. The major seismically active faults in the study area are presented in Figure 4.2.6.

The Keyf Malek anticline is a simple, box-like structure. It is asymmetrical, with the south-western limb dipping more steeply than the north-eastern one. The axis of the fold plunges slightly to the southeast ($141^{\circ}/06^{\circ}$) but, for practical purposes, it may be considered to be horizontal (MG co., 1993).

The strike and dip of the strata vary only slightly over the dam and powerhouse sites. The bedding has a fairly flat inclination at the top of the fold, but become rapidly steeper to the west of the axis where it generally dips 60° to 85° southwest. Mapping indicates that several strongly developed joint sets characterize the bedrock in the area. The bedding and joint set orientations are listed below in the order of development from the strongest to least developed. Poorly developed miscellaneous sets are excluded.

Discontinuity surveys were conducted on both sides of the river. Polar plot of these discontinuities (1 158 discontinuity planes) also the directions of principal stresses are presented on Figures 4.2.7; 4.2.8; 4.2.9 and 4.2.10. The strike and dip measurements quoted above are the ranges of the average measurements from each area. Joint set A is strongly developed at all locations in the project area. Joint sets B and C are more randomly developed and are absent at some locations.

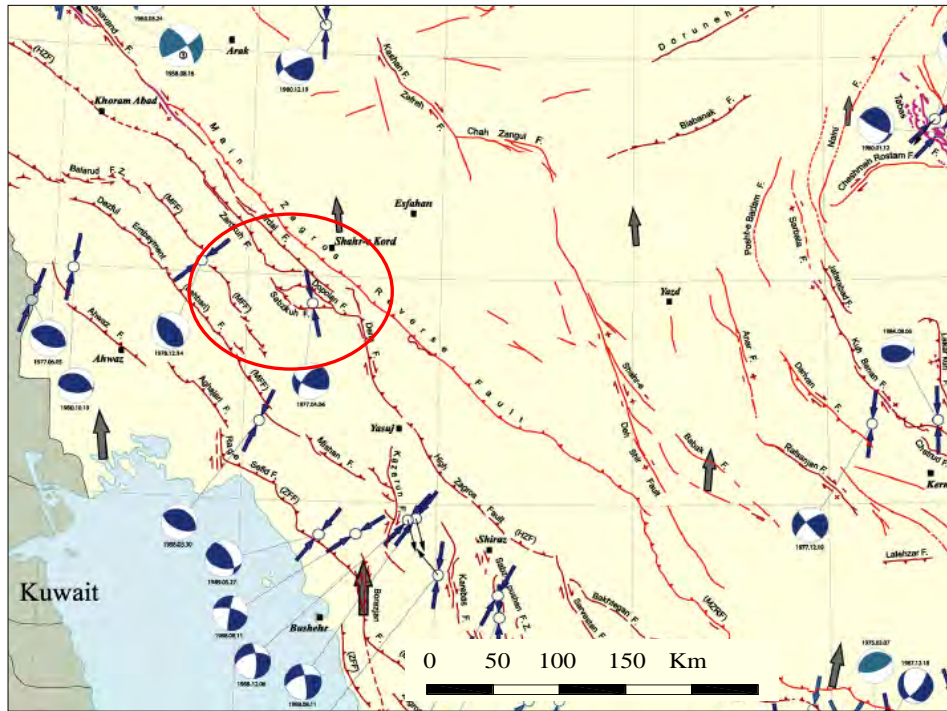


Figure 4.2.6. The major seismically active faults in the study area at the Zagros region. (after International Institute of Earthquake Engineering and Seismology- Iran, 2003).

Table 4.2.3. Bedding and joint sets orientation at the Karun-3 Dam site (after MG co., 1993).

Discontinuity Set	Dip Direction (°) / Dip-(°)	Spacing (m) Major Surfaces	Minor Surfaces	Continuity (m) Major Surfaces	Minor Surfaces
Bedding	223-234/50-90	5-20	1-3	500	100
A	126- 148 / 75-82	20-100	1-3	300	3-15
B	130-270/ 12-24	Only one major Surface mapped	1-20	300	3-20
C	310-338 /30-45	-----	5-10	-----	5-20

Bedding and joint surfaces are usually planar and rough. Joints are frequently open at surface, but usually closed at depth, although deep weathering along some joints was observed in drill core. Most joints exhibit some calcite filling and hematite staining. Rare to occasional clay coatings have been observed on some joint surfaces. Most joints are tension fractures which are characteristic of anticlines in the Asmari limestone of the simply folded zone. Slickensides were observed on joint surfaces in surface exposures and in drill core samples. Slickensided shear joints comprise 10% to 30% of the measured discontinuities in survey numbers R1, R2, R3, R7, R12, and L7 near the core of the anticline. Elsewhere, shear joints are rare and make up only 1% to 6% of the measurements. Exceptions are survey numbers R6 and R5 near the river downstream from the dam, where 20% of the measured discontinuities are slickensided shear joints.

4.2.3.1. Joint Study

4.2.3.1.1. Direction of Principal Stresses at Karun-3 Damsite

To determine the orientation of the principal stresses at the Karun-3 Dam, the numbers of 93 bedding planes, were measured in both abutments as input data, into Dips©, and the scatter plot, contour plot, major planes plot and rosette plot were analysed to determine the direction of principal stresses.

The directions of principal stresses (2D) are as follow:

σ_1 : 231°/ 0.0° (*max. Principal stress*)

σ_2 : 321°/ 0.0° (*intermediate principal stress*)

σ_3 : 0.0°/ 90° (*min. Principal stress*)

The direction of σ_1 coincides with the direction of shortening in the Zagros Fold thrust belt.

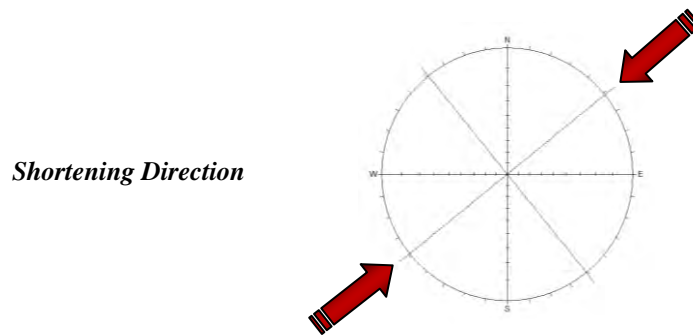


Figure 4.2.7. The direction of σ_1 / Shortening at Karun-3 dam site.

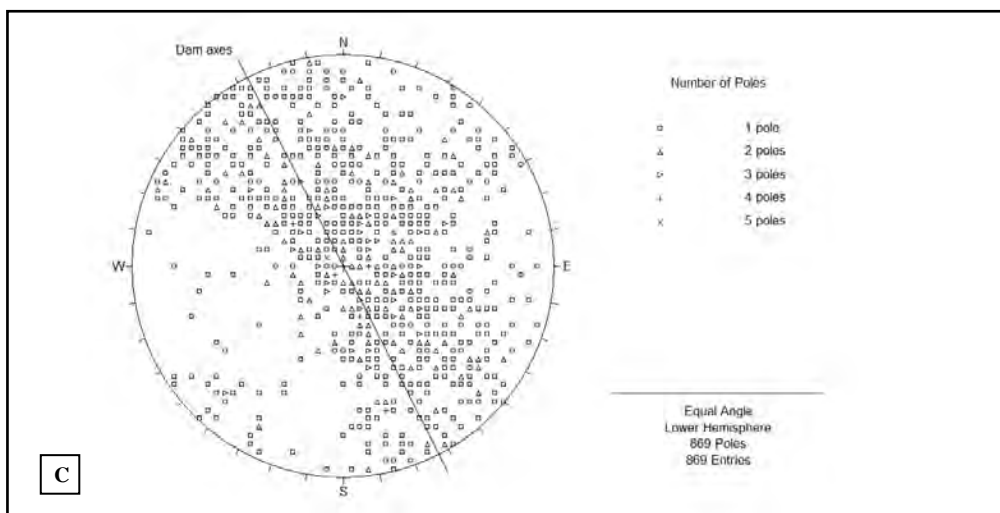
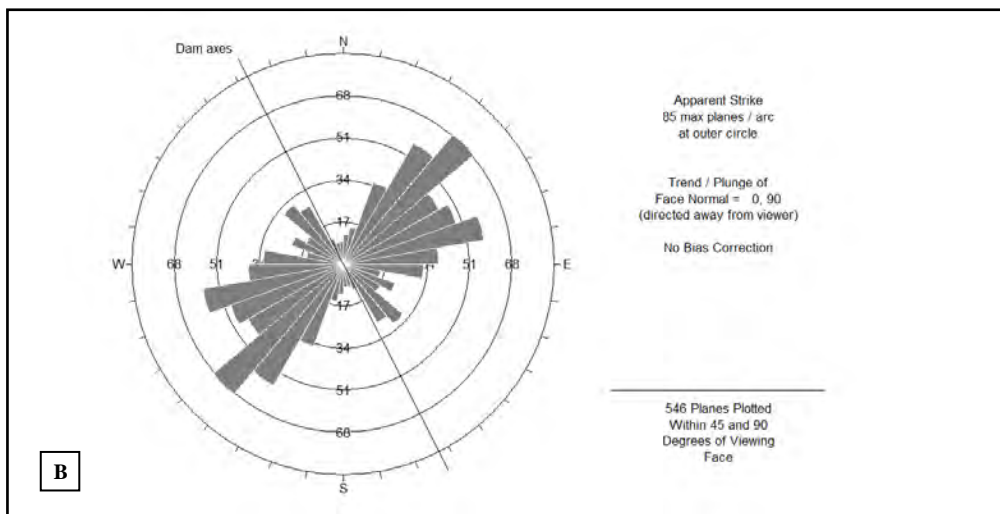
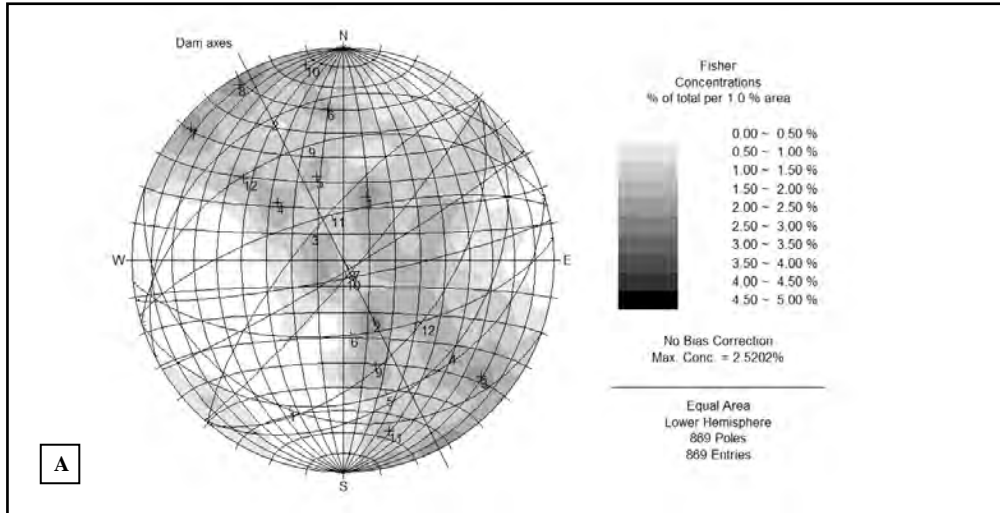


Figure 4.2.8. The Stereographic projection of joints at the right flank, A- Contour plot, B- Rosette plot, and C- Pole plot of joints (Dips \odot , equal area projection-Schmidt net, lower hemisphere).

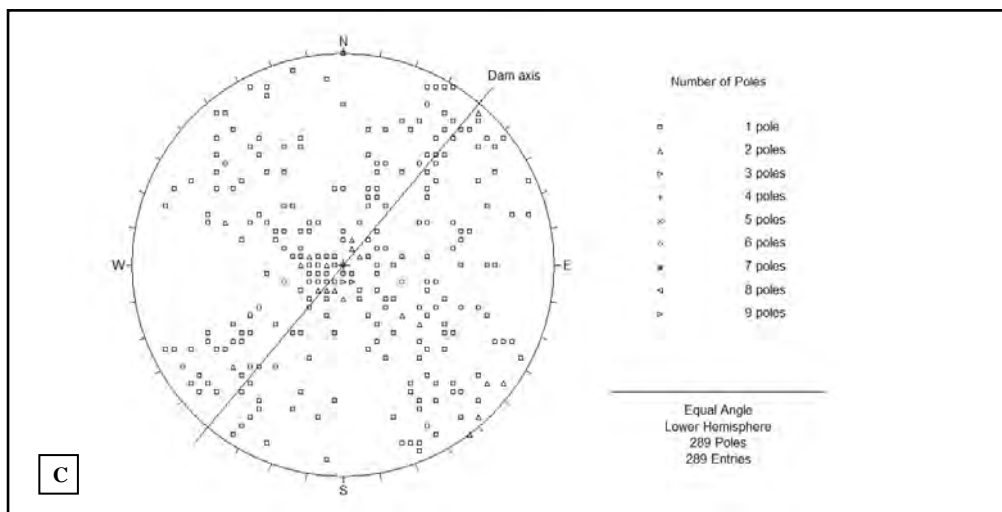
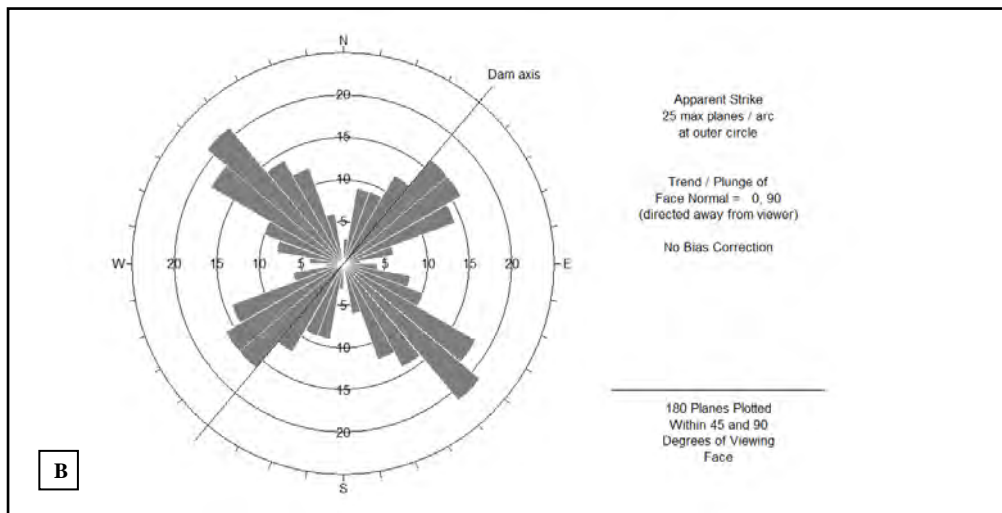
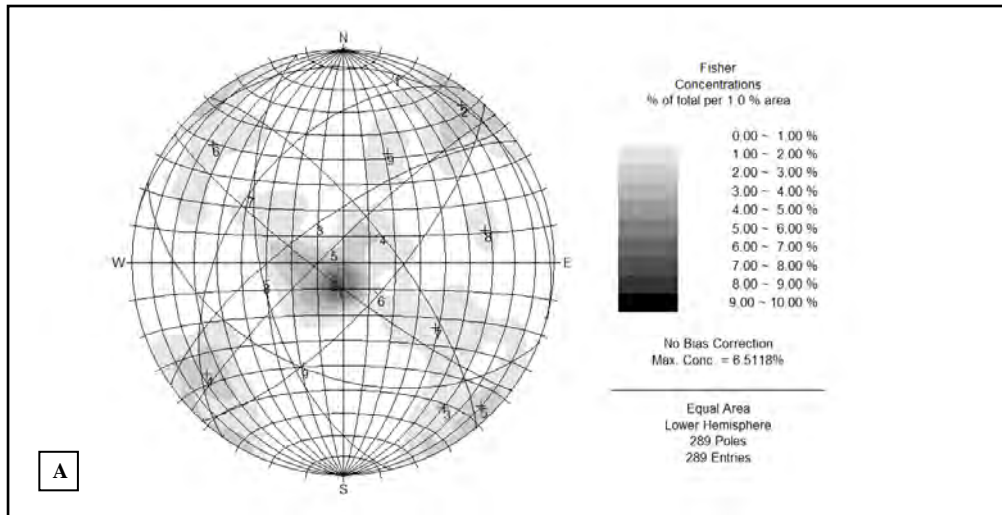


Figure 4.2.9. The Stereographic projection of joints at the left flank. A- Contour plot, B- Rosette plot, and C- Pole plot of joints (Dips©, equal area projection-Schmidt net, lower hemisphere).

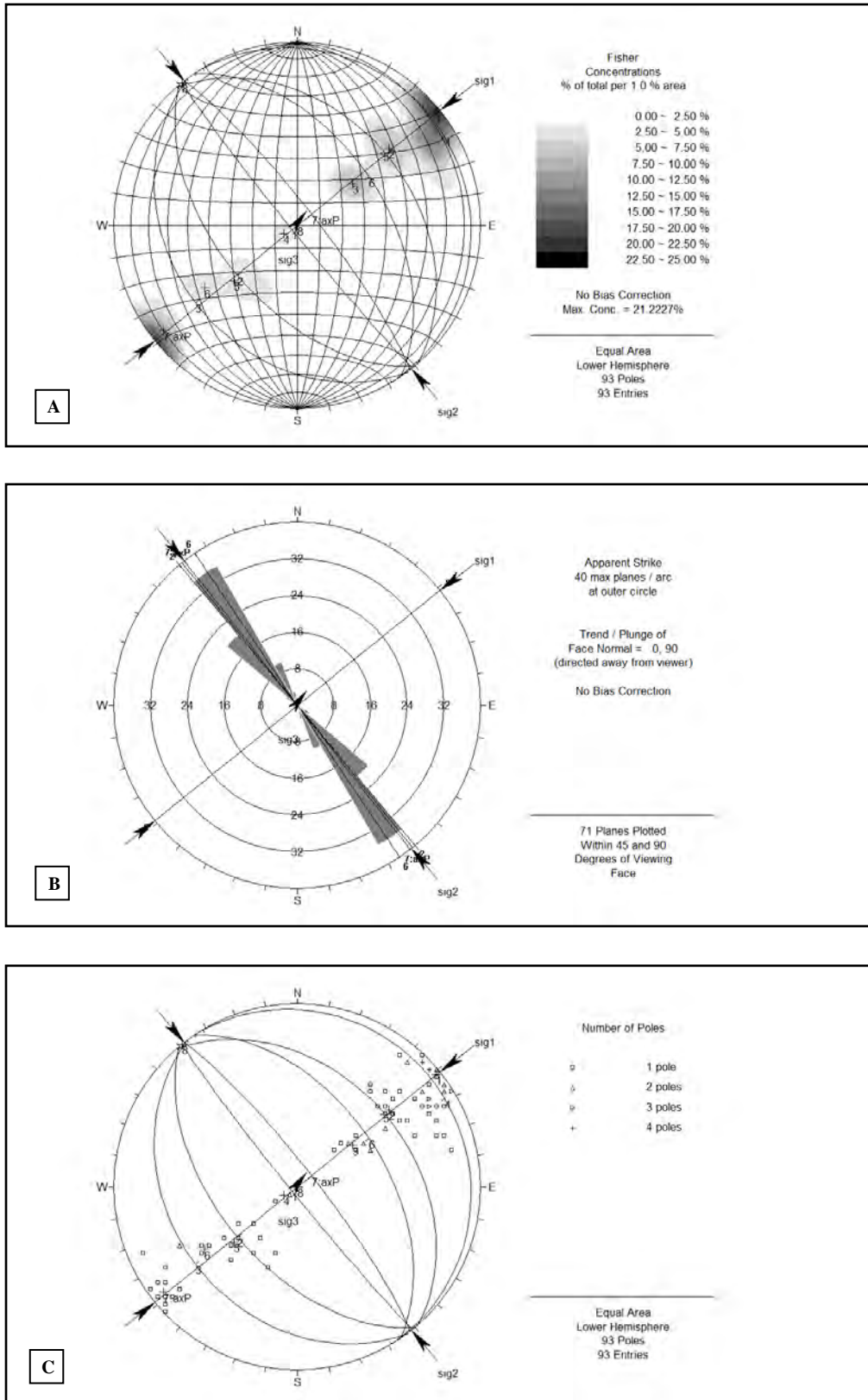


Figure 4.2.10. The Stereographic projection of bedding planes at the Karun-3 dam and identification of principal stresses that have impressed on dam site. The direction of σ_1 is coincident with direction of shortening in the Zagros Folded belt (Dips©, equal area projection-Schmidt net, lower hemisphere).

4.2.3.2. Regional Faults

It is likely that many important earthquake-generating faults are present in the basement rocks, although they do not necessarily have surface expressions. There are however a number of important surface faults in the site region. These are described in Table 4.2.4.

The only important regional fault along which earthquake activity has been documented is the Main Recent fault. This fault runs along the northwest boundary of the Khuzestan Seismotectonic province and is coincident with the Main Zagros thrust fault over most of its length. The project Definition Report lists seven major earthquakes which occurred along this fault over the past years. The largest measured event is the magnitude 7.4 Silakhor earthquake of January 1903 (Berberian, 1976).

Regional thrust and reverse faults shown in Table 4.1.4 have been described by Berberian (1976). Three of these faults, the Masjed Soleyman Fault, Ramhormoz Fault and an unnamed fault northeast of Masjed Soleyman, are Quaternary in age. In this study they are assumed to be seismically active even though no definite recent movement along them has been noted.

Table 4.2.4. Summary of Faults near the Karun-3 dam site (Berberian, 1976).

Name of Fault	Type	General Trend	Age of last Movement	Length (km)	Distance from Site (km)
Ramhormoz F.	Thrust- 20-25deg to NE	NW-SE	Quaternary	120.0	75.0 SW
Msjed soleman F.	Thrust 20 deg to NE	NW-SE	Quaternary	65.0	60.0 W
Unnamed F	Thrust	NW-SE	Quaternary	50.0	50.0 W
Unnamed F.	Thrust	NW-SE	Pre-Quaternary	95.0	17.0 NE
Unnamed F	High angle reverse 50-70 deg.NE	NW-SE	Pre-Quaternary	190.0	35.0 NE
Main Zagros F.	Thrust and angle reverse	NW-SE	Pre-Quaternary	1300.0	70.0 NE
Main Recent F.	Oblique slip with right lateral motion	NW-SE	Quaternary- Recent	1300.0	50.0- 70.0 NE
Behbahan line	Possibly large vertical movement ,right lateral	N-S	Pre-Quaternary	90.0 – 300.0	15.0 W

The Behbahan line while not proven to be a fault, is considered to have some potential for seismic activity. It is a 300 km long north-south trending lineament which runs transverse to the general structural trend of the Zagros Mountains and considered to pass approximately 15 km west of the site. In summary, the Behbahan line is not considered to have any significant impact on the Karun-3Dam (MG. co., 1993)

4.2.3.3. Local Faults

A number of small faults of lengths varying between 5 to 20 km occur within 20 km of the site. These faults probably developed during Pliocene- Quaternary time as a result of folding. Their short length suggests that they are probably not related to deep-seated basement structures and are not capable of generating large earthquakes even if they are still active. The most important fault is the Doshablori fault (Figure 4.2.11) which is 10 km long. This fault passes within 500 m of the left abutment of the dam and has been closely examined at several locations during the feasibility geology mapping program.

Fault A, which is about 500 m to 1 km long, cuts across the Pabdeh and Asmari limestone in the northeast side of the anticline, about 200 m upstream from the dam site. The fault strikes 15° and has a near vertical inclination. About 15 to 20 m of relative movement has occurred and the breccia zone is about 2 m wide at the uphill location and 5 to 7 m wide at the cliff

face. Slickensided fractures are abundant within and adjacent to the fault zone and bedding plane shears have been observed at many locations.



Figure 4.2.11. Karun-3 Dam and Power plant. The subunits of the Asmari Formation can be seen in both abutments. The Doshablori Fault strikes in a northwest-southeast direction and passes within 500 m southwest of the dam site.

4.3. Geology of the Karun-4 Dam and Power plant

The investigated project is located in Chahar Mahal Bakhtyari Province, 85 km south to southwest of Shahr kord. The geographical coordinates of the area are 50°, 24', 50"E and 31°, 35', 53" N. The most suitable access to the dam site is provided by the Izeh-Sharekord asphalt road about 85 km from Izeh.

The project area has high relief with some elevations at about 4 000 m. One of these mountains is Kuh Sefid with a height of about 3 100 m and is located near the dam site.

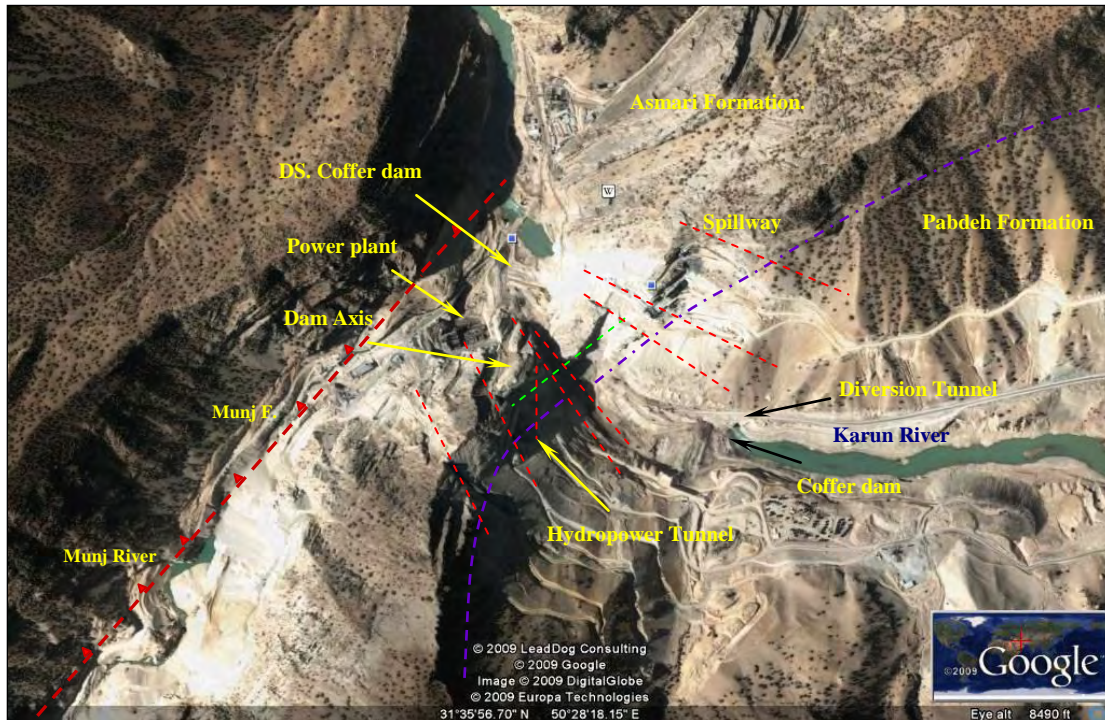


Figure 4.3.1. The satellite image of Karun-4 dam and power plant project on the Karun River. The dam site located on the southern flank of the Kuh Sefid Anticline and the foundation rocks is Asmari Formation limestone related to Oligomiocene in age. The various parts of the project can be observed as well (Google Earth, European Technology, 2009).

The Karun-4 dam and power plant project are located in the Karun River, almost 5 km downstream of the confluence Bazoft and Armand rivers in a steep U-shaped valley (about 70°) on the southwestern flank of the Kuh Sefid Anticline. This anticline has a northwest-southeast trend and is asymmetrical with a steeper south-western flank compared to the north-eastern one. The dam foundation rocks are of the Asmari and Pabdeh Formations.

Karun-4 is a double curvature concrete arch dam that is under construction. The dam has a height of 230 m and capacity of 2 190 million cubic metres. To divert the water of the Karun River during the dam construction, two tunnels in the right flank have been designed. The lengths of these tunnels are 610 m and 635 m and their excavated diameters are 11 m and 11.5 m respectively (9.5 m after final lining). The cofferdams are earth and rockfill structures. The spillway is a chute and orifice type, 124 m in length and 80 m high comprise five main bays located on the right flank (Figures 4.3.1 and 4.3.2).

The surface powerhouse contains four units with a total capacity of 1 000 MW (4× 250 MW).

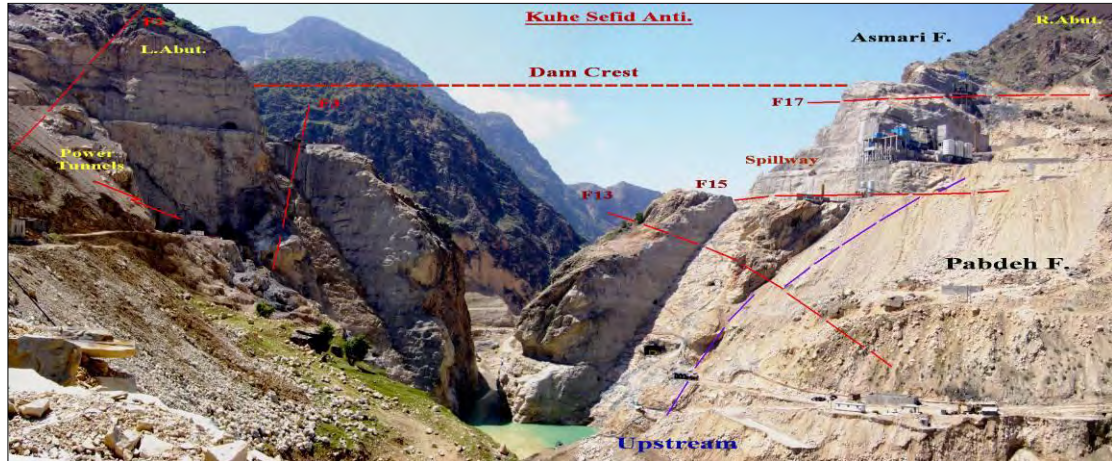


Figure 4.3.2. The Karun-4 dam site constructed at the southern flank of the Kuh Sefid Anticline (2006).

4.3.1. Objective and benefits of the project

- Generating annually 2 107 GWh electric energy
- Supply water for irrigating agricultural lands.
- Controlling floods
- Land reclamation

The general technical specifications of the dam project are shown in Table 4.3.1

Table 4.3.1. The technical specifications of the Karun-4 dam and power plant project (MG co., 1995- 1997).

Dam Type	Double curvature concrete arch dam
Height from the foundation	230.0 m
Length of the crest	440.0 m
Width of the dam at foundation	37.60.0 m
Width of the crest	7.0 m
Total volume of the reservoir	2190.0 million m ³
Power plant type	Ground
Capacity of the power plant	4 × 250 MW
Generate	2107 GWh/ year electricity energy
Foundation	Limestone (Asmari Formation)
Spillway	Chute, orifice types and free

4.3.2. Bedrock Geology of Project Area

Based on the geological map of the region at the project area, there are deposits from Cretaceous Age to the Present (Figures 1.4, 4.3.3 and 4.3.4). The geological formations in the project area are summarized in Table 4.3.2 and are as follow:

The Asmari Formation (500 m thickness) constitutes the main dam foundation rocks and divided into three units. The lower unit comprises limestone, porous limestone, and marly limestone with some marlstone, generally thick to very thickly bedded and highly karstic. The measured mean weighted RQD is between 55% to 83% which indicates fair to good quality rock mass.

The middle unit is located downstream of the dam and comprises alternating limestone, dolomitic limestone, marly limestone and, marl. Karstification is limited. The weighted mean RQD is between 53% to 84% which indicates fair to good quality rock mass.

The upper part consists alternating limestone (medium to thick layers), marly limestone and marl with slight karstification. The weighted mean RQD is between 45% to 78% which indicates poor to good quality rock mass.

Table 4.3.2. Geological formations around the project area.

Unit No.	RockFormation /Group	Lithology	Age
8	Quaternary deposit	River alluvium, colluvium deposits	Quaternary
7	Bakhtyari Formation	Massive conglomerate, sandstone	Late Pliocene to Pleistocene
6	Agha jari Formation	Brownish gray sandstone, red marlstone and siltstone	Late Miocene to Pliocene
5	Gachsaran Formation	Alternation of salt, anhydrite, gypsum, marlstone, marlylimestone, sandstone siltstone, reddish brown	Early Miocene
4	Asmari Formation	Alternation of fossiliferous light-brownish to grey limestone with marly limestone and marlstone and dolomitic limestone	OligoMiocene
3	Pabdeh Formation	Alternation of marly limestone calcareous marl and marlstone overlying purple shale	Late Paleocene to Oligocene
2	Gurpi Formation	Marly limestone and marlstone	Late Cretaceous
1	Bangestan group (Ilam, Sarvak and Kazhdumi formations)	Thick bedded grey limestone and marly limestone with shale interbeds, overlying bituminous shale (Kazhdumi Formation)	Upper Cretaceous

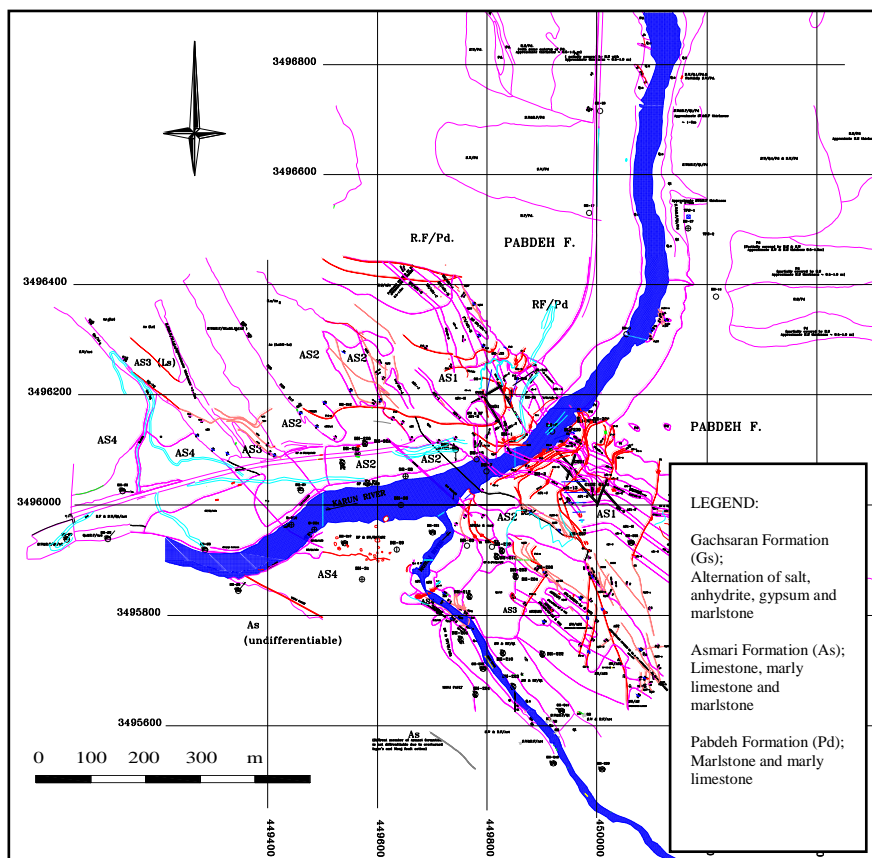


Figure 4.3.3. Geological map of the Karun-4 dam and power plant project in the Zagros Range of Iran. (after MG. co., 1989).

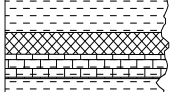
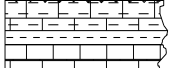
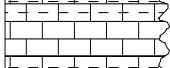
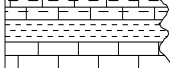
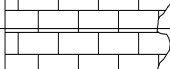
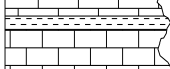
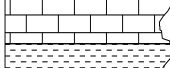
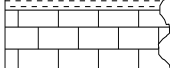
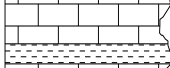

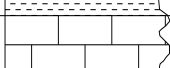
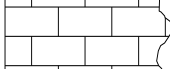
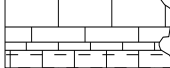


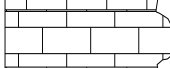
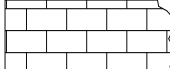


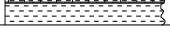
Formation	Thickness	Unit no.	Lithological column	Lithological description	Porosity%
Gachsaran Fm.				Alternation of salt, anhydrite, gypsum marl, marly limestone, limestone and shale	
ASMARI FORMATION 500.0 m	100.0 m	As.3		Marly limestone with Marlstone and sometimes Limestone interbedded	0.50
				Medium to thick bedded limestone and Marly limestone, sporadically marlstone interbedded,	2.25
				Intrabionomicrite, Mudstone to Wackstone Fracture/ vuggy porosity, bioclasts are Foraminifera such as Globigerina sp.	0.75
					5.00
	170.0 m	As.2		Medium to thick bedded limestone dolomitic limestone, marly limestone and marlstone frequency,	1.00
				Biontronicrite, Wackstone - Packstone Fracture/vuggy porosity, Bioclasts are mainly Foraminifera such as Miliolides, Austrorikina sp., Peneroplis sp., Dendritina sp., Echinoid shell fragments	7.00
					1.00
					1.50
					1.25
				Biodolomicrosparite, Wackstone, Dolomitization relatively developed	3.75
	230.0 m	As.1		Thick to very thick bedded, porous Limestone, grey to light grey, fine to medium grained, weak to relatively, strong, Fracture/vuggy porosity,	1.75
					1.50
				2.00	
			Marly limestone, medium to thick bedded grey, grey greenish, low Karstified weak to medium strength	11.00	
			Thick to very thick bedded Limestone grey to grey brownish, fine to medium grained, medium to high strength	5.00	
			Intrabionomicrite- Wackstone to Packstone Bioclastic elements are Foraminifera such as, Amphistegina sp., Rotalia sp., Heterostegina sp., Operculina sp., Elphidium sp., Lepidocyclina sp., Ditrupa Calcareous Red Algae, Echinoid shell Rudists shell fragments	3.35	
				2.10	
			Calcareous Marl, grey to green, fine grained, weak to relatively weak, Biontronicrite- wackstone,	0.30	
				15.2	
				3.00	
				0.75	
				1.50	
Pabdeh Fm.				Alternation of Marlstone, Marly limestone and shale	

Figure 4.3.4. Lithological column of the Asmari Formation at the Karun-4 dam site.

4.3.3. Hydrogeological Characteristic of the Dam Location

4.3.3.1. Karst Features, Porosity and Permeability

From a hydrogeological point of view, the permeability of the formation range from highly permeable to almost impermeable. The geological structure of the region also play an important role in its hydrogeology. The Ilam and Asmari formations are the most permeable formations of the region with very high flow springs present due to the influence of tectonic factors (mainly fracture porosity). The Asmari Formation is vuggy and karstic and has mostly relatively high permeability. Caves, karst channels, enlarged solution joints, stalagmites and stalactites can be observed in these carbonate rocks. At the Bazoft branch of the Karun-4 dam reservoir, there are springs with about 0.1- 3.0 cm/ min emerging from the Asmari Formation. In general, the porosity condition and permeability specifications at the dam axis are summarized in Table 4.3.3 and 4.3.4.

The petrographical and field investigations show that there are various types of porosity in the region but fracture porosity is predominant throughout the Asmari Formation succession (Figures 4.3.4 and 4.3.5). The fracture porosity constitutes about 40% of total porosity features. This shows the significant role of compressional tectonic movements that affected the area.

Table 4.3.3. The range of variation of porosity values classified on a logarithmic scale (Cherenyshev, Dearman, 1991).

Porosity %	< 0.01	0.01- 0.1	0.1- 1.0	1.0- 10	> 10
Descriptive terms	Very low porosity	Low porosity	Medium porosity	High porosity	Extremely High porosity

Table 4.3.4. The porosity (%) and permeability of the Asmari Formation units.

Asmari F. / Unit	Porosity Features	Porosity%	Permeability
U. Asmari/ As.3	Fracture, Intraparticle	0.5- 5.0 Medium to High	Impermeable to V. High
M. Asmari/ As.2	Fracture, Vuggy, Channel	1- 7.0 High	Impermeable to V. High
L. Asmari/ As.1	Fracture, Vuggy Intraparticle	1- 15.2 High to Ex. High	High (locally V. High)

Based on these values grouting will be necessary to reduce the conductivity and porosity of the dam foundation rocks. This will especially be necessary in the Lower Asmari unit which is highly karstified.

4.3.3.2. Watertightness of Reservoir

During site investigations, a total of 14 springs were recognized. The evaluation of spring data indicates that:

- With exception of two small springs, all of the springs are located above the reservoir level which is a positive indication from a reservoir watertightness point of view.
- 70% of springs originate from the Asmari Formation and is proof of the high water storage capacity and relatively high permeability in this formation.
- Springs which originate from Pabdeh, Gachsaran, Agha jari and Bakhtiari formations have low discharges and some of them may also dry up after few months into the hot season.

The distribution of large karst features in the Asmari Formation is limited and the only considerable observed cave with dimension about 15×4×3 m is on the left flank of the reservoir at elevation 1200 m (Figure 4.3.6).

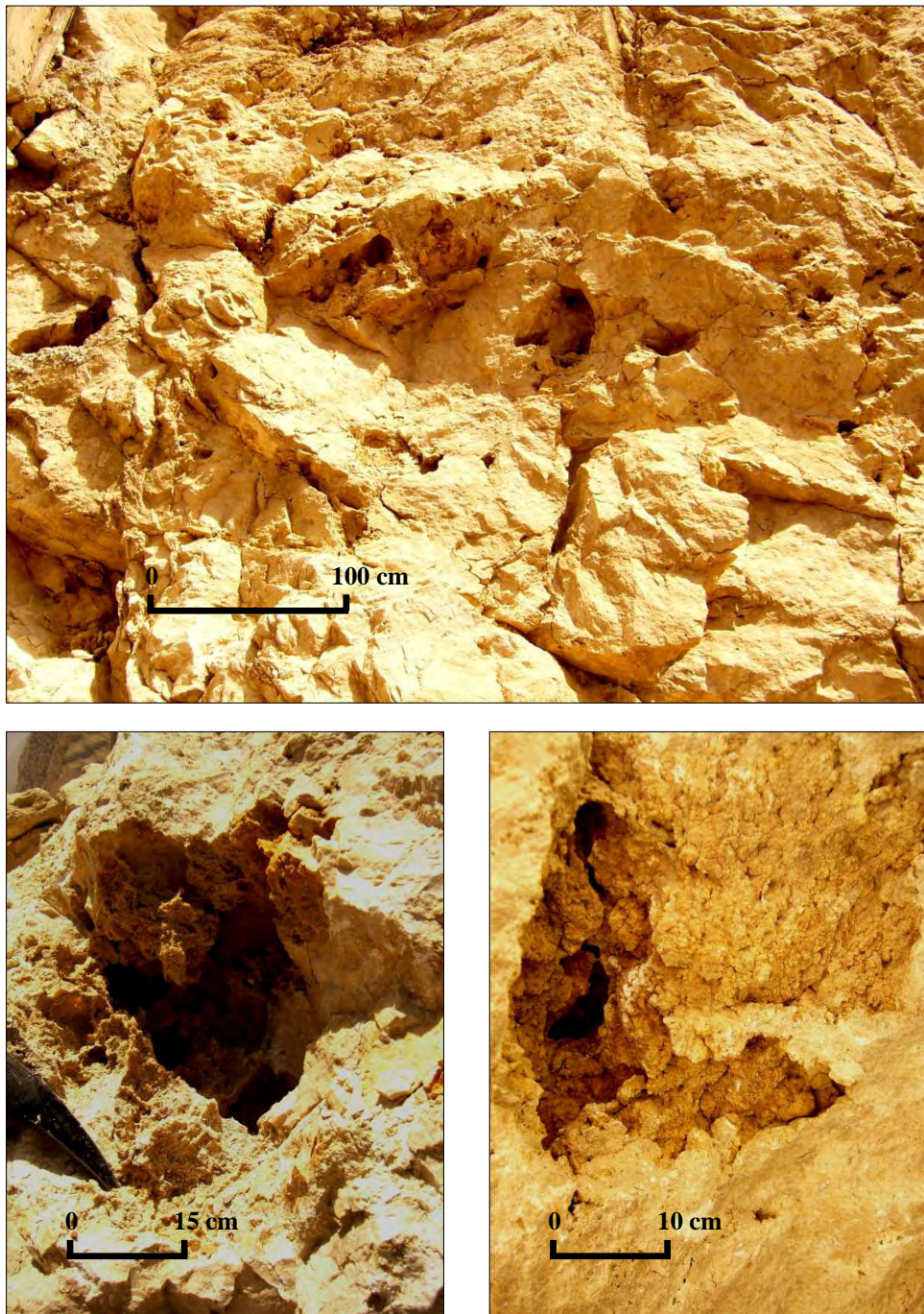


Figure 4.3.5. Some karstic features formed due to dissolution of limestone along discontinuity surfaces. The discontinuity surfaces mainly constituted by compressional tectonic movements at the region and then enlarged by water dissolution. The small fibrous cement, dog tooth calcite crystals and micritic cement overgrowth on vuggs and fractures surface.

Almost all caves have longitudinal shapes with a general direction parallel to bedding also along the intersection between bedding and joints. The shape of the channels is circular or elliptical and the dimensions vary between 30 cm to 100 cm.



Figure 4.3.6. The reservoir area of the Karun-4 dam surrounded partly by the Kuh Sefid Anticline. The Pabdeh Formation constitutes reservoir bed rock near dam location. This formation lithologically comprise impervious succession of marlstone and marly limestone (2006).

Distribution of geological formations in the reservoir area is not uniform. The reservoir can be divided in two parts based on outcrop of formations:

- a) From dam site area up to, about 2 km upstream of Armand and Bazoft confluence and along Armand and up to about 11.5 km along Bazoft River, the bedrock is mostly composed of the Pabdeh and Gurpi formations, Asmari Formation outcrops above the reservoir elevation.
- b) The second part of the reservoir with its particular bedrock characteristics is considered from 11.5 km to 20 km upstream. This part of the reservoir is made up of the Asmari, Gachsaran and Agha Jari formation.

The Pabdeh/ Gurpi (30%- impermeable rocks) and Asmari (29%- permeable) have the most distribution and Bakhtiari has the lowest distribution.

4.3.4. Structural Geology

The Zagros Mountains are considered as a geosynclinal folded belt which appeared as synclinal and anticlinal folds due to the Alpine Orogeny during the Pliocene period, with a general trend of northwest- southeast. Figure 4.3.6 indicates the situation at the Karun-4 dam site.

4.3.4.1. Regional Faults

The Bazoft Fault is about 8 km from the dam site at the nearest point. Its trend is northwest-southeast and the length is about 28 km. It has a thrust mechanism and dips northeast.

The Khajeh – Anvar Fault with a northwest- southeast trend, about 35 km length and thrust mechanism, this fault is 13 km from the dam site at the closest point.

Dopolan Fault is a thrust fault with northwest- southeast trend, more than 70 km long and more than 30 km distant from the dam site.

The Maforon Fault extends in a northwest- southeast trend and is 80 km long and 50 km away from the dam site at the closest point. It has a thrust mechanism with thrust dip towards the northeast.

4.3.4.2. Local Faults

Generally, 20 faults were identified at the dam centerline of which 11 faults are situated on the left flank and 9 faults on the right flank. They are mostly reverse or strike slip faults that show influence of compressional tectonic movement at the dam location (Figures 4.3.8, 4.3.9 and 4.3.10). The local faults and their specifications are listed in Table 4.3.5.

Faults with a length of more than 100 m and 10 m to 60 m displacement (F1, F2, F3, F4 and F15) were observed in the Asmari Formation at the dam axis. The fault zone width varies between centimetres to 5 m and are filled with brecciated rocks, clay minerals, calcite and oxidized rock material (iron oxide).

The variations of fault dip and dip direction are between 25° to 85° and 45° to 355° respectively. About 44% of faults have dip directions between 60° to 85° and 56% faults between 100° to 355°.

The stereographic projection of faults at the dam axis are presented in Figure 4.3.11.

Based on stereographic projection of reverse faults the directions of major principal stresses (2D) are as follows (Figure 4.3.7):

σ_1 : 247° / 0.0° (*max. principal stress*)

σ_2 : 337° / 0.0° (*intermediate principal stress*)

σ_3 : 0.0° / 90° (*min. principal stress*)

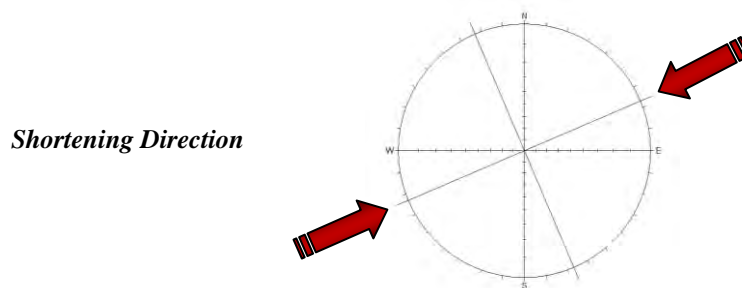


Figure 4.3.7. The direction of σ_1 / Shortening at Karun-4 dam site.

This coincides with the compressional tectonic regime of the Zagros Folded belt.

Table 4.3.5. The faults identifications at the Kaun-4 dam axis.

Fault No.	Location	Type	Dip°	DD°	Fault zone (m)	Gouge	Length (m)	Displacement (m)
F1	L.Flank	Reverse	55	50	1- 2 m		>100	60
F2	L. Flank	Reverse	70- 80	80	1- 2 m	Covered by talus	>100	60
F3	L. Flank	Reverse	35- 55	65- 100	0.5- 5 m	--	>100	15-30
F3a	L. Flank	Sinistral	50	140	--	--	--	2.5
F3b	L. Flank	Sinistral	55	130	--	--	--	2
F3c	L. Flank	Sinistral	60	135	--	--	--	1.5
F3d	L. Flank	Rev/Dex	40	40- 65	1- 2 m	R.Fr,CA,CL	>50	1.5-2
F3e	L. Flank	Normal	50- 70	310	--	--	30-40	1
F4	L. Flank	Dextral	80	75- 85	2- 5 m	Breccia	>100	10
F4a	L. Flank	Reverse	30- 45	70- 100	0- 15cm	Healded,R.Fr	>50	0.5-1.5
F5	L. Flank	Sinistral	70	95- 135	--	CL,Breccia	75	1-3
F6	L. Flank	Sinistral	45	140	--	--	60	3-4
F6a	L. Flank	Reverse	30-40	40- 70	--	--	>100	0.5-20
F7	L. Flank	Rev/Dex	40- 55	110- 140	1- 10cm	CL,CA,R.Fr	100	4-6
F8	L. Flank	Sinistral	40- 55	45	--	--	20	2
F8a	L. Flank	Dextral	40	45	--	--	50	1
F9	L. Flank	Sinistral	40	120	1- 16cm	R.Fr	50	1
F10	L. Flank	Strike slip	30	130	--	--	60	1
F10a	L. Flank	Sinistral	57-60	135-145	--	CA	40	--
F11	R. Flank	Rev/Sin	25-42	350- 45	5- 50cm	CL,CA,R.Fr	70	1.5
F12	R. Flank	?	35- 45	65	1- 1.5m	--	70	?
F13	R. Flank	Strike slip	35-40	350- 10	10-100cm	CA,CL,Marl	345	--
F14	R. Flank	---	--	--	--	--	--	--
F15	R. Flank	Rev/Sin	25- 55	35- 50	1-2cm	R.Fr,CA,CL	>100	40-55
F16	R. Flank	Rev/Sin	15- 20	300-310	10-50cm	CA&R.Fr	>25	3
F17	R. Flank	Rev/Sin	--	35- 75	--	--	>90	2-2.5
F18	R. Flank	--	45- 55	110	10-15cm	R.Fr&CA	>85	?
F56	Adit G4	--	85	75	20-30cm	CL,CA	--	--
F57	Adit G4	--	50-60	145	1.5m	--	--	0.3
F19	R. Flank	Sinistral	60-65	25-30	--	--	--	100-150
F20	L. Flank	Sinistral	55	147	--	--	--	1.5-2

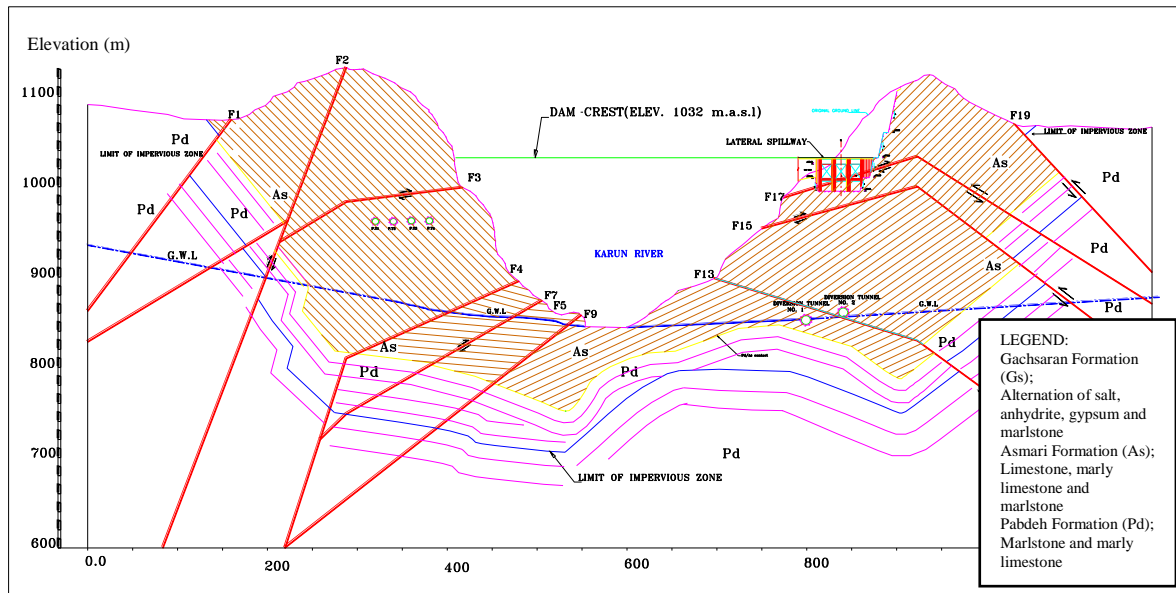


Figure 4.3.8. Engineering geological section of the Karun-4 along Dam axis (after MG co., 2010).

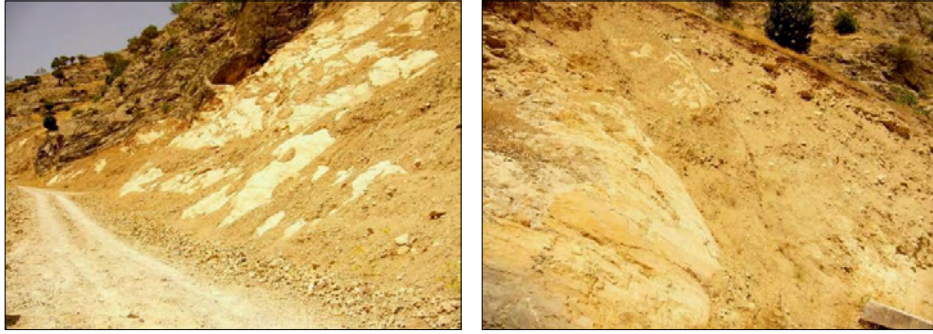


Figure 4.3.9. The reverse faults F. 15 and F. 17 (slickenside) at the right flank.



Figure 4.3.10. The small scale repetitive reverse faults due to compression movements in the Asmari Formation rocks the rigid layer of limestone embedded between two ductile layers of marlstone (northeastern limb of the Kuh Sefid Anticline).

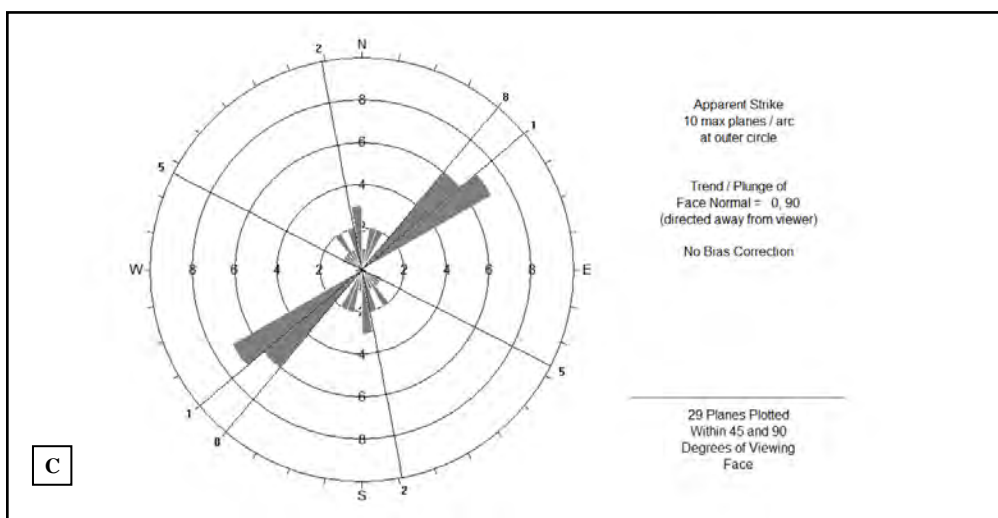
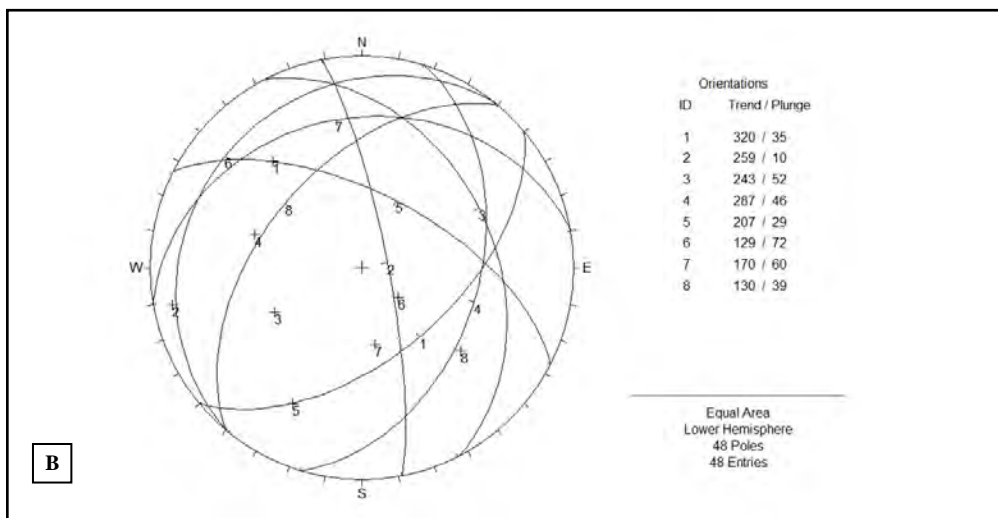
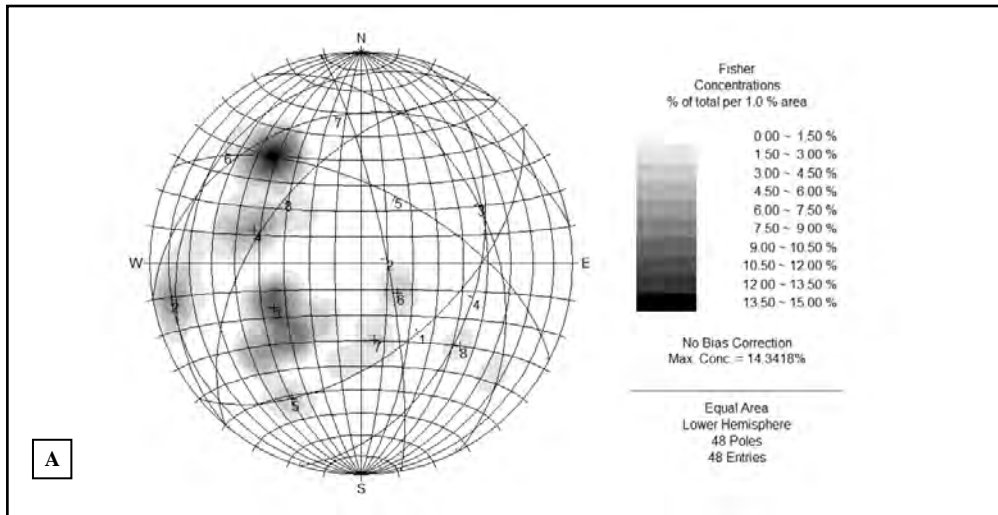


Figure 4.3.11. Stereographic projection of faults which are located on the dam axis of the Karun-4. A- Contour plot, B- Major planes plot and C- Rosette plot. (Dips©, equal area projection-Schmidt net, lower hemisphere).

4.3.4.3. Joint Study

For the joint study at the Karun-4 dam centerline, 77 joints in the right abutment and 116 joints in the left abutment have been measured (totally 193 joints). Based on the concentration of discontinuity planes in the stereographic projection (Dips©), the major joint sets on both abutments are shown in Figures 4.3.12 and 4.3.13.

Almost 47% of total joints are filled with calcite, 45% by calcite- clay and in situ soil and 8% by other gouge materials.

The bedding plane aperture varies between 2 and 100 mm on the surface and decrease in depth.

The major joint set orientations in the right flank are:

- Js.1: 036°/ 31°
- Js.2: 128°/ 40°
- Js.3 (Bedding planes): 221°/ 68°

The major joint sets on the left flank are:

- Js.1: 128°/ 33°
- Js.2: 57°/ 30°
- Js.3: 06°/ 21°
- Js.8: (Bedding planes): 215°/ 72°
- Js.4: 323°/ 31°
- Js.5: 291°/ 36°
- Js.6: 300°/ 69°
- Js.7: 89°/ 66°

The two abutments of the dam have slopes of between 75° to 77° while decrease to 30° at higher elevations (over 950 m). There seems to be some rock wedge instability on both sides of the dam foundation, but with consideration of the stereographic projection of joint sets and their intersection points, internal friction angle (38°- 45°) and aspect of the slope face, there are not any unstable rock blocks on both dam abutments.

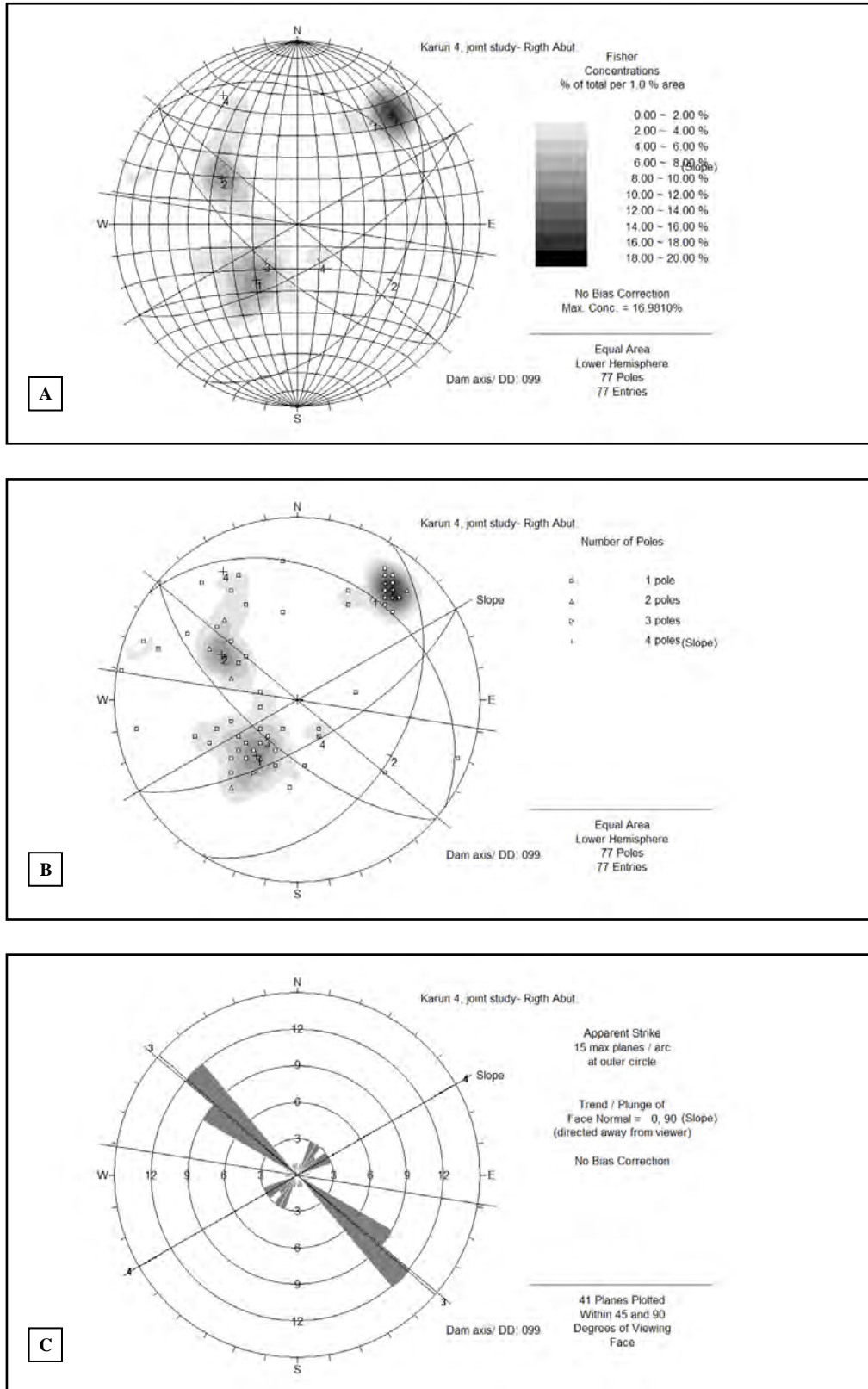


Figure 4.3.12. Stereographic projection of joints (discontinuity distribution) at the right flank of the Karun-4 dam site. A- Contour plot, B- Scatter plot and Rosette plot (Dips©, equal area projection-Schmidt net, lower hemisphere).

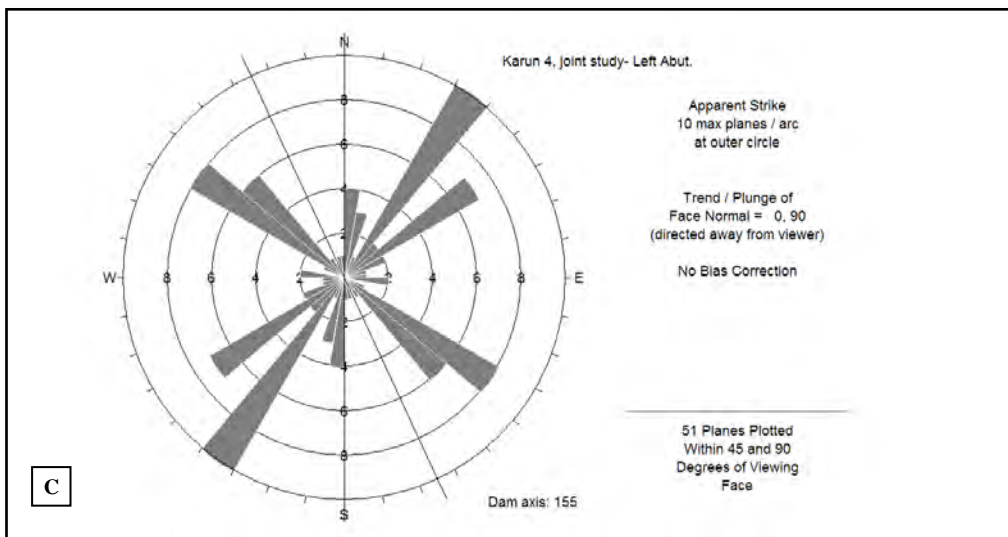
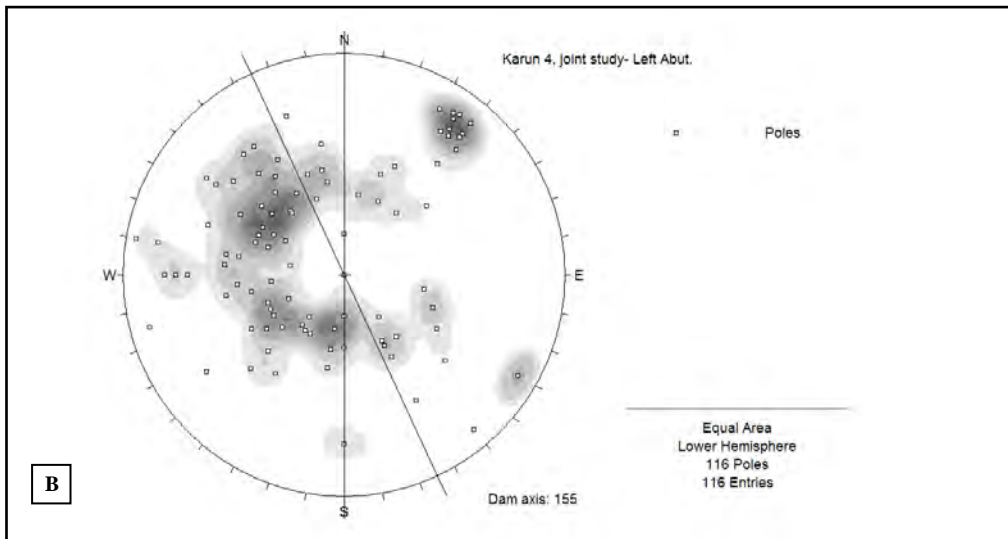
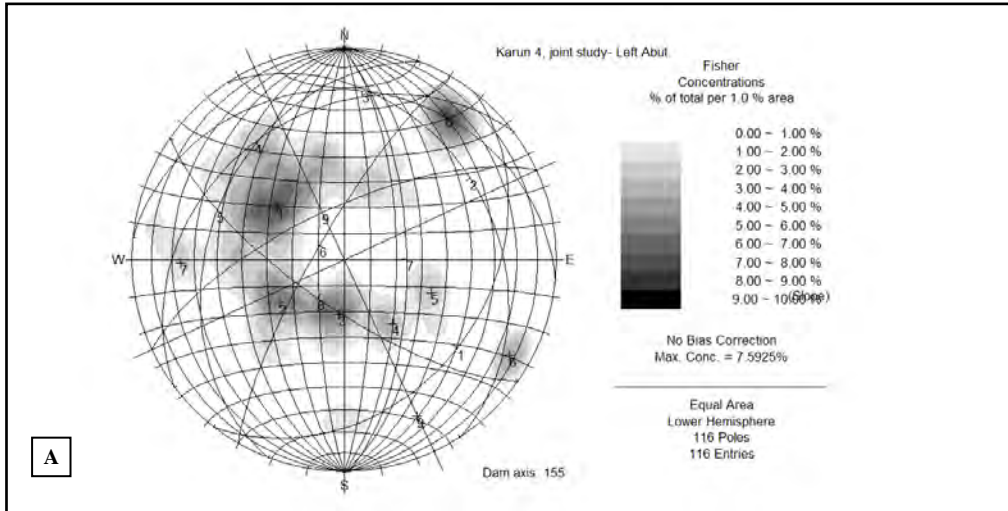


Figure 4.3.13. Stereographic projection of joints (discontinuity distribution) at the left flank of the Karun-4 dam site. A- Contour plot, B- Scatter plot and Rosette plot (Dips©, equal area projection-Schmidt net, lower hemisphere).

4.4. Geology of the Marun Dam and Power plant

The Marun Dam and Power Plant is situated in the Zagros Mountain Range at Tange Takab (gorge) approximately 19 km northeast of Behbahan in the Khuzestan Province. The Marun Dam (rockfill) was constructed on the Marun River and is at 165 m high, the second highest embankment dam in Iran with a crest length of 345 m. The construction was started in 1987 and completed in 1999.

The main objectives of this project are to regulate the Marun River and provide a dependable water resource for irrigation in the four plains of Behbahan, Jayezan, Khalafabad and Shadegan.

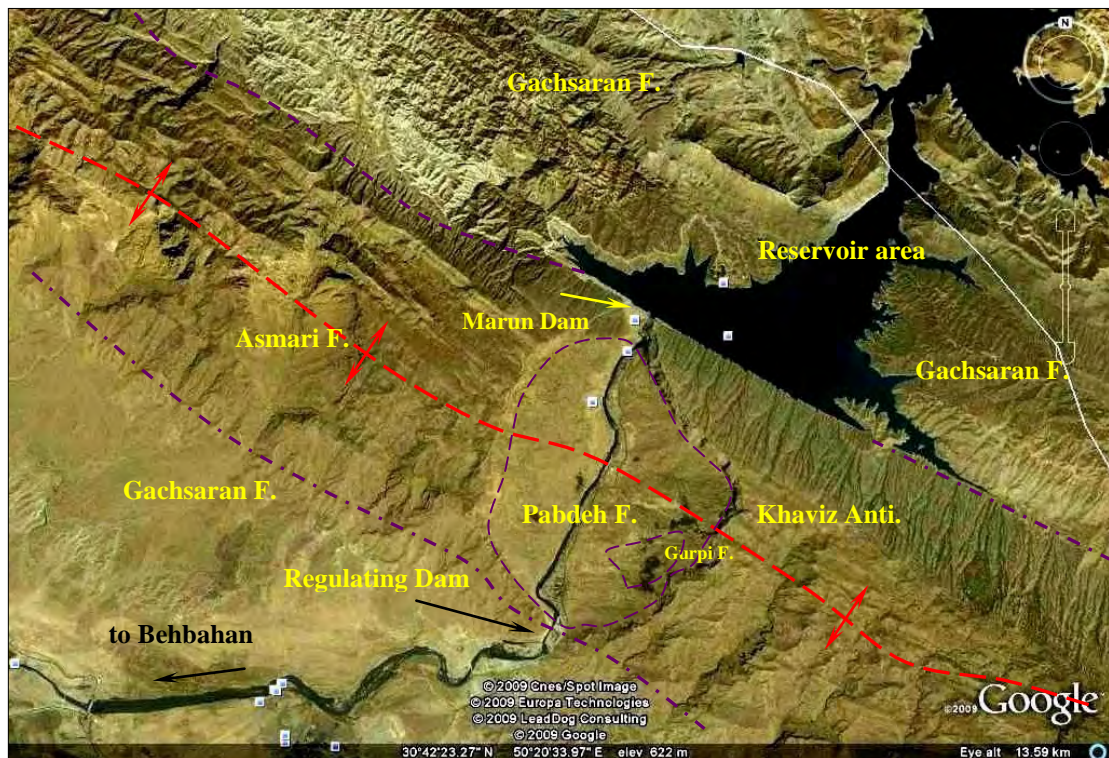


Figure 4.4.1. The satellite image of the Marun dam site on the northern flank of the Khaviz Anticline. The Marun rock fill dam constructed at Tange Takab (gorge) approximately 19 km northeast of Behbahan in Khuzestan Province of Iran (Google Earth, European Technology, 2009).

At the project area, a stratigraphic sequence from upper Cretaceous to Quaternary time can be observed. The Asmari Formation rocks of Oligomiocene age form the main dam foundation and comprise limestone, marly limestone and dolomitic limestone interbedded with marlstone, dipping at 32°-36° to the northeast. The dam is located on the northeastern flank of the Khaviz Anticline (35 km long and 8 km wide) which has a northwest-southeast trend (Figures 4.4.1 and 4.4.2).

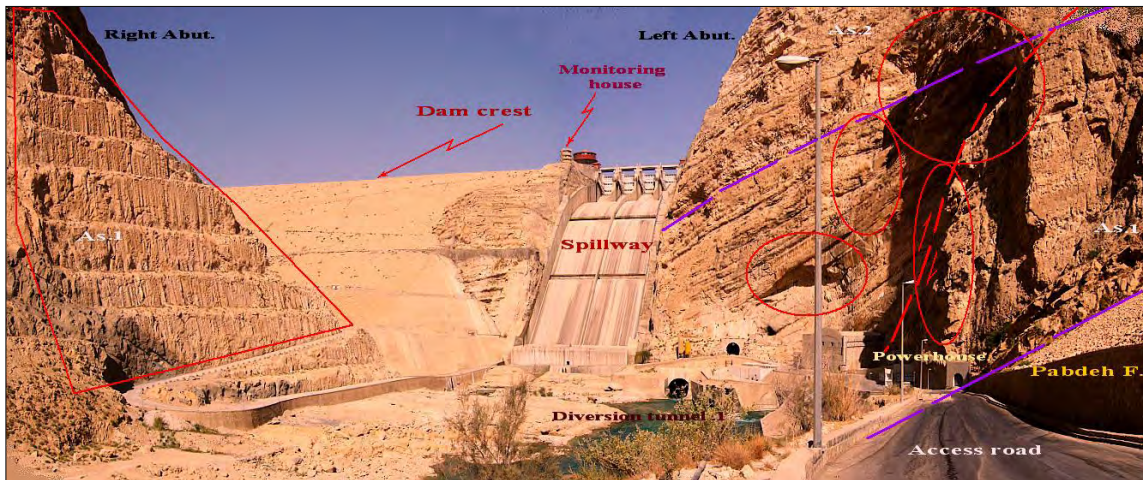


Figure 4.4.2. The Marun rock fill dam constructed on the northern flank of the Khaviz Anticline. The various parts of dam such as semi underground power plant, spillway, diversion tunnels and access road to the dam crest can be seen. The closed red lines indicate some important instability with high risk of falling rock hazard.

4.4.1. Objectives and benefits of the project

- Generating annually 385 GWh hydroelectric energy by two vertical axis turbines and two generators.
- Supply water for irrigating of 55 000 ha of agricultural lands at Behbahan, Jayezan, Khalafabad and Shadegan.
- Controlling floods and regulating the Marun River
- Land reclamation

The general technical specifications of the dam project are listed in Table 4.4.1.

Table 4.4.1. Marun dam and power plant project specifications (after MG co., 1986).

Dam Type	Rock fill dam with clay core
Height from the foundation	165.0 m
Length of the crest	345.0 m
Dam body volume	85863040.0 m ³
Total volume of the reservoir	1200 million m ³
Power plant type	Semi underground
Spillway	Gated spillway- four radial gates combined, ending in a ski jump
Water diversion system	U/S and D/S cofferdam and two diversion tunnels with 505 m and 640 m length and 10.7 m, 13 m dia.
Capacity of the power plant	145 MW (4 units)

4.4.2. Bedrock Geology of Project Area

Figure 1.4 shows the sedimentary succession from the Upper Cretaceous to Quaternary age with a summary of the geological formations in Table 4.4.2. The geological formations are discussed below.

The Asmari Formation constitutes the two flanks of the Khaviz Anticline and comprise alternating grey to light brown limestone, marly limestone and marlstone, which lies on fossiliferous thickly bedded limestone. Based on the petrographical analysis, physical and mechanical properties, the Asmari Formation succession can be divided into three main units (Figures 4.4.3 and 4.4.4).

Table 4.4.2. Geological formations around project area.

Unit No.	Rock Formation /Group	Lithology	Age
7	Quaternary deposit	River alluvium, colluvium deposits	Quaternary
6	Bakhtyari Formation	Massive conglomerate, sandstone	Late Pliocene to Pleistocene
5	Agha jari Formation	Brownish gray sandstone, red marlstone and siltstone	Late Miocene to Pliocene
4	Gachsaran Formation	Alternation of salt, anhydrite, gypsum, marlstone, marly limestone, sandstone siltstone, reddish brown	Early Miocene
3	Asmari Formation	Alternation of fossiliferous light-brownish to grey limestone with marly limestone and marlstone and dolomitic limestone	Oligomiocene
2	Pabdeh Formation	Alternation of marly limestone calcareous marl and marlstone overlying purple shale	Late Paleocene to Oligocene
1	Gurpi Formation	Marly limestone and marlstone	Late Cretaceous

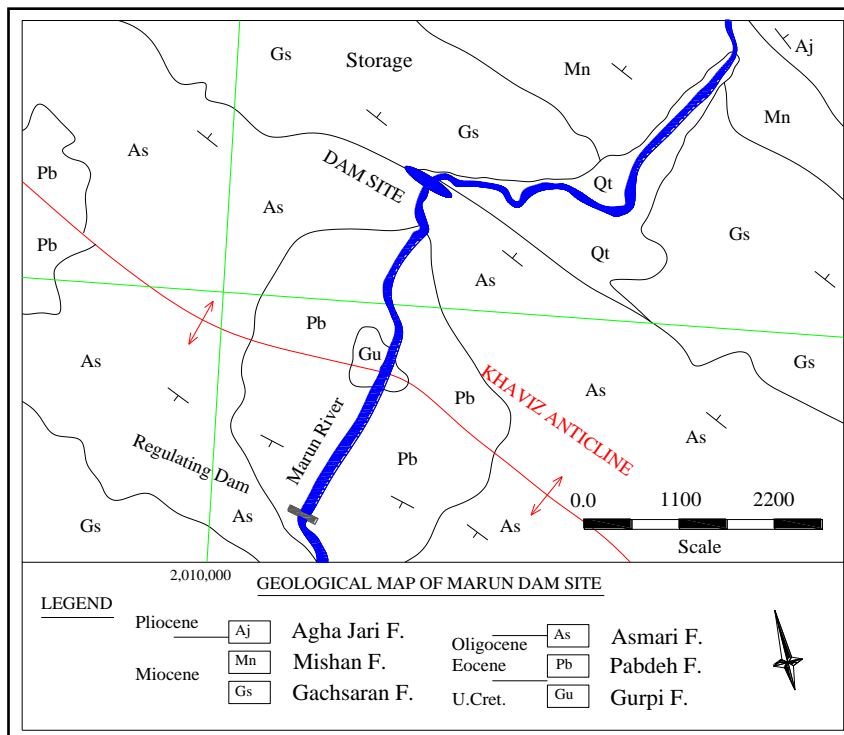


Figure 4.4.3. The geological map of Marun dam and power plant project in the Zagros Range of Iran. The dam foundation is limestone, marly limestone, marlstone and dolomitic limestone of the Asmari Formation (after MG co., 2010).

The lower Asmari consists of 180 m massive to thickly bedded, high strength, microcrystalline limestone and marly limestone with thin intercalations of marl and shale, light grey to grey in color and is relatively highly karstified. Petrographical analysis shows high porosity that in some places constitutes 15% of the rock volume.

The middle unit consists of 110 m medium bedded karstified microcrystalline limestone and marly limestone with frequent thin beds of marlstone. The porosity is relatively high and reaches up to 11% locally. The microfauna's components are mainly Foraminifera, Calcareous Red Algae, Echinoid and Pelecypoda shell fragments.

The upper unit consists of 80 m medium to thinly bedded limestone, marly limestone and dolomitic limestone, light grey to yellow in color. Karstification is well developed in the upper part of the unit and the porosity values vary between 2% and 5.4%.

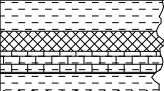
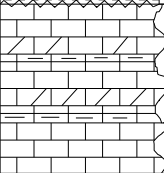
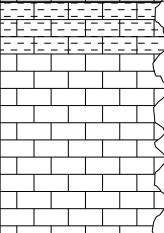
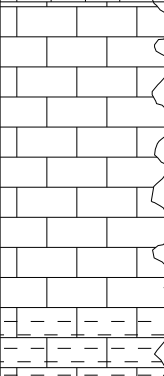
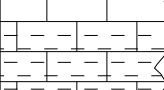
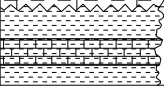
Formation	Thickness	Unit no.	Lithological column	Lithological description	Porosity%
Gachsaran Fm.				Alternation of salt, anhydrite, gypsum marl, marly limestone, limestone and shale	
ASMARI FORMATION 370.0 m	80.0 m	As.3		Medium to thin bedded limestone and marly limestone, vuggy and fracture porosity, light grey to yellow, with some dolomitic limestone. Microfossils are; Foraminifera such as Dendritina sp., Miliolides and Echinoid shell	5.40 3.70 2.12 2.70
	110.0 m	As.2		Marly limestone, vuggy and channel porosity, Medium bedded of Microcrystalline limestone with thin bedded of marlstone frequency. Biopelmicrite- wackstone to Biolitic boundstone, bioclasts are; Foraminifera such as Peneroplis sp., Miliolides, Austrorilina sp., Rotalia sp., and fragments of Pelecypoda, Echinoid shell and Red Algae	9.62 1.40 11.00 3.80 1.80
	180.0 m	As.1		Massive to very thick bedded limestone, microcrystalline, light grey to grey, dense, high strength, with interbedded of thin marls/ shale. Vuggy, channel, intraparticle, fracture porosity and karstic zones. Intra-biomicrite- wackstone to packstone. Organic components are Foraminifera. Such as Asterigerina sp., Dendritina sp., Heterostegina sp., Haplofragium sp., Pseudotaberina sp., Miliolides, calcareous Red Algae, Echinoid and Pelecypoda shell.	3.60 10.90 1.33 12.70 4.75 4.00
				Marly limestone, thick to medium bedded Biomicrite- packstone, bioclasts are; Foraminifera shell such as Operculina sp., Rotalia sp., Miliolides, Pelecypoda shell	14.90 1.63
Pabdeh Fm.				Alternation of Marlstone, Marly limestone and shale	

Figure 4.4.4. Lithological column of the Asmari Formation at the Marun dam site. The Asmari Formation consists of 370 m limestone, dolomitic limestone, marly limestone and divided into three main units.

4.4.3. Hydrogeological Characteristic of the Dam Location

4.4.3.1. Karst Features, Porosity and Permeability

Petrographical studies of samples and field investigation at the Marun Dam showed that the Asmari Formation is the only formation which has relatively high porosity. The karstification varies from karstified to highly karstified (Figures 4.4.4 and 4.4.5).

The formation has high potential for water storage due to both porosity and karstification. Some springs that originate from the Asmari Formation have potable water with a normal taste but there are also lots of salty and sulfur springs in the region that originate from the Gachsaran Formation (Fars Group). At 500-1500 m from Godaar Nargoon Village, there are

three sulfur springs with 10 to 600 l/m discharge. Some small iron springs with 1-2 l/m discharge were observed in the Pabdeh Formation.

On surface, there are perpendicular fractures almost 10 m long and 15 – 20 m deep that are partly filled by Quaternary deposits and observations in exploration galleries and boreholes also indicate cemented breccias and crystallized minerals inside the fracture zones. These structures originated from tectonic movements but have been enlarged due to dissolution.

The main part of the reservoir underlain by the *Fars Group* Formation is composed of gypsum, sandstone marl, shale and a thin layer of limestone (Figure 4.4.6). Lithologically, this succession seems impervious, but at the contact with the Asmari and Gachsaran Formations, at the dam and in the reservoir intense karstification caused both probable discharge conditions. It should be mentioned that the water from the Fars Group can produce active solutions which can influence the carbonate rocks of the Asmari Formation and development of karst zones.

The fracture and fissure densities in the lower unit are low but become more abundant in the middle and upper parts of the Asmari Formation.

The lower part of Asmari Formation consists of massive to very thickly bedded limestone with well developed karst features such as cavities and dissolution zones, especially at the base. The porosity values based on petrographical analysis are high to extremely high and reduce in some places almost 15% of the rock volume.

The middle part consists of medium bedded microcrystalline limestone, marly limestone and marlstone with dissolution features. Holes and cavities that are partly filled by calcite and clayey materials indicate acidic water dissolution. The range variation of porosity values is high to extremely high and reach in some places in the middle and upper part 9- 11% of the unit volume.

The upper part of the Asmari Formation consists of 80 m of medium to thinly bedded limestone and dolomitic limestone. Karstification is relatively widespread especially in the upper part of the unit. Karstification phenomena on bedding planes and through fracture zones are well developed. The maximum porosity value reaches 5.4% which relates to high porosity. At the intersection of the main fractures and some bedding planes, the dissolution of limestone due to aggressive water is well developed.

In the Tables 4.4.3, 4.4.4 and 4.4.5, the porosity and permeability results of three units of the Asmari Formation, based on petrographical studies and lugeon tests, are listed. The quantity and quality criteria for permeability classification are:

Table 4.4.3. The quantity and quality criteria for permeability classification (Lewis et al., 2006).

Permeability	Quantity (Lu)	0- 3	3- 10	10- 30	30- 60	> 60
	Quality	Non	Low	Moderate	High	V. High

Table 4.4.4. The range of variation of porosity values classified on a logarithmic scale. (Cherenyshev, Dearman, 1991).

Porosity %	< 0.01	0.01- 0.1	0.1- 1.0	1.0- 10	> 10
Descriptive terms	Very low porosity	Low porosity	Medium porosity	High porosity	Extremely High porosity

Based on hydraulic conductivity, porosity and permeability results, it seems that some water leakages occur especially in the upper and middle Asmari at the dam foundation and cut-off curtain. Here the cut-off curtain is suspended in the middle Asmari unit.

The design of the grouting curtain was not modified and this has caused the excessive leakage after the first impoundment of the reservoir. It was decided to impound the reservoir during the summer of 1996 for agricultural purposes.

Table 4.4.5. The porosity and permeability values of the Asmari Formation units.

Asmari F. / Unit	Porosity Features	Porosity%	Permeability
U. Asmari/ As.3	Vuggy, Fracture	2- 5.4 High	Moderate to High
M. Asmari/ As.2	Vuggy, Channel	1.4- 11 High	Low to Moderate
L. Asmari/ As.1	Vuggy, Channel, Fracture,	1.6- 14.9 High to Ex. High	Low to Moderate

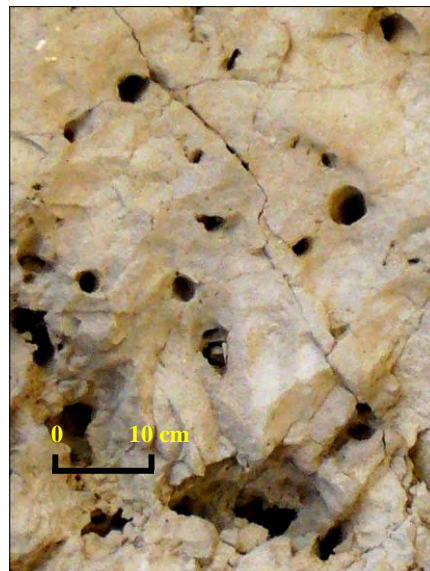
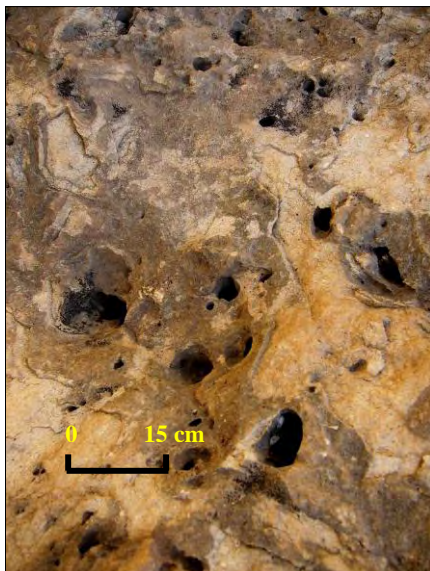


Figure 4.4.5. Some karstic features due to acidic water dissolution in the Asmari Formation limestone. The porosities mostly seem channel porosity, but in some places at intersection between bedding planes and discontinuities, karstification is well developed because of limestone dissolution.

With the fuse shell, temporary impoundment became possible to satisfy the agricultural demand and minimize delay in construction activities at the same time. By March 1997, the embankment had been constructed to 80% of its final height (165 m).



Figure 4.4.6. The reservoir area of the Marun dam site that situated on northeast flank of the Khaviz Anticline. The upper Asmari Formation limestone as main dam foundation and evaporite rocks of Gachsaran Formation that constitute a part of reservoir area can be observed.

Immediately after impoundment, considerable leakage was observed in the pressure tunnel and efforts to open the stoplogs failed. At the same time an embankment was constructed and subsequent grouting controlled the leakage in the pressure tunnel. The embankment was overtopped with increasing water elevation, and considerable leakage of up to $7 \text{ m}^3/\text{sec}$ occurred from weak zones upstream of the plug.

The major flow of approximately $4.5 \text{ m}^3/\text{sec}$ was from two large solution channels and leakage around the concrete plug. The remaining flow was from the access tunnel and the grouting adit ($2.3 \text{ m}^3/\text{sec}$). Drain holes in the dam body at the toe were dry.

The rock strata at the site comprise a series of karstic limestones interbedded with water sensitive marls which dip towards the reservoir. In addition, there are two major joint sets, the first parallel to the bedding, and the second perpendicular to the bedding. The water entered the fissure system upstream of the plug and passed along the fissures, washed out the marls interbeds forming large cavities. Water was leaking into all tunnels and the dam, and prevented entry into some tunnels due to high water flows. It was reported that all springs received their water from the same fissure. Efforts to control the leakage by grouting failed due to excessive flows and even chemical grouting appeared to be ineffective in blocking the flow.

The experience clearly indicates that the limestone Asmari Formation is karstified and a porous succession with a highly potential for water leakage. This succession is accompanied by some very weak rock layers such as marlstone which is highly susceptible to erosion under the high hydraulic pressure of the reservoir.

The water tightness of the dam site and reservoir should be investigated in detail to identify the karstified zones in the Asmari and Gachsaran Formations in addition to the contact zones between the two formations.

4.4.4. Tectonic Setting

The pre Quaternary formations from the upper Cretaceous to Pliocene are folded due to tectonic activities dating from Plio- Pleistocene times. The main tectonic structures are the Khaviz and Bangestan Anticlines. The dam site is located on the northeastern flank of the Khaviz Anticline and the Bangestan Anticline as the northern limit of the reservoir.

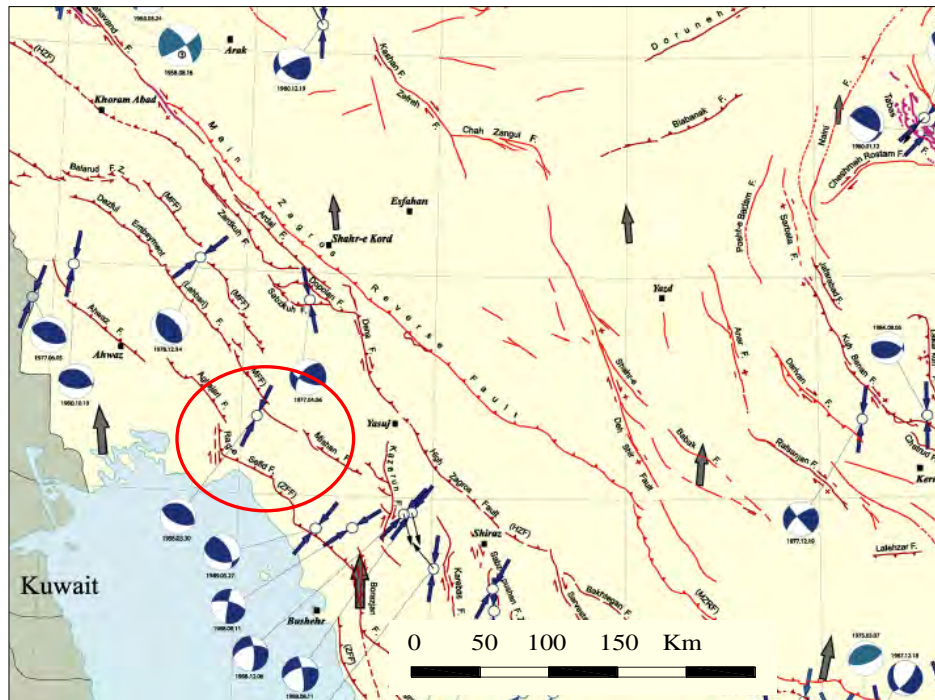


Figure 4.4.7. The major seismically active faults in the study area in the Zagros region. This map shows the distribution of active faults and demonstrates the relationship between the slip vectors and compressive axis, obtained from the determination of the focal mechanism of the earthquakes, and GPS velocities (after International Institute of Earthquake Engineering and Seismology- Iran, 2003).

The two anticlines are asymmetrical with their axes almost parallel trending northwest-southeast, which is the typical of the main structural trend in the Zagros Region (Figure 4.4.7). The younger formations in the Fars Group (Mio-Pliocene) have an abnormal position in the syncline between the Khaviz and Bangestan anticlines. They are extensively eroded and deformed (folded) due to their flexural and plastic characteristics (mainly evaporites and marls).

The Asmari Formation in the northeastern part of the reservoir (about 10 km from the dam location) is thrust over the Mishan and Bakhtyari Formations due to a thrust fault dipping to the northeast, which imply high compressional movement in the region. In addition some small displacements and landslides occur in the Fars Group succession. These phenomena may be the main cause of slope instability after impoundment of the reservoir. The Asmari Formation was also deformed by a high angle reverse fault with a northwest-southeast trend near the power plant location on the left flank. This fault caused some slope instability such as rock falls and suspended blocks which have enormous potential of falling (Figure 4.4.8). The main discontinuity planes in this area are:

- a) Bedding planes with azimuth 120° to 125° and dip 30° - 35° to the northeast. The planes have apertures from millimetres to 15 cm partly filled with clay minerals and carbonate sediments. The surfaces are wavy and rough and are influenced by slight weathering and karstification.

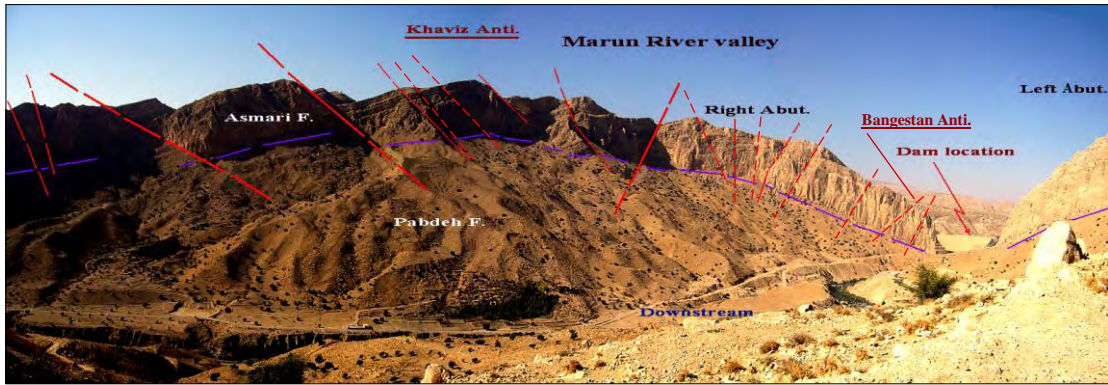


Figure 4.4.8. Panoramic view of the Khaviz Anticline and Marun dam location with the main faults and fracture systems. The Keystone graben caused by extensional process at outer core of anticline during compressional regime can be observed.

- b) Joints trending parallel to sub parallel to the bedding planes. These joints have azimuths 196° to 215° and dip 40° to 50° in the middle Asmari and 60° to 75° in the other parts of the Asmari succession. Some of these joints pass through all three units with small displacement and seem to be small faults. The displacement varies from 0.7 to 1m. In some places slickensides can also be observed. On surface the fractures are 10 m in length and 15 m to 20 m deep and are partly filled by Quaternary deposits. In some localities the infill is composed of brecciated, cemented materials and recrystallized minerals such as calcite. Field investigations show that there are not any traces of recent movement along these surfaces.
- c) Secondary joints with azimuth 200° to 210° and 60° to 80° dip to the southwest also influenced the Asmari strata on surface. These fractures are tight at the surface but open near the slopes. They are 5 m in length and 5 m deep with apertures between 5 and 15 cm. They are perpendicular to the river valley.
- d) Joints with azimuth 290° - 300° and 110° to 120° with dip between 70° to 80° .

A lot of fractures, fissures and small faults with short displacements are present in the Asmari Formation (Figure 4.4.8).

4.4.4.1. Joint Study

A joint survey including 123 joints was taken on both abutments. A stereographic projection showing the concentrations of the major joint sets is shown in Figure 4.4.10. The contour plot, rosette plot and pole plot of the discontinuities (equal area projection, lower hemisphere) are represented in diagram 4.4.10.

The major joint set specifications on the dam axis are as follow:

- Js1 (Bedding planes): $033^{\circ}/ 34^{\circ}$
- Js3: $209^{\circ}/ 74^{\circ}$
- Js4: $296^{\circ}/ 88^{\circ}$
- Js5: $033^{\circ}/ 79^{\circ}$
- Js6: $207^{\circ}/ 54^{\circ}$

The surface of the bedding planes is generally rough and wavy and filled with clay minerals and calcite cement. The apertures of the discontinuities are from millimetres to between 10 -15 centimetres.

The pattern of joint systems as well as the high angle morphology on both abutments, especially on the left flank (negative angles) create planar sliding and rock fall hazards (Figure 4.4.2).

Based on the stereographic projection of bedding plane dip directions on both flanks of the Khaviz Anticline the direction of major principal stresses (2D) can be calculated as follows (Figure 4.4.10):

σ_1 : 213°/ 0.0° (*max. principal stress*)

σ_2 : 303°/ 0.0° (*intermediate principal stress*)

σ_3 : 0.0°/ 90° (*min. principal stress*)

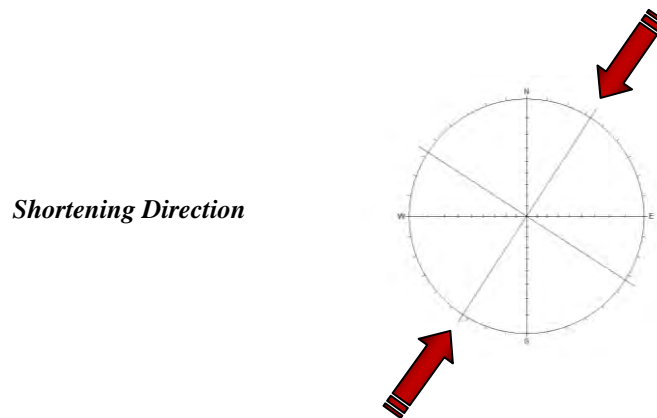


Figure 4.4.9. The direction of σ_1 / Shortening at Marun dam site.

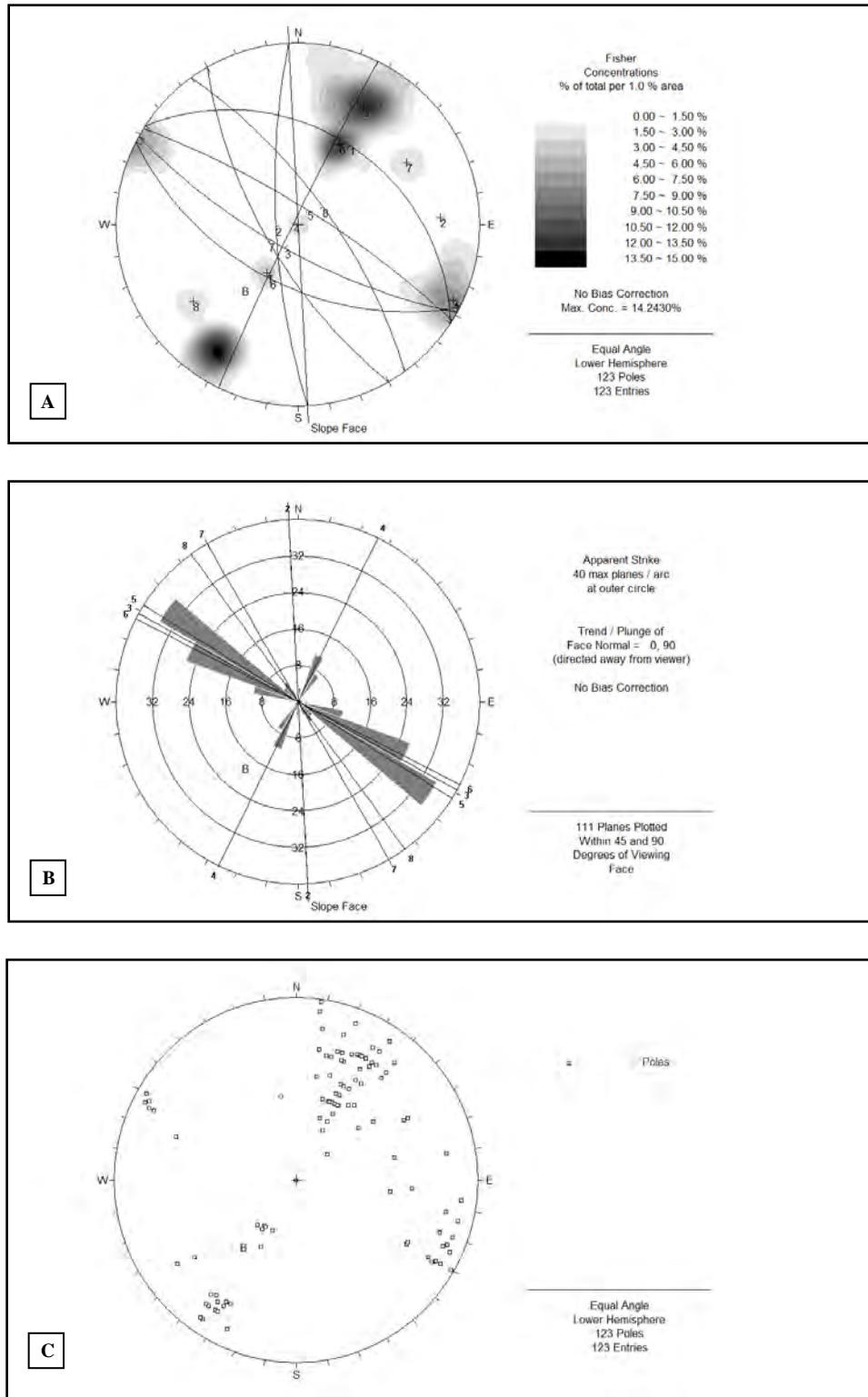


Figure 4.4.10. Stereographic projection of joints at the Marun Dam. A- Contour plot, B- Rosette plot and C- Pole plot of discontinuities (Dips©, equal area projection-Schmidt net, lower hemisphere).

4.5. Geology of the Seymareh Dam and Power plant

The Seymareh dam and power plant project is constructed in the Seymareh River at the entrance of the gorge of the Ravandi Anticline. The dam is accessible from the Darreh Shahr–Ilam main road in the Ilam Province of Iran.

The river valley is U shaped with relatively high cliff angles and locally negative angles in some cases. The geomorphology is basically controlled by the lithology, tectonic history and climate of the region. The two flanks of dam have very steep slopes below on elevation of 760 m but decrease to 25 degrees above this elevation. The river bed is about 35 to 40 m in width that gradually increases down stream of the dam position.

Due to some sliding events (according to the surface and subsurface stratigraphic investigations we found that 4.5 m landslide/rock fall debris underlying about 28 m of lake deposits and 5.5 m recent river alluvium that is widespread throughout the upstream area of Seymareh Dam locality), the direction of river flow changed from northwest-southeast to northeast southwest near the entrance to the gorge (Figure 4.5.1). The river cuts through the anticline axis and southern anticline flank and flow northwest- southeast into the Talkhab Plain and finally converge with the Karkheh River.

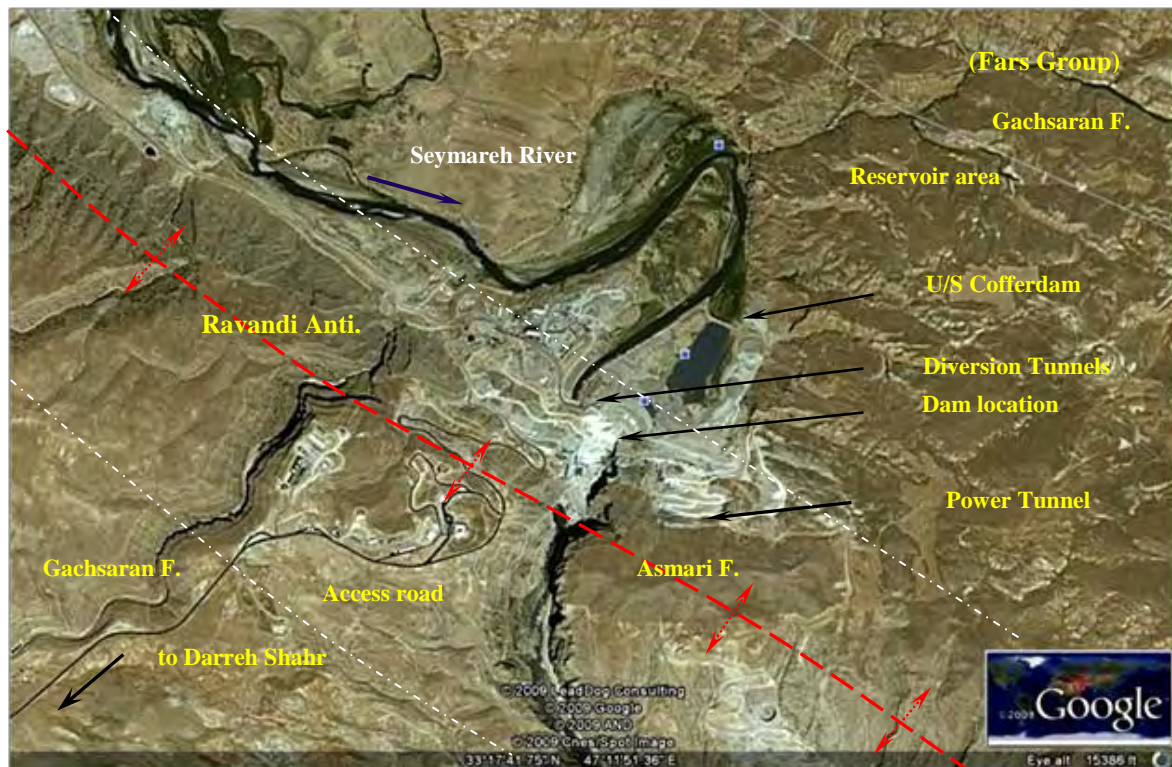


Figure 4.5.1. Satellite image of the Seymareh dam site on the northern flank of the Ravandi Anticline with a northwest-southeast trend. The Seymareh concrete arch dam is constructed in the Seymareh river valley approximately 106 km southeast of Ilam city at Ilam Province of Iran (Google Earth, European Technology 2009).

The dam foundation rocks are the Asmari Formation limestone dipping at 25°- 35° at the entrance of the gorge (dam axis) and gradually decreasing to 10°- 15° downstream near the anticline axis. The dam is located on the north- eastern flank of the Ravandi Anticline which has a northwest- southeast trend and is asymmetrical (Figures 4.5.2 and 4.5.3).

The Seymareh dam is a double curvature concrete dam which is presently under construction. This dam, with a gated spillway, has a height of 180 m and reservoir volume of 3215 m³.

Other structures consist of upstream and downstream cofferdams and two diversion tunnels at the right flank. The diversion tunnels are 473 m, and 397 m long with 10.5 m and 8.3 m diameter respectively. The cofferdams are earth and rock fill structures.

The powerhouse contains three units with a total capacity of 480 MW that generates 843GWh/year electricity.

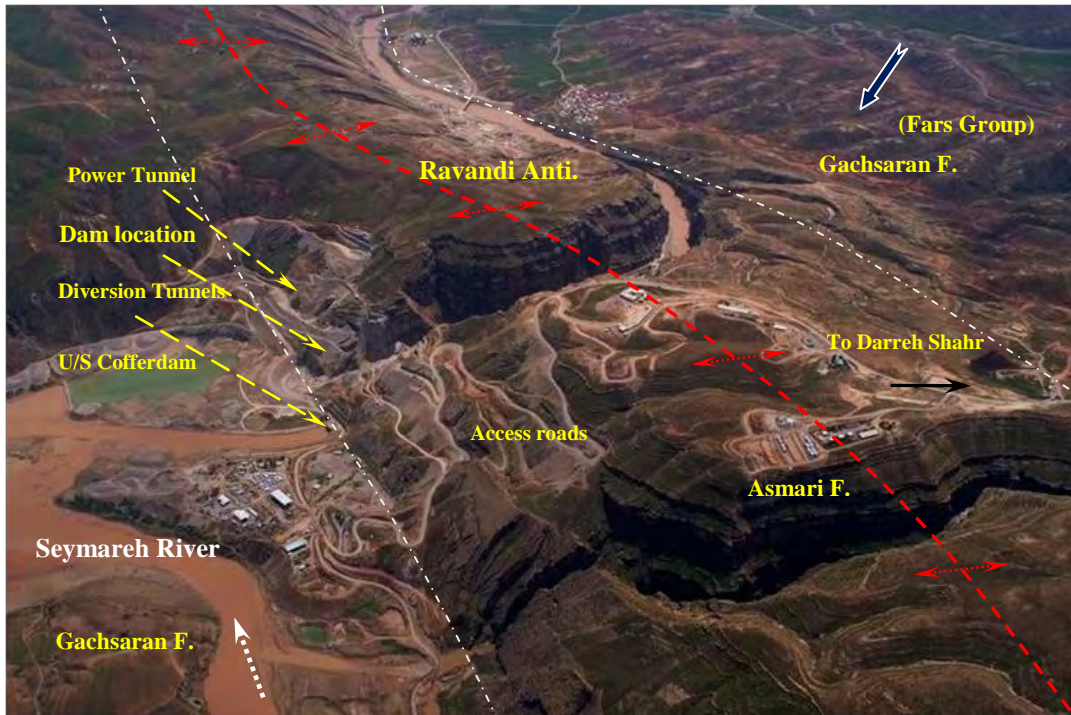


Figure 4.5.2. Aerial view of Seymareh dam site being constructed on the northern flank of the Ravandi Anticline (after khoshboresh, 2007).

4.5.1. Objective and benefits of the project

- a) Generating annually 843 million kWh hydroelectric energy via three units' power plant.
- b) Supply water for irrigation of agricultural lands.
- c) Controlling flooding in the Seymareh River.
- d) Land reclamation
- e) Approximately 40 million dollars of annual income due to electricity generated by this project

The general technical specifications of the dam project are summarized in Table 4.5.1.

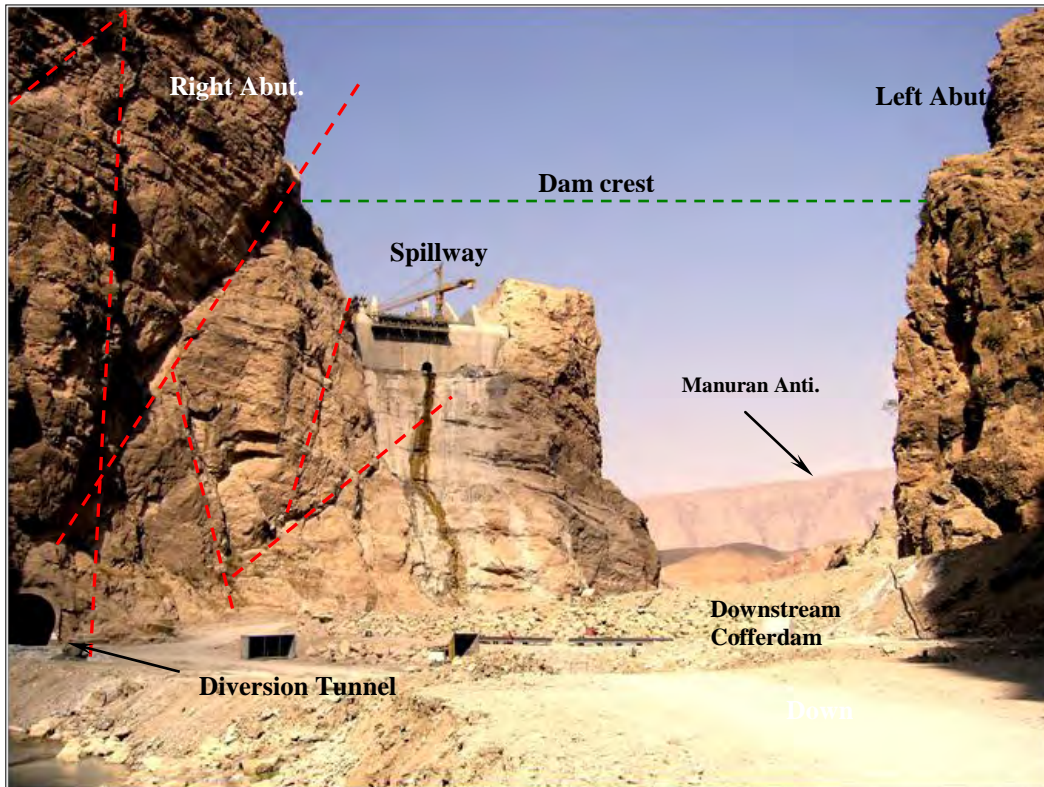


Figure 4.5.3. The Seymareh dam foundation rocks and associated structures such as diversion tunnels, spillway and downstream cofferdam. The dam foundation rock is Asmari Formation limestone (2007).

Table 4.5.1. The technical specifications of the Seymareh dam and power plant project.

Dam Type	Double curvature concrete type
Height from the foundation	180.0 m
Length of the crest	202.0 m
Dam body volume	500,000 m ³
Total volume of the reservoir	3215 million m ³
Power plant type	Ground, 2.5 km down stream
Spillway	1-Gated spillway, 2- Free on dam body
Water diversion system	U/S and D/S cofferdam and two diversion tunnel with 473 m, 397 m long and 10.5m, 8.3 m. diameters
Capacity of the power plant	480 MW (3 units of 160 MW)

4.5.2. Bedrock Geology of Project Area

Based on the geological map of the region at the project area, there are deposits from Oligocene to Quaternary Era (Figure 1.4). The geological formations in the project area are summarized in Table 4.5.2.

The Asmari Formation as the main foundation rocks is divided into three units; The lower unit lithologically comprises 188 m medium bedded, fossiliferous marly limestone and microcrystalline limestone. The porosity varies between 1.4% to 5.2% that indicates a high porosity index. The rock quality designation (RQD) is about 80% which indicates good quality rock mass. The permeability values vary from non to medium permeability for this unit. The uniaxial compressive strength (UCS), based on Schmidt hammer field tests and laboratory tests is about 95 MPa.

The middle unit lithologically comprises 238 m massive to thickly bedded, crystalline limestone, dolomitic limestone and marly limestone light to dark grey in colour. Except for the first part of the diversion tunnels, all dam structures are constructed in this unit. Karstification features can be observed throughout the unit. The porosity value in the lower part is 7.5% which implies high porosity and decrease gradually to 0.95% in the upper part. The permeability, based on lugeon test results, indicates low to high values (Figure 4.5.5). The UCS and RQD are 70-100 MPa and 75%- 95% (good quality) respectively.

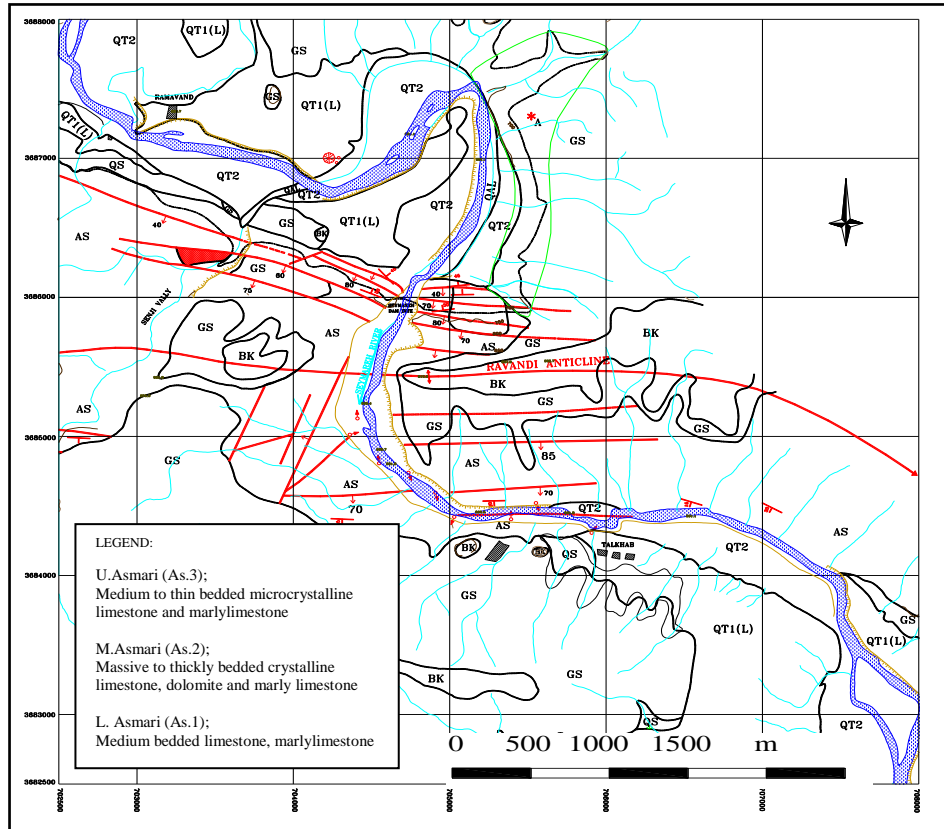


Figure 4.5.4. The engineering geological map of the Seymareh dam and power plant project. Asmari Formation constitutes the dam foundation rocks and comprise grey to light grey limestone, dolomitic limestone and marly limestone Oligomiocene age (after MG co., 2010).

Table 4.5.2. The geological formations at the Seymareh dam site.

Unit No.	Rock Formation/ Group	Lithology	Age
4	Quaternary deposit	River alluvium, colluvium deposits	Quaternary
3	Bakhtiary Formation	Unconformably massive conglomerate and sandstone	Late Pliocene to Pleistocene
2	Gachsaran Formation	Alternation of salt, anhydrite, gypsum, marlstone, marlylimestone, sandstone siltstone, reddish brown	Early Miocene
1	Asmari Formation	Cream to brown limestone, marly limestone dolomitic limestone and marl, fossiliferous	OligoMiocene

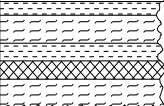
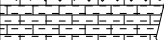


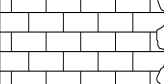
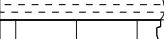
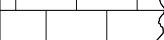


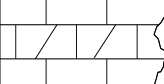

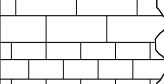
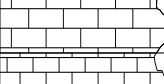
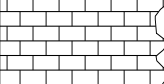
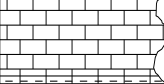
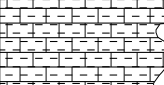
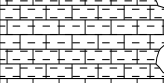
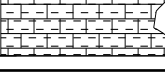
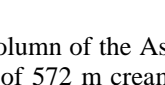
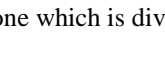

Formation	Thickness	Unit no.	Lithological column	Lithological description	Porosity%
Gachsaran F.				Alternation of salt, anhydrite, gypsum marl, marly limestone, limestone and shale	
ASMARI FORMATION 572.0 m	1500 m	As.3		Marly limestone	0.75
				Vuggy to fracture porosity Biopelmicrite, packstone, Bioclasts are: Planktonic Foraminifera, Spogiomorphides, Borelis sp, Meandrospira sp, Milialides	1.50
				Crystalline bioclastic limestone grey to dark grey, partly recrystallized Intrapelbiomicrite, wackstone- packstone	1.00
				Vuggy porosity, partly filled by coarse Sparry calcite cement, Bioclasts are; Borelis sp, Rotalia sp, Milialides, Ditrupa Echinoid shell and Red Algae,	2.00
				Marlstone	2.20
	2380 m	As.2		Marly limestone, fossiliferous	4.40
				Crystalline dolomitic limestone with Extensive dolomitization	0.90
				Bioturbated dolomite, wackstone- packstone Vuggy to fracture porosity	0.00
				Bioclasts are Lepidocyclina sp., Red Algae	1.00
				Crystalline dolomitic limestone Massive to thick bedded	0.60
1880m	As.1		Dolobionomicrite, wackstone, vuggy porosity Karstified, partly filled by microsparry Calcite cement, micritic cement partly changed to rhombohedral crystals of Dolomite, Bioclasts are Operculin sp, Echinoid shell fragments	1.25	
			Microcrystalline and fossiliferous limestone, thin to medium bedded	3.70	
			Biomicrite, packstone, bioclasts are Echinoid, Pelecypoda shell fragments Vuggy porosity karstified	7.50	
			Microcrystalline limestone, dark grey Vuggy porosity, partly filled by coarse blocky to microsparry calcite cement	3.00	
			Pelmicrite, wackstone micritic cement partly recrystallized to microsparry calcite cement	1.40	
1880m	As.1		Fossiliferous marly limestone dark grey in color, vuggy porosity	1.40	
			Intrabionomicrite, wackstone to packstone Bioclasts are Archais sp, Peneroplis sp. Milialides, Austrotrilina sp, Dendritina sp. Rotalia sp, Bryozoa, Red Algae, Echinoida Spongia and Pelecypoda shell fragments	2.20	
			Marly limestone	4.50	
			Marly limestone	2.50	
			Marly limestone	5.20	

Figure 4.5.5. Lithological column of the Asmari Formation at the Seymareh dam site. The Asmari Formation consists of 572 m cream to light grey limestone, dolomitic limestone, marly limestone and marlstone which is divided into three main units.

The upper unit lithologically comprises 150 m grey to dark grey microcrystalline limestone, bioclastic limestone and marly limestone, karstified and medium to thinly bedded (Figure 4.5.5).

The porosity values are between 0.75% to 4.4% that indicate medium to high porosity. The permeability is high to very high. The UCS and RQD values based on laboratory tests are 60-100 MPa and 65%- 94% (fair to good quality) respectively.

4.5.3. Hydrogeological Characteristics of the Dam Location

4.5.3.1. Karst Features, Porosity and Permeability

The hydrogeology at the dam site includes formations with very high permeability to almost impermeable. The limestone rocks of the Asmari Formation are the most susceptible to dissolution and karstification.

The main factors influencing the permeability of the rocks are the occurrence of joints and fractures due to tectonic movements and this can intensify karstification. Tectonic activities can cause extensive joint systems along water which can flow through the rock mass. The joints play a main role in the development of karstification. These joints constitute a continuous path for movement of mineral waters causing dissolution and karstification.

The most important features are extensional joints caused by high shear stress on bedding planes. These joints constitute a continuous path for water flow and the extension of karstification.

Exploratory drilling results and lugeon tests (dam axis) indicate that the permeability near the fault zones show relatively high values. For example in borehole HM23 and HM12 on the right flank, the average permeability is 6 and 31 lugeon respectively, but in boreholes HM15 and HM16 which are located near the crushed zones the permeability values are very high.

On the left flank in boreholes HM5 and HM22 permeability are 12 and 48 lugeon respectively which indicate moderate to high permeability and for the river section the values are 10 to 23 lugeon.

In general, the permeability conditions of the three units are as follows:

- Upper Asmari between 30 to 74.4 lugeon
- Middle Asmari between 4 to 45 lugeon
- Lower Asmari between < 1 to 19 lugeon

Petrographical analysis and field investigations indicated that the cavities can be divided into two types:

- Cavities due to dissolution and karstification processes (secondary process).

The diameter of the cavities generally vary from 10 - 150 cm and reach tens of metres downstream partly filled by clay minerals and calcite. These cavities have been caused by extensive dissolution of limestone through discontinuity surfaces such as joint sets and bedding planes especially at their intersections (Figure 4.5.6 and Figure 4.5.7.A, B).

- Cavities due to diagenetic processes.

These cavities generally are circular and elliptical shapes with maximum diameter of 10 cm and constitute maximum of 7.5% of total volume of rocks, partly filled by calcite cement. It seems not to have any hydrogeological connection with each other (Figure 4.5.7.B, C).

There is a cavity 30 m long, 7 m width, and 10 m deep 600 m downstream of the anticlinal axis in the Kaffeh Nila Gorge. Recent exploratory drilling (by MG. co., 2007) also indicated a large karst cavity in the lower Asmari unit underneath the river bed which had not been observed during phases 1 and 2 of the investigations. These karst features were caused by extensive dissolution activities of acidic water through the Asmari limestone succession. In general, there are a lot of springs in the area between the dam site and Iron Bridge near the Talkhab Village that are obviously related to fracture systems and enlarged bedding planes due to dissolution. The discharge values vary between less than 1 l/sec for the seasonal springs to a maximum of 140 l/sec for non seasonal springs. The water temperature is 19°-20° and has a constant temperature throughout the year. The hydrochemical analysis of spring water indicates high *calcium sulphate* and *sodium chloride* content.

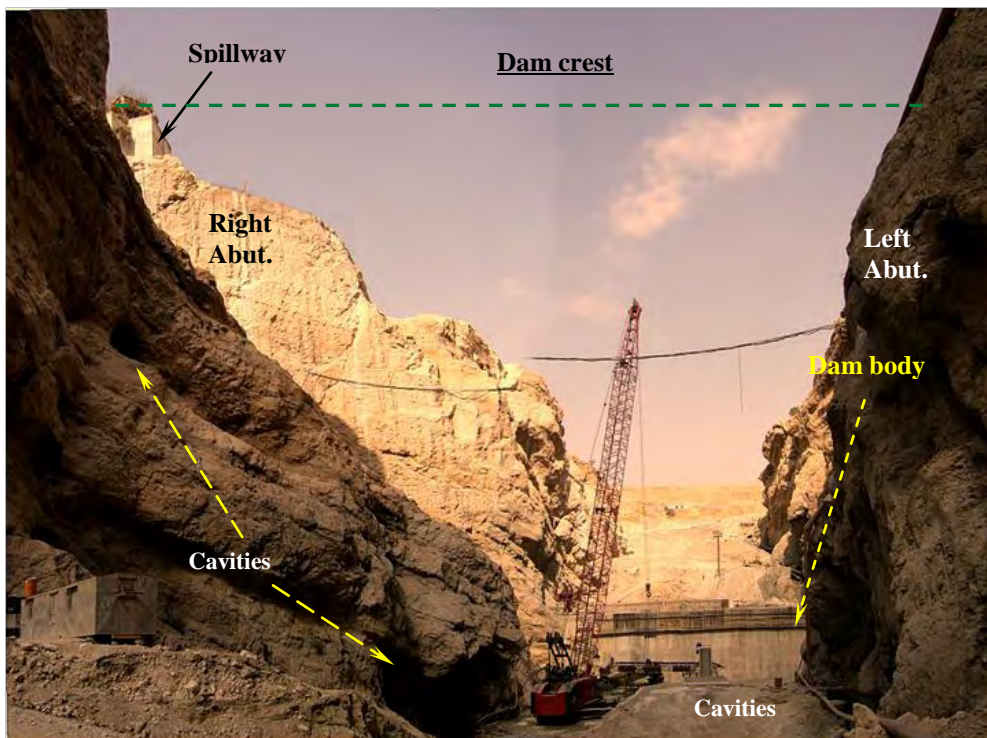


Figure 4.5.6. The large cavities due to dissolution of limestone mainly along bedding planes downstream of the dam axis. These features can be observed high on both flanks of the dam foundation (2007).

Dye tests have been carried out to determine the hydrogeological connection between the Gachsaran and Asmari formations but apparently any dye traces have been observed in the Asmari Formation rocks. The hydrochemical analyses of spring waters in the down stream indicate high calcium sulphate and sodium chloride which imply hydraulic connection between the two formations. Future exploratory investigations to identify the hydrogeological conditions at the dam location and in the reservoir area will be necessary.

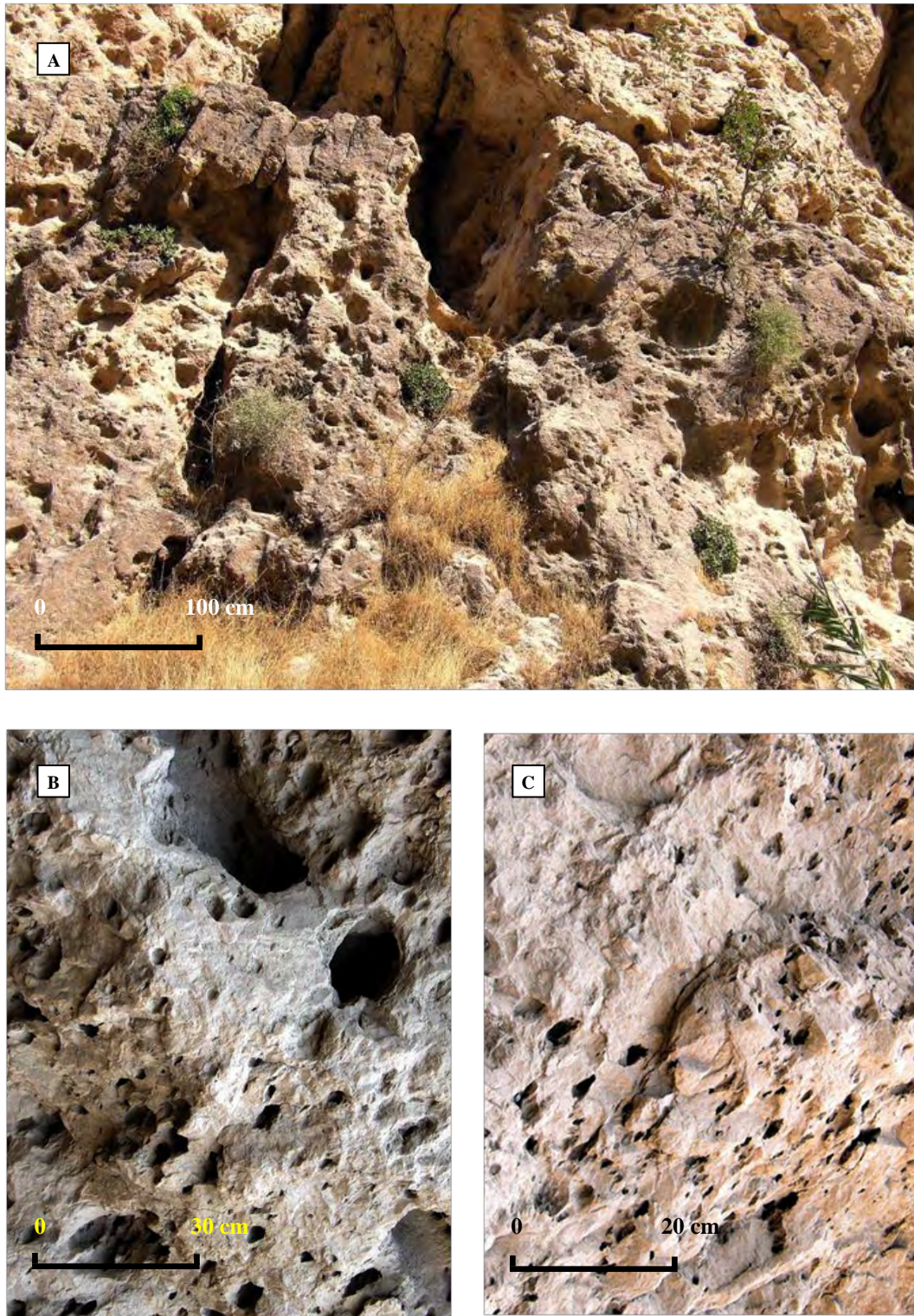


Figure 4.5.7. Some karstic features related to dissolution of limestone through discontinuity surfaces by aggressive water with dimensions from 10 cm to metres (A, B) and cavities related to diagenetic process with small dimensions (B, C).

4.5.4. Tectonic Setting

4.5.4.1. Regional Tectonic

The Seymareh dam site and its reservoir are located in the tectonic province of south-western Iran, the Zagros folded belt (Figure 4.5.8). The dam is constructed on the northern flank of the Ravandi Anticline (Figure 4.5.9) which is an asymmetrical and double plunging fold where the northern flank dips have shallower gradient than the southern one (25° - 30°). The Ravandi Anticline, with a northwest- southeast trend, follows the general trend of the Zagros Mountains. Satellite images indicate variable strike due to tectonic stresses. At the dam axis it is about east- west in the southern part it is $N123^{\circ}E$ and in the northern part the strike changes to $N115^{\circ}E$. The anticline layers comprise the Asmari Formation limestone that dips 25° - 30° northeast at the dam axis. The dip of the bedding planes in the upstream part increases to 50° based on exploratory drilling and in the downstream it gradually decrease and finally reaches to about 0° (horizontal) near the anticline axis. The southern flank of the anticline shows more regular dip at the bedding than the northern flank.

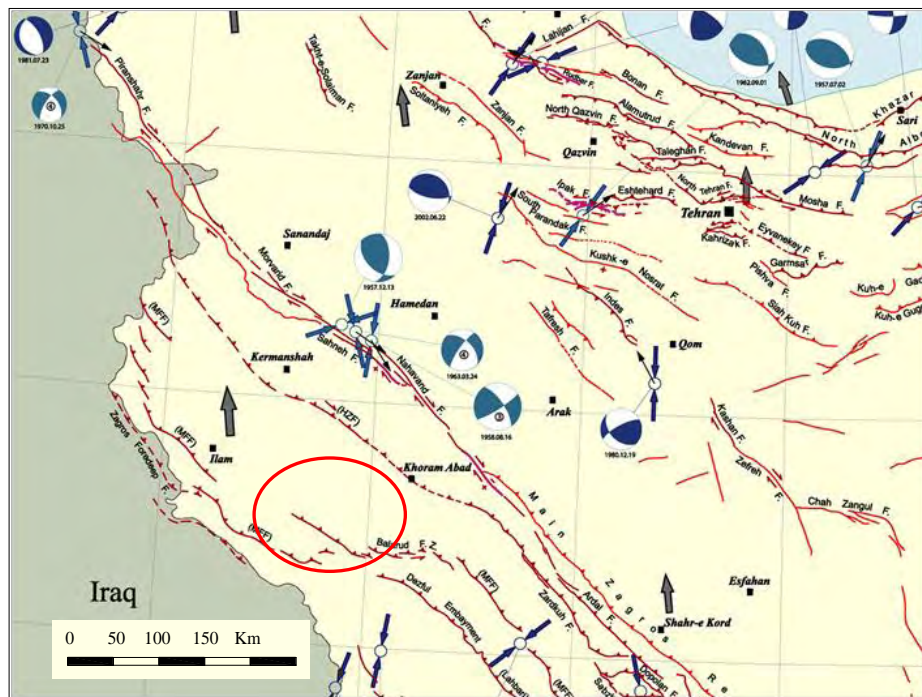


Figure 4.5.8. The major seismically active faults in the study area in the Zagros region. This map shows the distribution of active faults and demonstrates the relationship between the slip vectors and compressive axis obtained from the solution of the focal mechanism of the earthquakes, and GPS velocities (after International Institute of Earthquake Engineering and Seismology- Iran, 2003).

The reservoir area is limited by the Ravandi Anticline on the southern rim and the Manuran Anticline on the northern rim. The Manuran Anticline is also an asymmetrically folded structure which axis follows the Zagros Mountains that are relatively parallel to each other. The azimuth of the Manuran Anticline axis is about $N104^{\circ}E$. The other important fold structure which is situated between the two main folds is the Bunch Har Anticline with axis trending $N107^{\circ}E$.

Related to these fold structures, are parasitic folding due to compressional stresses in syncline between the two fold structures. The Fars Group, especially the Gachsaran Formation with

plastic and soluble characteristics was extensively subjected to small scale folding and faulting. This cause a major problem for watertightness in the reservoir.

4.5.4.2. Small Scale Faults and Direction of Principal Stresses at the Seymareh Dam site

A total of 16 faults have been recognized at the dam site. They are generally classified as reverse and normal faults. The reverse faults are mainly situated at the dam axis and the normal types are mainly in the area around the anticline axis. Due to compressional stress, which is the main factor causing the reverse faults, an extensional area is created at the top of the anticline and the normal faults took place due to gravity processes (Figure 4.5.10).

The identified faults can be divided into two groups;

a) Vertical to very steep faults

These faults with small displacements of between 0.5 to 1 m are mostly observed in the area between the anticline axis and dam axis. These faults have not significantly influenced the geomorphology of the area due to small displacements and constitute the small scale *key stone graben* in the area around the anticline axis. The structures were caused by gravitational processes (Figures 4.5.9 and 4.5.10).

The only fault, F10, with a brecciated zone of 0.5 to 2 m wide occurs at the dam axis.

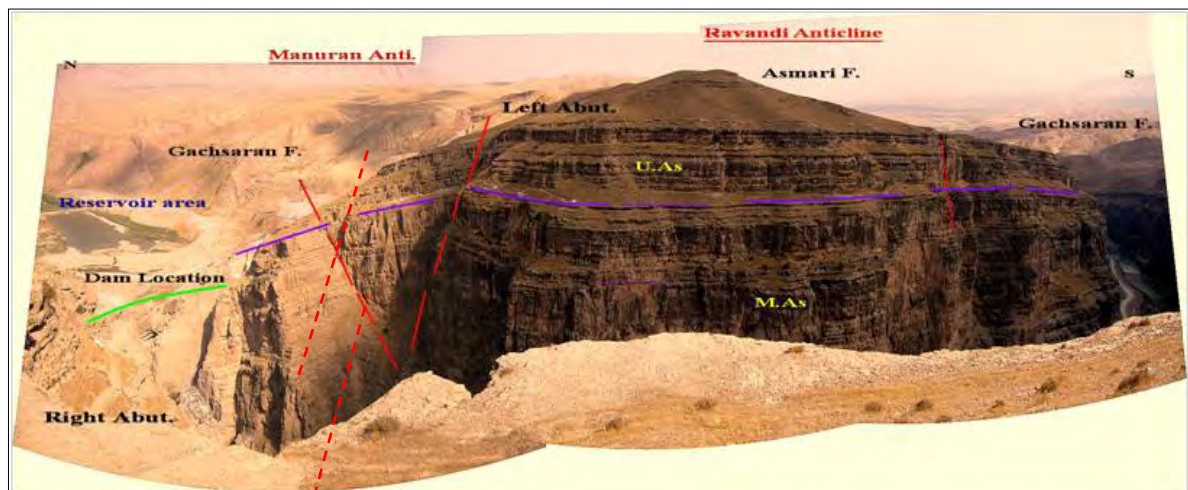


Figure 4.5.9. Panoramic view of the Seymareh river valley at the Ravandi Anticline with the Seymareh dam location on the northern flank of the anticline. The reservoir with 3 215 million cubic metres volume and upstream cofferdam as well as the Manuran Anticline are also shows.

All faults have a trend of between W-E to N-S. In some places faults have displacements of 20 to 30 cm.

b) Oblique faults

These faults with 45° to 70° dip are commonly reverse faults and can be observed around the dam axis (Faults no. F10, F7, F4 and F1) with dips of 70° , 45° , 65° and 45° respectively. Their strike is relatively parallel to the bedding planes (Figure 4.5.11). These faults with small displacements also appear toward the anticline axis and generally belong to the extensional- gravitational processes (normal faults).



Figure 4.5.10. Small scale normal faults (key stone graben) on the right side of the Seymareh River valley. These structures occur in the area around the anticline axis where extensional area was created at the top, then followed by vertical displacement of blocks due to gravity.

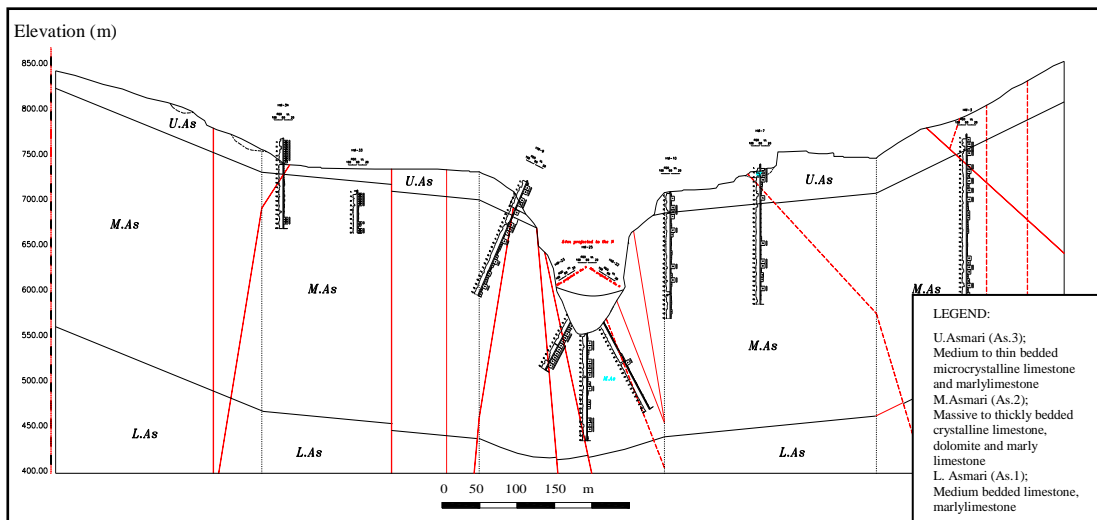


Figure 4.5.11. The engineering geological cross section of the Asmari Formation along the dam axis. The Asmari limestone units were subjected to faulting and folding due to compressional stresses. The faults are mainly reverse faults with small displacements. The exploratory boreholes BH5, BH7, BH9, BH10, BH33 and BH34 indicate the RQD and permeability values of the rock mass (after MG co., 2009).

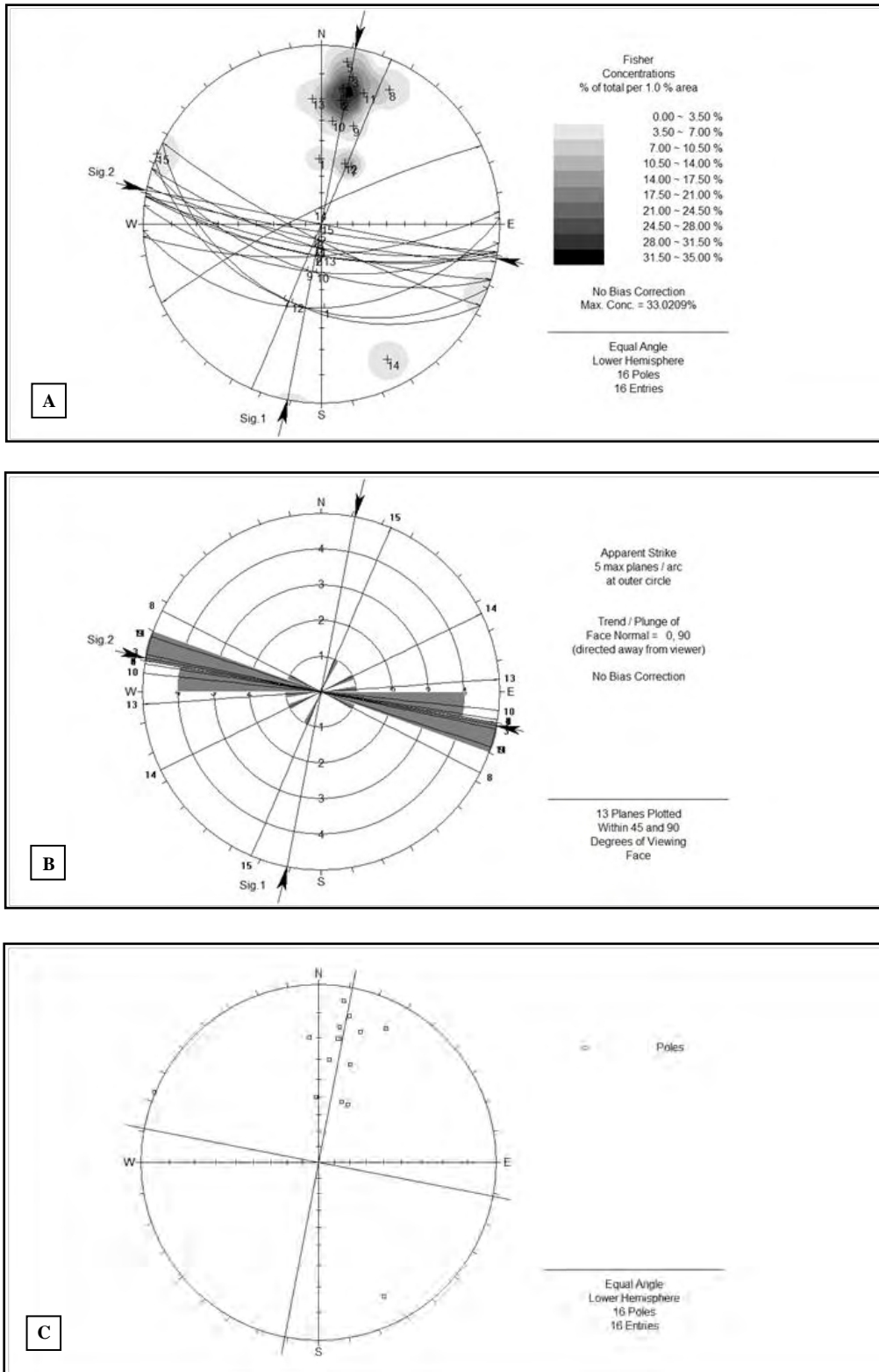


Figure 4.5.12. Stereographic projection of faults (general orientation of small- scale faults) at the two abutments of dam site A- Contour plot, B- Rosette plot, and C- Pole plot of faults with field stress directions (Dips©, equal area projection-Schmidt net, lower hemisphere).

Figure 4.5.11 shows the engineering and structural geology at the dam axis. The three units of the Asmari Formation are completely influenced by the 14 faults with hidden faults which are covered by relatively thick river alluvium deposits (~50 m). In Figure 4.4.12 the stereographic projection of faults including contour plot, rosette plot and scatter plot in Dips©. These plots are based on the poles concentration. The field stress in 2D, are identified as follows (Figure 4.5.13):

- σ_1 : 191°/ 0.0° (*max. principal stress*)
 σ_2 : 281°/ 0.0° (*intermediate principal stress*)
 σ_3 : 0.0°/ 90° (*min. principal stress*)

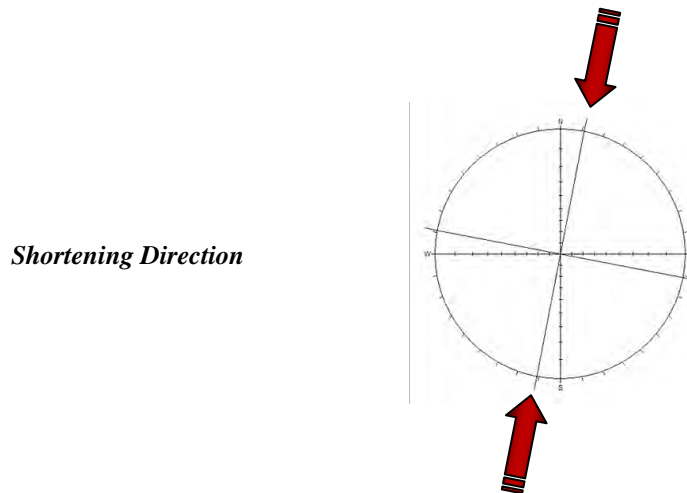


Figure 4.5.13. The direction of σ_1 / Shortening at Seymareh dam site.

4.5.4.3. Joint Study

A total of 89 joints from the two abutments of dam the have been measured and presented contour plot, rosette plot and pole plot of joints (Figure 4.5.14). Based on the stereographic projection of joints in Figure 4.5.14 excluding the bedding planes another three joint sets can be identified at the dam location were Js.1, Js.2 the main joint sets and the Js.3 is an accessory joint set.

The bedding planes and joint sets have the following orientations:

- Js.1 170°- 175°/ 65°- 75°
- Js.2 270°- 275°/ 80°- 90°
- Js.3 120°- 130°/ 70°- 80°
- Bedding planes 10°- 20°/ 25°- 35°

The average lengths of the Joint sets are:

- Js.1 More than 10 m
- Js.2 3- 10 m
- Js.3 1- 3 m

The discontinuity surfaces are rough and wavy with apertures of less than 2 mm. Discontinuity fillings are mostly calcite, clay minerals and rare detrital materials but in some places joints without any fill materials can be observed. Iron oxides commonly stain

discontinuity surfaces without any fill. The spacing of Js.1, Js.2 and Js.3 are 55, 65 and 140 cm respectively.

It can be assumed that the joints Js.1 and Js.2 are extensional with Js.3 a shear joint if the orientation of the anticlinal axes and field stress directions are taken into account. The azimuth of Js.1 is parallel and the Js.2 perpendicular to the anticline axis.

An important technical problem is the instability of rock blocks from upper Asmari unit on the northern flank of the Ravandi Anticline around the dam location. At an elevation between 620 to 800 m, there is an area of 250 m x 300 m which is covered by unstable blocks due to the intersection of Js.1, Js.2 and bedding planes on the left flank (200 m east of the dam axis). On the basis of the stereographic projection of joint sets (Figure 4.5.15), the bedding planes will be the main rock sliding surface for all blocks, if failure takes place (planar failure). The thickness of the sliding zone is estimated to be 20 to 25 m.

Such blocks formed by the same structures can be observed on the right side of the northern flank of the Ravandi Anticline. The satellite image of the dam site (Figures 4.5.1 and 4.5.2) shows a sudden change in the river flow direction from northwest- southeast ($N120^{\circ}E$) parallel with anticline axis, to northeast-southwest ($N56^{\circ}E$), which constitutes a sharp river meander about 500 to 600 m from the dam location. This structure was most probably caused by a huge landslide of the right flank in historic times (exploratory drilling investigation indicates 4.5 m slope wash debris including fine materials to angular boulders of limestone and rockfall debris underlie 28 m silty clay of lacustrine deposits).

Consideration of structural evidence mentioned above and seismic data, the sliding phenomena is expected on the northern flank of the anticline where the inlets of the diversion tunnels and hydropower tunnel structures may be at risk. Water overtopping due to a huge landslide after impoundment should also be considered.

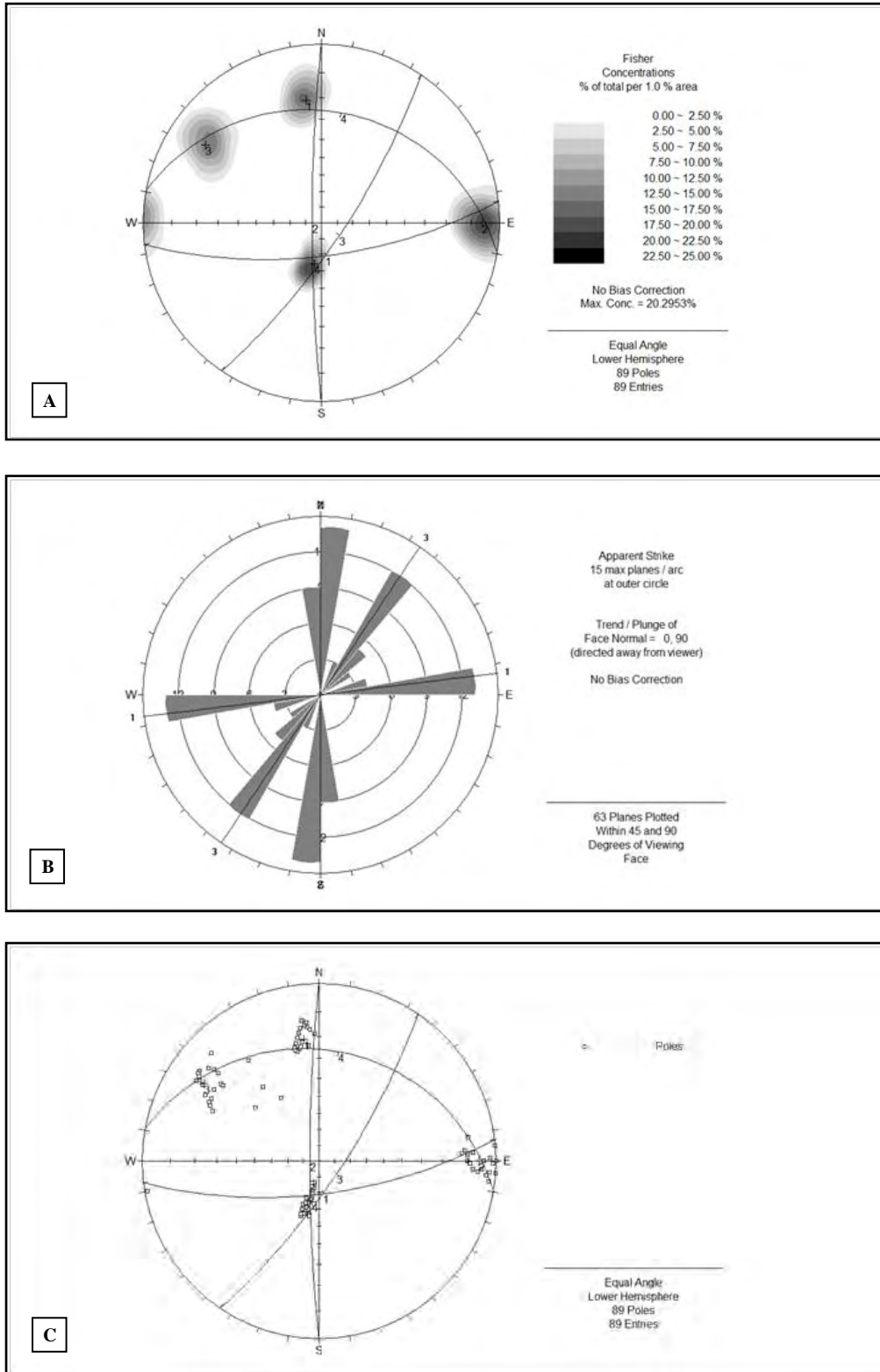


Figure 4.5.14. Stereographic projection of joints (discontinuities distribution) at Seymareh dam site A- Contour plot, B- Rosette plot, and C- Pole plot of joints (Dips©, equal area projection-Schmidt net, lower hemisphere).

4.6. Geology of the Salman Farsi Dam and Power plant

The Salman Farsi dam project is located at the entrance of the Karzin Gorge in the Ghareh Agahaj River, about 140 km south of Shiraz city and 12 km northeast of Ghir Town in the so called folded foothills belt of the Zagros Mountains. This tectonic province in southern Iran is characterized by a simple folded sedimentary sequence, of which only post Permian and younger than Oligocene to Pliocene rocks are exposed (Figure 4.6.1).

In the project area, the stratigraphic sequences are of the upper Cretaceous to the Present. The dam foundation rocks are of the Asmari Formation of the Oligomiocene and generally comprise limestone, marly limestone, dolomitic limestone and marlstone.



Figure 4.6.1. Satellite image of the Salman Farsi dam site and surrounding area on the northern flank of the Changel Anticline (Google Earth, European Technology 2006).

The dam with a gated spillway is 125 m high and has a capacity of 1 400 million m³. The spillway contains three main bays with eight combined radial gates, ending in a ski jump (Figure 4.6.2).

Other structures consist of upstream and downstream cofferdams and a diversion tunnel in the left flank. The cofferdams are earth and rockfill structures and the diversion tunnel is about 375 m long and 15 m in diameter. The powerhouse contains two small units with a total capacity of 13MW (2×6.5MW) that will generate 50 GWh/year.

4.6.1. Objective and benefits of the project

- a) Generating annually 50 million kWh hydroelectric energy via a 13MW power plant.
- b) Supply water for irrigating 32 000 ha of agricultural lands.
- c) Controlling floods.
- d) Land reclamation

The general technical specifications of the dam project can be observed in Table 4.6.1.



Figure 4.6.2. Salman Farsi (Ghir) dam is a concrete arch gravity dam 125 m high and is under construction on the Ghareh Agahaj River.

Table 4.6.1. Salman Farsi dam and power plant project specifications.

Dam type	Concrete arch gravity
Height from the foundation	125.0 m
Length of the crest	345.0 m
Dam body volume	750,000 m ³
Total volume of the reservoir	1400 million m ³
Power plant type	Ground
Spillway	Gated spillway- eight radial gates combined, ending in a ski jump
Water diversion system	U/S and D/S cofferdam and a diversion tunnel with 375m long and 15m. diameter
Capacity of the power plant	13MW (2 units of 6.5MW)

4.6.2. Bedrock Geology of Project Area

A summary of the principal bedrock formations present in the project area is given in Table 4.6.2. At the project area, a continuous stratigraphic sequence of sediments from the upper Cretaceous period (K) to the Pliocene (N) stage are present with a salt dome of the Hurmoz Formation of Precambrian age intruded to the upper strata (Figure 1.4). The Asmari Formation in the study area is divided into three units: The Asmari Formation divisions are according to their engineering and petrographical properties (Figures 4.6.3 and 4.6.4).

Table 4.6.2. A summary of the principal formations in the project area.

Unit No.	Rock Formation/ Group	Lithology	Age
8	Quaternary deposit	River alluvium, colluvium deposits	Quaternary
7	Bakhtiary Formation	conglomerate and sandstone	Plio- Pleistocene
6	Agha Jari Formation	Calcareous sandstone, red marls and siltstone	Late Miocene to Pliocene
5	Mishan Formation	Grey marl and shelly limestone	Early to M.Miocene
4	Razak Formation	Alternating red shale and siltstone with marl and gypsum	Early Miocene
3	Asmari Formation	Cream to brown limestone, marly limestone dolomitic limestone and marl, fossiliferous	OligoMiocene
2	Pabdeh Formations	Cherty, fossiliferous limestone, marly limestone, shale	Late Paleocene to Oligocene
1	Gurpi Formations	Bluish grey marl and shale	Late Cretaceous

The lower Asmari is about 230 m thick and is situated downstream of the dam site and lithologically, comprises regularly bedded fined grained, brown limestone and marls.

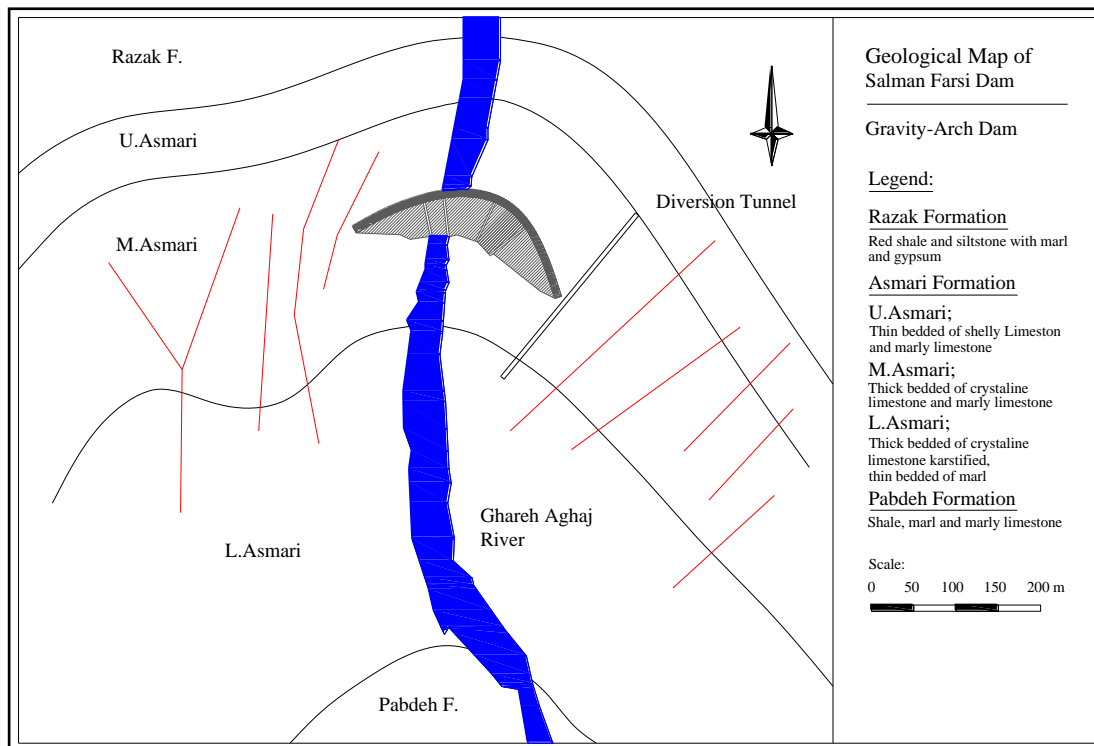


Figure 4.6.3. Simplified geological map of the Salman Farsi dam and power plant project. Several small-scale strike slip faults. (after MG co., 2009).

The middle Asmari comprises 270 m heterogeneous and thickly bedded crystalline limestone, dolomite, and dolomitic limestone with some rare marly limestone interbeds. The dam and grout curtain are situated in this unit. Karst features are well developed.

The upper unit outcrops upstream of the dam axis and form the eastern and western reservoir flanks immediately upstream of the dam site. This unit comprises, alternating thinly bedded limestone, marl and marly limestone with some thin dolomitic limestone and siltstone interbeds. It is less permeable than the Middle and Lower units. The thickness of the unit is about 150 m.

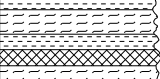
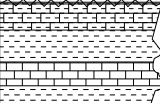
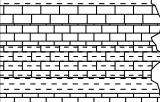
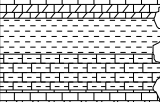
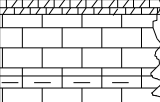
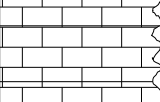
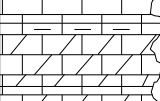

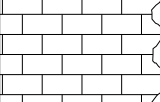
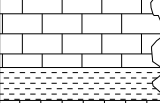
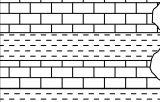
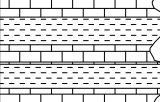
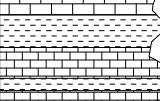
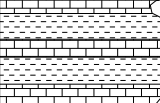
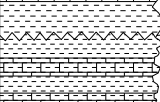
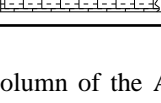
Formation	Thickness	Unit no.	Lithological column	Lithological description	Porosity%
Razak F.	>1000 m			Siltstone and Shales, with few gypsum beds and marls	Reservoir area
ASMARI FORMATION 650.0 m	150.0 m	As.3		Thrust zone Heterogeneous alternating of thinly bedded Shelly Limestone, and marly limestone with Marls and Siltstone Moderate to weak strength	19.40
				Biointrasparite, Grainstone Fossil contents are Archais sp., Miliolide and Pelecypoda shell fragments	1.60
				Dolomitic limestone, marly limestone and marl, Biadolomicrite, Wackstone vuggy and channel porosity, Thinly bedded Fossil contents are Rotalia sp., Miliolides Nummulites sp. Operculina sp.	4.25
				Dolomitic limestone, marly limestone and marl, Biadolomicrite, Wackstone vuggy and channel porosity, Thinly bedded Fossil contents are Rotalia sp., Miliolides Nummulites sp. Operculina sp.	1.50
				Dolomitic limestone, marly limestone and marl, Biadolomicrite, Wackstone vuggy and channel porosity, Thinly bedded Fossil contents are Rotalia sp., Miliolides Nummulites sp. Operculina sp.	7.50
	270.0 m	As.2		Homogeneous and thickly bedded Crystalline limestone, marly limestone Vuggy, intraparticle porosity Intrabiosparite, Grainstone (calcareonite), fossil contents are Peneroplis sp., Miliolides, Textulariidae sp.	4.00
				Echinoid shell and skeletal fragments fine grained cherty limestone Intermediate to high strength	8.00
				Dolomitic limestone and Dolomite Thickly bedded, low karstified Dolopelmicrite, Wackstone Fossil contents are Nummulites sp. Miliolides and Echinoid shell fragments	4.00
				Thick bedded, Hstrength Fine grained crystalline limestone Biopelmicrite, Wackstone-bioclasts are Operculina sp. and Echinoid shell debris Vug, channel, intraparticle porosity	0.30
				Thick bedded, Hstrength Fine grained crystalline limestone Biopelmicrite, Wackstone-bioclasts are Operculina sp. and Echinoid shell debris Vug, channel, intraparticle porosity	3.00
230.0m	As.1		Regularly bedded of fined grained Brown limestone and marls Bionicrite, Wackstone vug and fracture porosity Fossil contents are Operculina sp. and some Planktonic species Ostracoda shell and Echinoid shell fragments	1.00	
			Moderate to High strength Locally strong karstified layer	1.20	
			Thin to v.thin bedded limestone and marl Bionicrite, Packstone to Boundstone vug, channel, fenestral, fracture porosity Fossil contents are Foraminifera: Operculina sp., Heterostegina sp. Rotalia sp., Echinoid shell and spines calcareous Red Algae, Bryozoon such as Onychocella sp.	1.90	
			Thin to v.thin bedded limestone and marl Bionicrite, Packstone to Boundstone vug, channel, fenestral, fracture porosity Fossil contents are Foraminifera: Operculina sp., Heterostegina sp. Rotalia sp., Echinoid shell and spines calcareous Red Algae, Bryozoon such as Onychocella sp.	1.00	
			Thin to v.thin bedded limestone and marl Bionicrite, Packstone to Boundstone vug, channel, fenestral, fracture porosity Fossil contents are Foraminifera: Operculina sp., Heterostegina sp. Rotalia sp., Echinoid shell and spines calcareous Red Algae, Bryozoon such as Onychocella sp.	5.60	
Pabdeh Fm.			Fossiliferous limestone passing into shale interbedded with thinly bedded marly limestone	Impervious	

Figure 4.6.4. Lithological column of the Asmari Formation and petrographic analysis interpretations at Salman Farsi (Ghir) dam.

4.6.3. Hydrogeological Characteristic of the Dam Location

4.6.3.1. Karst Features and Porosity

Most of the rocks exposed at the dam site show secondary porosity such as vuggy, channel, cavern and fracture features. The bedding planes and other discontinuities are also enlarged by dissolution of limestone and well developed karstification especially in the middle unit of the Asmari Formation rocks (Figure 4.6.5). Primary porosity due to an incomplete diagenetic recrystallization and compaction can also be observed locally. Based on field observations and petrographical studies the lower unit has isolated cavities and the porosity reaches a maximum of 5.6% locally (lower most part of the unit).

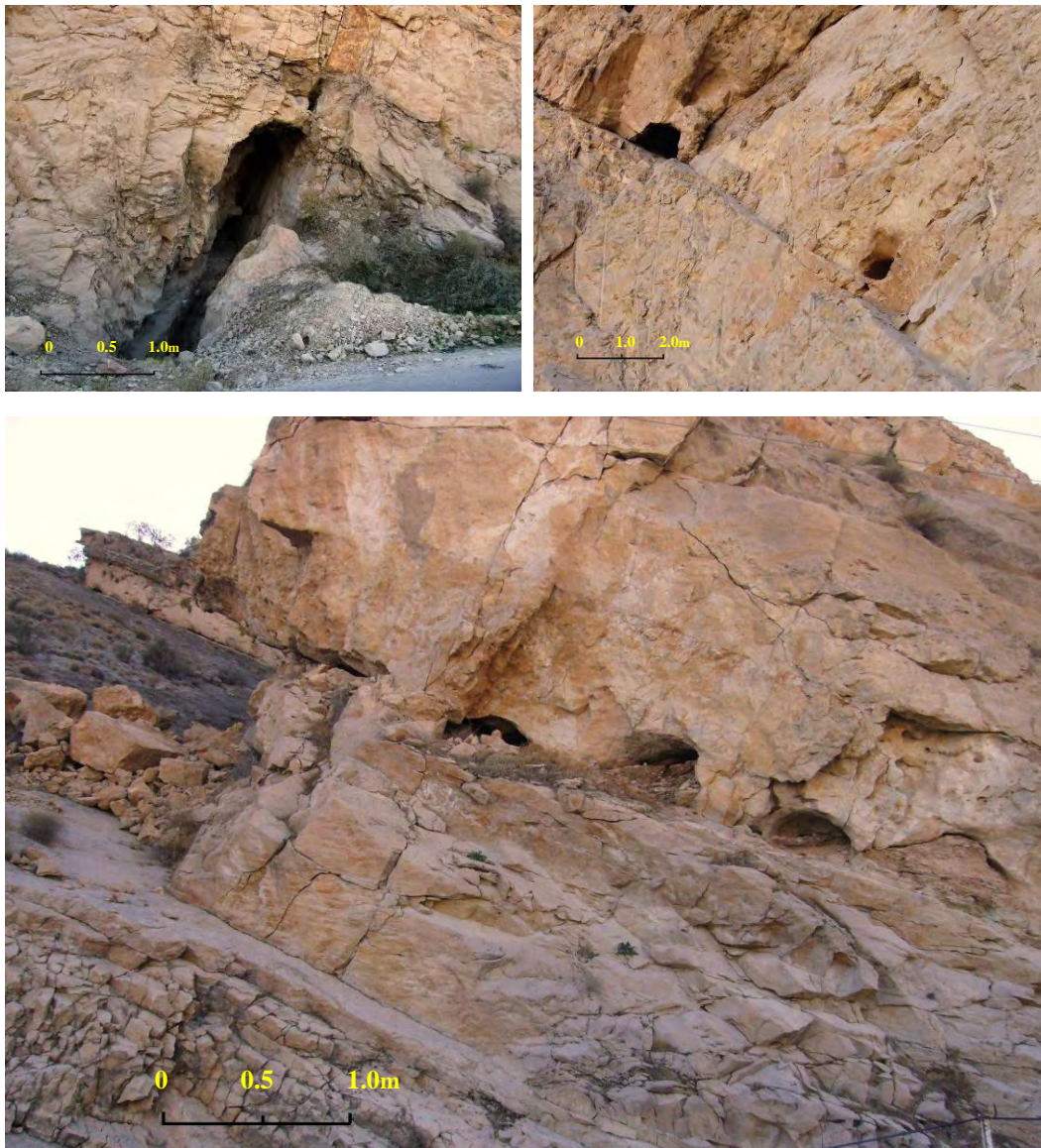


Figure 4.6.5. Some karstic features due to dissolution of limestone along discontinuity surfaces in the upper part of the middle unit of the Asmari Formation. These features constitute a 3D network of channels, which somewhere converge into huge caverns.

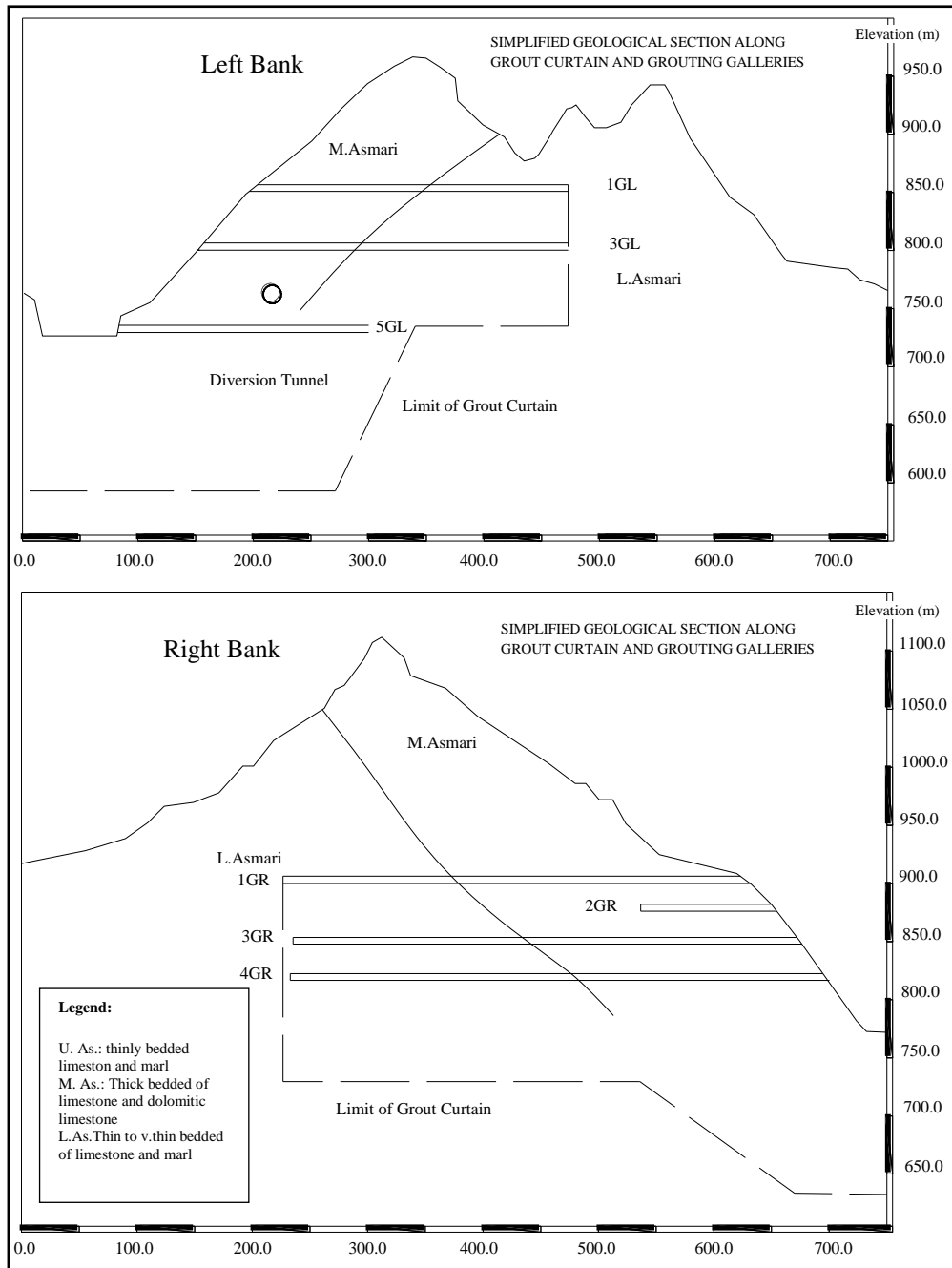


Figure 4.6.6. The engineering geological section of the Asmari Formation at the right and left flanks of the Salman Farsi dam. The exploration and grouting galleries, limit of cut-off curtain and section of diversion tunnel can be observed (after MG co., 2009).

In the middle unit, karstification is well developed with the largest karst zones present in the upper part of the unit, whereas karst features are seldom seen in the lower part. The petrographic analyses show the general porosity reaching a maximum of 8.0% in the upper part of the unit. Chimneys and karsts are extensively developed on the intersection of bedding planes and joints and are due to water dissolution (Figure 4.6.5).

Except for the lower most part of the unit, the karst features in the upper unit are restricted. The porosity comprises very small cavities that follow the limestone bedding planes and joints. In the upper most part of the unit where the Asmari Formation locally is thrust on to the Razak Formation, the crushed zone shows high porosity that was gradually increased due

to infiltrating meteoric water (epigenic karst) and hydrothermal waters (hypogenic karst) (Klimchouk, 2007).

Three factors caused the development of karst; the lithology, distribution of rock type, and the occurrence of discontinuities. From the lithological point of view, there is a general tendency for strong dissolution of the porous, vuggy, micritic limestone compared to the more resistant, less porous, recrystallized, finely to medium-grained calcarenite. Fossiliferous and finely grained cherty limestone of the middle unit is rarely showing weathering, whereas marls and marly limestones are impervious. Observations through exploration galleries clearly show that the cavities are initiated at the intersections of the bedding and joints and enlarged along the bedding planes.

The general shape of the karst features results in metres long oblate chimneys of several decimetre diameter following the steeply dipping bedding in the middle unit. It has been suggested that the karst in the middle unit, is a mature system (JV. Stucky/Electrowatt., 1992, Koleini et al., 2012), generated during a period of strong hydrothermal activity (hypogenic karst), because signs of highly mineralized former ground water circulation are common. This hypothesis may be supported by the presence of hot springs and suggests that the karst should also have developed in depth. The field observations show about 24 springs present at the dam site of which 11 springs are hot water springs with temperatures of 30°- 40°.

In general, it is possible to zone the units into three principal zones correlating with the stratigraphy. The upper zone of the Asmari Formation comprises a very heterogeneous alternation of thinly bedded limestones with marls and siltstones resulting in a fairly impervious rock mass of moderate to weak rocks.

The central zone is more homogeneous and thickly bedded. Characteristic lithology are the vuggy, porous limestone. The rock strength is generally intermediate to high and karst features are well developed (Figure 4.6.6).

Finally, the lower zone of the Asmari Formation is characterized by a very regularly bedded, fine grained brown limestone at the top, very thickly bedded cherty limestone in the centre and an extremely regularly alternation of thinly bedded limestone with thin marly beds at the base. The strength is moderate to high and the permeability is low, but locally strong karstified layers have been observed.

4.6.3.2. Speleological Reconnaissance

The exact identification of the three dimensional cavern developments is key to the final decision on how to plug or to circumvent the karst systems in the most economical and most efficient way, and how to incorporate the plugging of these structures into the grout curtain. For this reason, all detected caverns have to be speleologically investigated as well as geologically surveyed.

During the excavation of adits and grout galleries, seven large caverns were discovered. The two largest are Golshani's Cave, GG 802 on the right flank and Saidi Cave, GG 835 in the left flank (Figures 4.6.7, 4.6.8 and 4.6.9). Golshani's cave (150 000 m³, Fazeli, 2007) was investigated from elevation 802 m down to elevation 740 m. The bedding planes and joint set Js1 are the main discontinuities in this cave. It is obvious that several channels that belong to this cavern extended above 802 m and others below 740 m. The vertical dimension of the cavern is more than 70 m and horizontally more than 40 m. The origin of Saidi Cave was caused by different discontinuities, although joint system Js.1 played a primary role.



Figure 4.6.7. Several channels related to cavern development in the right flank. The bedding planes and Js.1 are mainly responsible for cave development.

4.6.3.3. *Permeability at the Dam site*

Permeability values between 1.2×10^{-4} - 1.2×10^{-6} cm/s, represents very low fractured and very low permeable rocks, from 1.2×10^{-3} - 1.2×10^{-4} indicate low fractured and low permeable rocks, and permeabilities from 1.2×10^{-2} - 1.2×10^{-3} cm/s, indicate permeable but low karstified rocks. Only the range from 1.2×10^{-1} - 1.2×10^{-2} cm/s, indicate karstified or strongly karstified rocks. The permeability of intensively karstified and fractured rocks is usually more than 1.2×10^{-1} cm/s (MG.co, 1993).

Consequently, from a leakage point of view, it is obvious that a rock mass with a permeability of more than 1.2×10^{-3} cm/s plays a key role, but permeability of more than 1.2×10^{-2} cm/s has a decisive influence on the successful design of the anti seepage treatment.

Based on the borehole logs and Lugeon tests only, the rock mass at the dam site appears not to be highly karstified. Some Lugeon tests do indicate the presence of karstification, but during the drilling program, no karst voids were encountered. This fact was surprising. There is a pronounced anisotropy in the permeability due to steep and subvertical discontinuities, which display different Lugeon values for vertical and inclined boreholes.

The hydrogeological features at the dam site are the consequence of the regional geological setting. The impervious and compressed anticline core seems to be a barrier for underground water filtration from the upper erosion base levels to the lower steps. A number of springs (phreatic water as well as thermal water) discharge along the gorge section upstream of the barrier.

Apparently, there is no hydrogeological possibility for the underground water to penetrate downstream. Water movement towards the regional base level (Ghir Plain) has been interrupted by a deep long and wide hydrogeological barrier consisting of the Pabdeh and partially of the Lower Asmari Formations.

Under these circumstances, the bottom of the gorge is a local, but the only active erosion base for all upstream waters. The rapid post- Pliocene uplift (one mm/year) caused a rapid fluvial

process where the bottom of the Karzin gorge is cut by rapid fast fluvial erosion perpendicular to the anticline axis.

Well developed subvertical fracture systems, together with frequent and steep joint systems along with the bedding planes created a fully connected network for preferential filtration of water. i.e. the limestone rock mass is fully exposed to karstification processes. The karst aquifer is in constant adjustment to the level of the gorge bottom. As the discharge zone became progressively lowered, the hydraulic gradients towards the gorge bottom increased. Consequently, turbulent underground flows eroded the walls of initial karst conduits producing the large channels and caverns.

The karst features could only develop up to the gorge (limestone bedrock), i.e., approximately to elevation 740 - 735 m. This is the real base of the karstification in the gorge area. Therefore, it has to be assumed that down to elevation 735 m karst conduits exist. Theoretically, a siphonal circulation of phreatic water could provoke karstification deeper than the erosion base level, but in the Karzin gorge there is apparently no evidence for such a process. Deeper karstification can also be the consequence of upward hot water flows. As referred to before, the limestone ridges on either side of the dam site are subparallel systems of vertical and subvertical discontinuities (shears, faults), running across the axis of the Chngal Anticline. Karstic features developed along these discontinuities and along the steeply dipping bedding planes. They can possibly provide a direct hydraulic connection between the reservoir and the gorge downstream of the dam, i.e., there is the possibility of substantial seepage from the reservoir bypassing the dam. Thus, the grout curtain has to be placed in such a way to intersect these discontinuities.

Generally, the hydrogeological anisotropy is one of the important characteristics of the dam site. Karst porosity dominates in the upper part of the Middle Asmari limestone unit as referred to before. A number of karst channels have been discovered in the rock mass from reservoir elevation (855 m), down to this level. Most frequently, karst chimneys with apertures from a few centimetres to a few metres have been detected. In addition, large caves with volumes of thousands of cubic metres have been discovered on both valley sides. The volume of the largest one found on the right flank (Golshani Cave) is 150 000 m³ (Figure 4.6.8 and 4.6.9). These large caves are partially filled with huge limestone blocks with some blocks more than 10 m³ in size.

The exact depth of the Karstic features is uncertain but the speleological investigations are not finalized yet. According to the thermal field, measured in only one deep hole drilled from river level, permeability due to karstification is indicated only at elevation 690 m- 710 m. In the same hole the permeability tests show more than 100 Lu at elevation 725 m. Some negligible peaks at elevations 620 m and 590 m of less than 10 Lu are too small to be interpreted as due to karstification.

The geophysical logs did not detect any particularly problematic geological conditions along the boreholes and wells.

In general the Lugeon tests on the dam axis indicate the permeability of the Asmari Formation as follows:

- a) Upper Asmari, fairly impervious
- b) Middle Asmari, very low to very high in the upper part
- c) Lower Asmari, generally low but locally very high

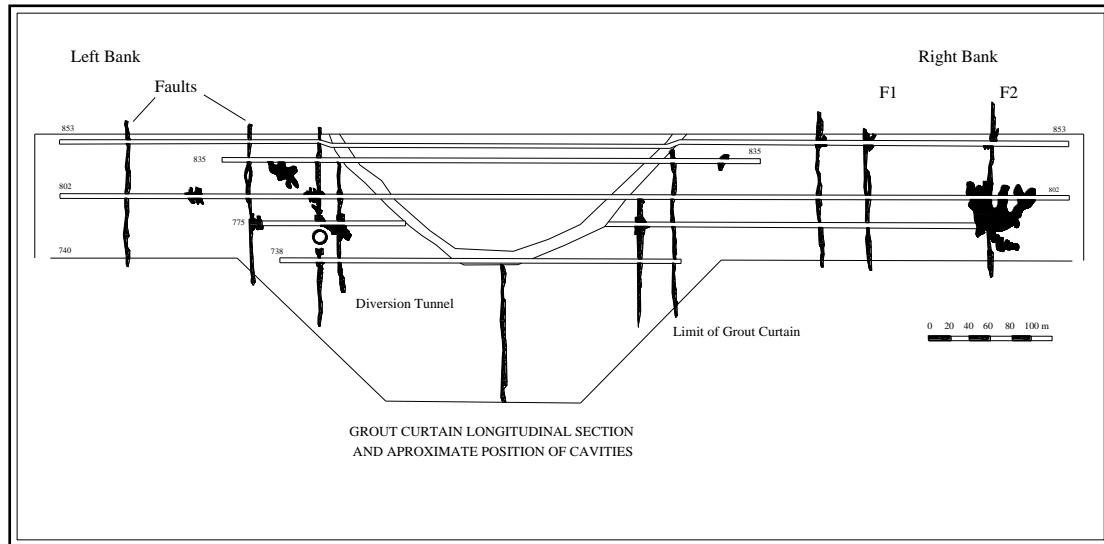


Figure 4.6.8. Schematic presentation of the longitudinal section of the grout curtain and approximate positions of cavities at the Salman Farsi dam (after Stucky-Electrowatt, 2001).

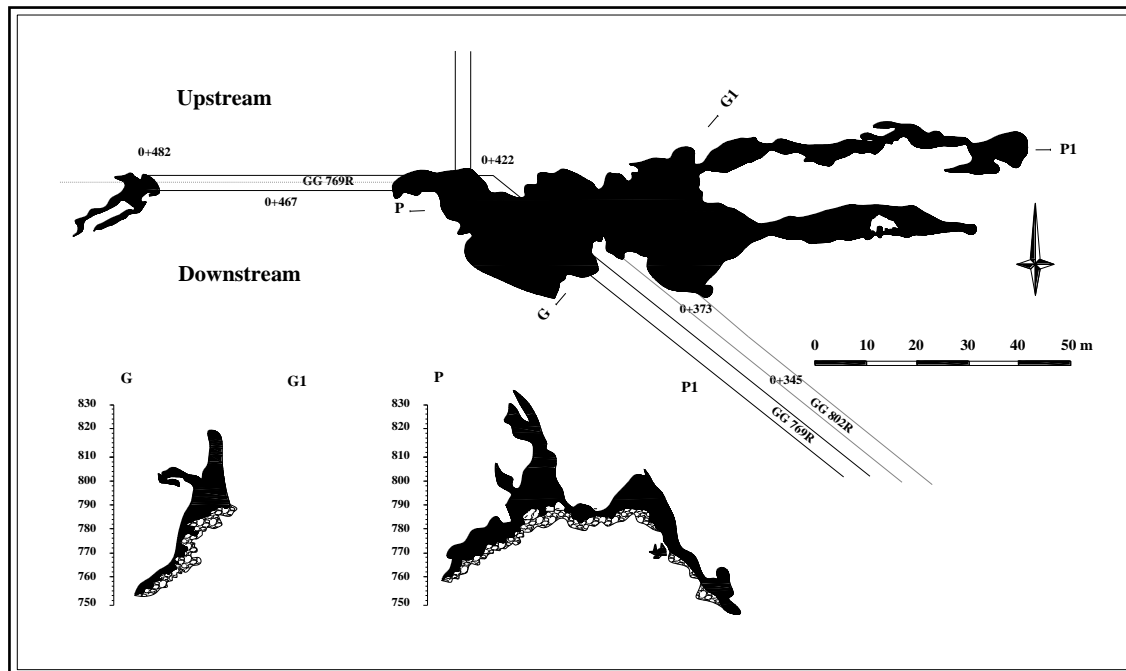


Figure 4.6.9. The geological map and section of Golshani Cave in the right flank of the Salman Farsi dam (after Stucky-Electrowatt, 2001).

4.6.3.4. Reservoir Watertightness

The Salman Farsi reservoir is located in a valley composed of the following generally impermeable formations.

- Razak; red shale, siltstone, marls and gypsum
- Mishan; grey marl and shelly limestone
- Bakhtiary; unconformable deposited massive conglomerate and sandstone.

The reservoir will partially be in contact with the almost impermeable Upper Asmari formation. The youngest sediments in the reservoir are widespread alluvial gravel and terraces (Figure 4.6.10).

Only in a few localities, close to the dam site, will the reservoir water come into direct contact with karstified limestone. In addition, the Yarg Spring area is a questionable location for seepage. In the reservoir area, no drilling investigations have been executed, except for three boreholes in the vicinity of the Yarg Spring.



Figure 4.6.10. The southern part of the reservoir area of the Salman Farsi dam project on the northern limb of the Changal Anticline. The bedrock consists of almost impermeable rock successions of the Fars Group. The Karbasi Anticline, which forms the northeastern boundary of the reservoir can be seen as well (2007).

4.6.4. Tectonic Setting

4.6.4.1. Regional Tectonic

The Salman Farsi dam site and reservoir are situated in the Zagros Mountains tectonic province of southwestern Iran (Figure 4.6.11). The dam is situated on the northern flank of the Changal Anticline (Figure 4.6.10) in the Karzin Gorge which follows the Zagros trend. With regards to the reservoir, the relevant anticlines are Changal, Palang and Karbasi. The axes of these anticlines are parallel to each other. The Karbasi Anticline represents the northern rim and Changal represent the southern rim of the future reservoir.

These folded structures are situated between the reservoir area and the lower erosion base level (Ghir Plain). It is an asymmetrically folded structure, striking generally WNW-ESE and plunges steeply northwards. The fold axis is oriented $295^{\circ}/15^{\circ}$. Related to this fold is a parasitic anticline that is very important for the water tightness of the reservoir on the northwestern part of the dam site (fold axis $285^{\circ}/05^{\circ}$). The Changal Anticline is separated from the Palang Anticline by a very tight northwest plunging syncline.

The dip of the Asmari Limestone layers at the site area is 50° - 60° NNE. The very steep, NE dipping and reverse Dareh Siah Fault cuts the core of the Changal Anticline downstream from the dam site. Genetically, this fault belongs to the folding phase. The Asmari Formation has been thrust on to the Razak Formation in the northwestern part of the site due to the Dareh Siah Fault activity (Figures 4.6.12 and 4.6.13).

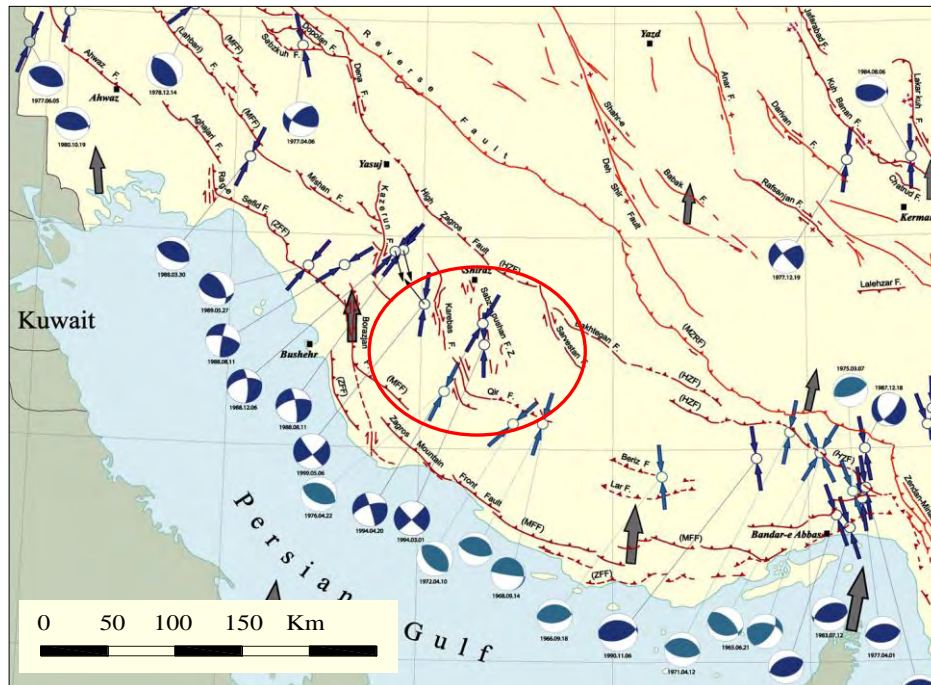


Figure 4.6.11. The major seismically active faults in the study area. The map shows the distribution of active faults and demonstrates the relationship between the slip vectors and compressive axis, obtained from the solution of the focal mechanism of earthquakes, and GPS velocities (International Institute of Earthquake Engineering and Seismology- Iran, 2003).

Due to the presence of the Precambrian Hormus Salt Formation, deduced from the frequent salt domes, the sedimentary pile has been detached from the basement explaining the N-S to NNE-SSW oriented tectonic transport direction and the well exposed sequence of gentle long whale back anticlines separated by strongly folded and sometimes very tight synclines.

The deformation started in the Pliocene as signaled by the unconformable deposition of the fluvial, deltaic Bakhtiary conglomerates on the Agha Jari and Mishan formations, as the erosion products of rising anticlinal hills. The folding continued through the Pleistocene tilting the Bakhtiary beds within the synclines. At the same time high angle thrust faults developed.

At a later tectonic stage, important right-handed strike slip faults developed, cutting and displacing the anticlines by several kilometres. The most important of these structures are from west to east the Karbasi, Sarvestan, Lar and the Bakhtegan Faults. Like in the case of the Karbasi Fault, salt domes are associated with the strike slip portion of these structures, which extend through the entire sedimentary cover, perhaps reaching the basement. These faults accommodated the oblique deformation within the fold belt caused by thrust and slip movements along the Kazerun and Main Zagros faults (Figure 4.6.11).

The present tectonic phase is expressed by strong seismicity. Fault plane solutions and the focal depth of the recent earthquakes indicate that the seismicity is related to northwest

southeast striking high angle reverse faults (dipping NE or SW) of 8 to 20 km depth in the uppermost basement.

The fact that several ductile salt layers are distributed within the sedimentary cover absorbing the deformation, explains the absence of directly related surface faults (Zagros-Type Earthquakes along buried faults). One of these buried seismic trends, based on historical destructive earthquakes in the Ghir area is located about 15 km south-southwest of the dam site. Reactivation of earlier surface discontinuities and sympathetic faulting have also been observed.

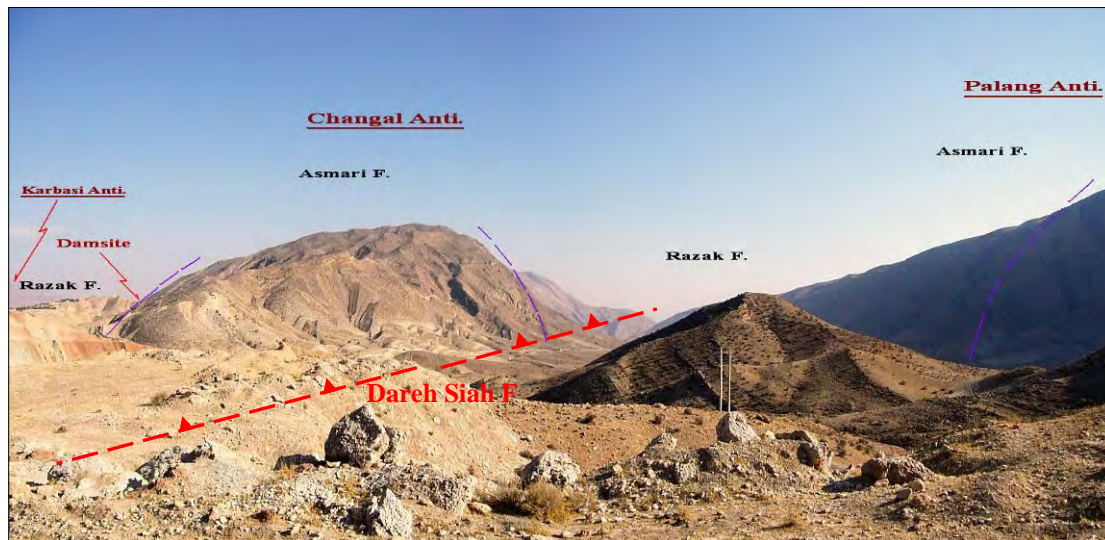


Figure 4.6.12. The Salman Farsi dam site is situated on the northern flank of the Changal Anticline which follows the Zagros trend. The Karbasi Anticline represents the northern rim and the Changal Anticline represents the southern rim of the future reservoir (2007).

4.6.4.2. Large Scale Structures in the Project Area

- a) A small salt dome and a system of left-handed strike slip faults cutting the Kaftar Anticline. The importance of this structure for the seismic hazard has to be verified in the field.
- b) The Karbasi Anticline (Asmari-Jahrum Formation) which borders the northern part of the future reservoir.
- c) A large syncline in the reservoir area created by disharmonic, strongly folded Pliocene to Pleistocene rocks (Razak, Mishan, and Bakhtiary formations) and Quaternary cemented mainly gravely alluvium. The syncline is bordered to the northwest by the two arms of the southeast plunging limestones of the Naura Anticline. The Ghareh Agahaj River flows in the axial depression of the syncline.
- d) The Changal Anticline which rims the reservoir to the south. Related to this fold is a parasitic fold which is very important for the water tightness of the reservoir and which has been mapped northwest of the dam site.
- e) The Dareh Siah Fault cutting the core of the Changal Anticline (Figures 4.6.12 and 4.6.13).
- f) A very tight northwest plunging syncline separating the Changal Anticline from the Palang Anticline.

- g) The South Dashte Ghir Fault to the south of the large Ghir plain. The seismotectonic importance of this high angle reverse fault has already been discussed.



Figure 4.6.13. The Dareh Siah Thrust Fault cuts the core of the Changal Anticline then continues to the northwest of the dam site and caused the Asmari Formation thrust on to the Razak evaporites Formation.

4.6.4.3. Joint Study and Direction of Principal Stresses at the Salman Farsi Dam site

Apart from the bedding planes of sedimentary origin, six different kinds of discontinuities (small-scale faults and joints) which reduce the quality of the rock mass and decrease the slope stability rate can be identified at the dam site.

The stereographic projections of discontinuities including a Contour plot, Rosette plot and Pole plot (Dips©) are shown in Figure 4.6.14. The principal sets of discontinuities are Js.1, Js.2, Js.3 and Bp. (bedding plane). Two less important of the discontinuity sets that are accessory joint sets are Js.4 and Js.5.

Bedding planes are the most evident feature forming structures spaced 0.4 to 1.2 m in the limestone, 0.1 to 0.6 m in the marly limestone and less than 5 cm in the marlstone, and also represent the preferred detachment surface according to the mechanical competence contrast of the rock wall.

Small-scale faults of maximum 10 m length and 2 m displacement can be observed in the upper unit of the Asmari Formation. The discontinuity apertures are from mm to cm and filled by small fault breccia not washed out by erosion. In the central and lower units, the faults are mostly left-handed, less frequent but longer. On the right bank a very clearly visible structure can be observed about 100 m west of the dam, displacing the beds of the middle unit about 1m. The fault surface is rough, the opening very small and the wall rock fractured. This structure is more than 100 m long and may extend the same distance downwards, but is covered by colluvial deposits.

On the left flank, a fault has been followed from the outlet of the diversion tunnel up to the ridge. The displacement varies from few centimetres to 1.5 m. The aperture is few centimetres, washed out in the upper parts and filled by fault breccia at lower levels where a

hot water spring occurs. The general orientations of the faults coincide with joint systems Js.1 and Js.2. The stereographic projections of faults are indicated in Figure 4.6.15.

Joint system Js.1, Js.2 and Js.3 dips very steep. These discontinuities often rough surfaces are closed without filling with spacing between 0.5 and 3 m. Joints on the left flank are uniformly oriented and generally belong to system Js.2 but on the right flank the distribution is more scattered. The distribution of discontinuities according to the rock units and abutment side is shown in Figure 4.6.14. Flat lying joints have been exclusively measured in the upper units of the right flank.

The bedding planes on the left abutment are very uniformly orientated and are mainly of system Js.2. The joint distribution on the right abutment shows Js.1 and Js.2 almost present in equal density.

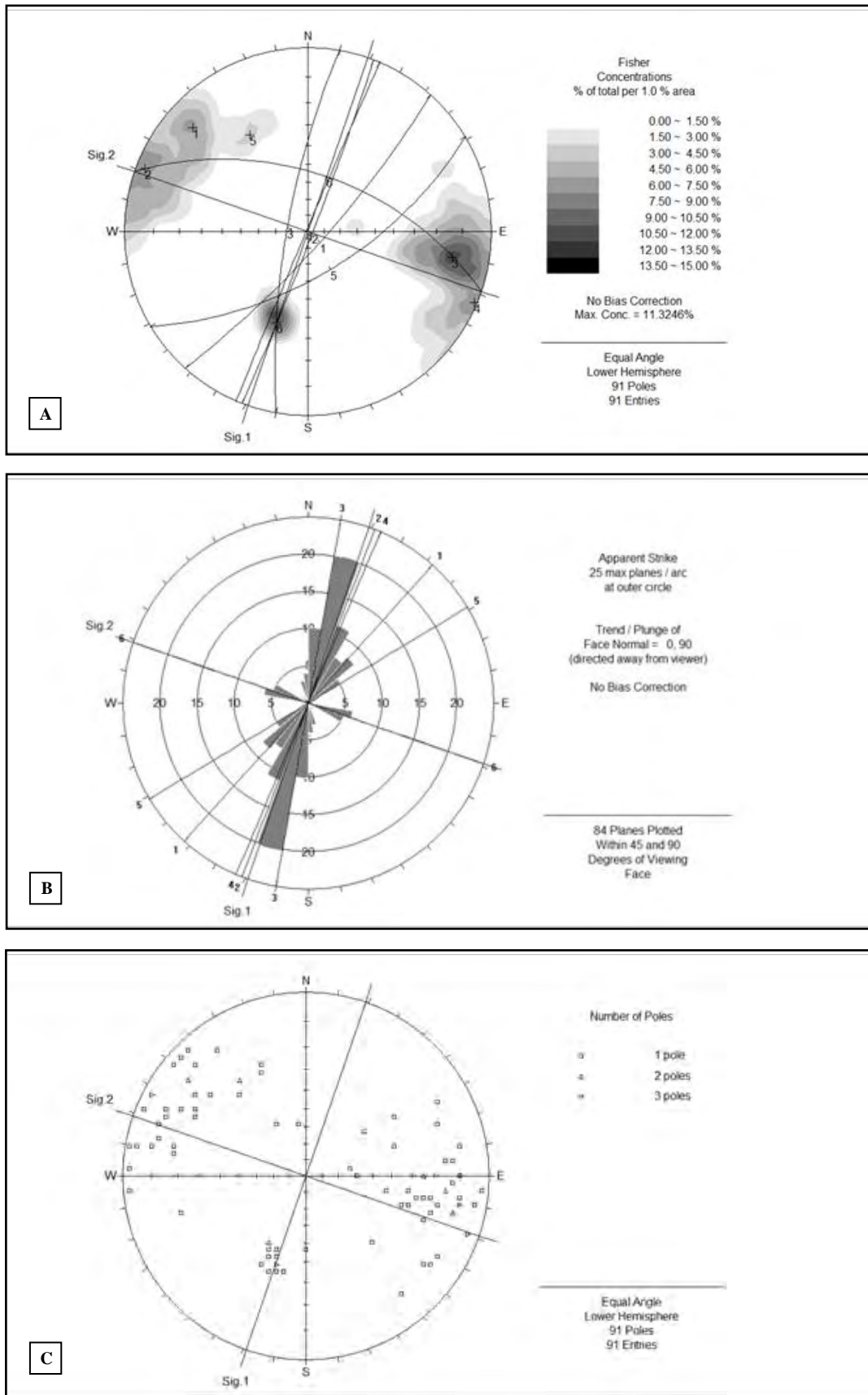


Figure 4.6.14. Stereographic projection of joints (discontinuity distribution) of the Salman Farsi dam foundation rocks. A- Contour plot, B- Rosette plot, and C- Scatter plot of joints (Dips©, equal area projection-Schmidt net, lower hemisphere).

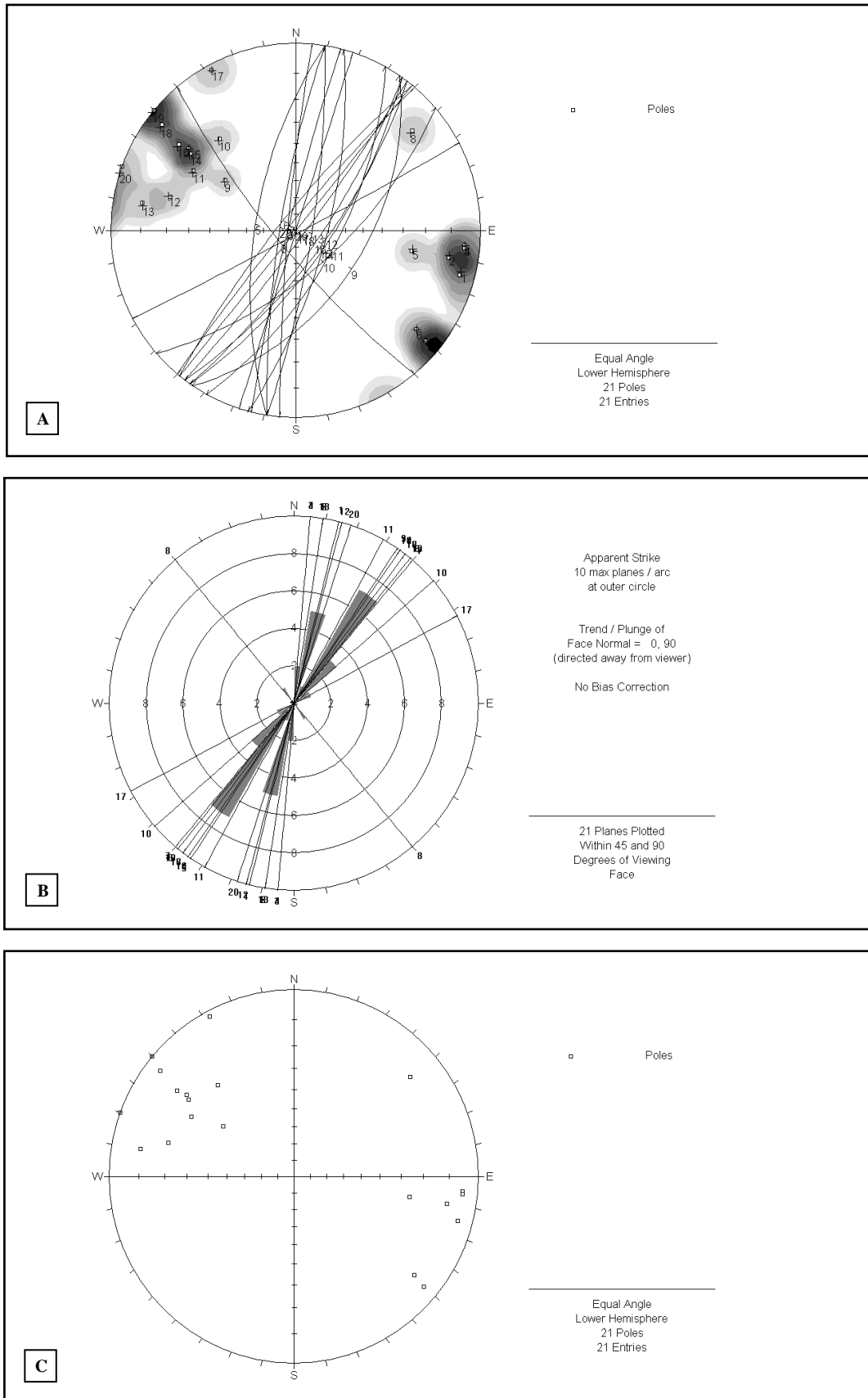


Figure 4.6.15. Stereographic projection of faults (general orientation of small-scale faults) at the two abutments of the dam site A- Contour plot, B- Rosette plot, and C- Scatter plot of faults (Dips $^{\circ}$, equal area projection-Schmidt net, lower hemisphere).

The bedding planes have a more scattered distribution. Figure 4.6.16 represents the calculated main great circle orientations of the major joint systems and bedding planes and their intersections on both sides of the dam foundation. The other joint systems Js.4 and Js.5 are poorly developed and their occurrence is very local, but because of their steep dip can be considered to decrease the stability.

The major joint sets based on the stereographic projections are as follows:

- Js.1: 131°/ 81°
- Js.2: 115°/ 85°
- Js.3: 280°/ 77°
- Js.4: 294°/ 89°
- Js.5: 149°/ 63°
- (B.p) bedding planes: 019°/ 55°

The direction of the major principal stresses based on the discontinuity systems especially the bedding planes dip/direction in 2D view, are as follows:

σ_1 : 205°/ 0.0° (*max. principal stress*)

σ_2 : 295°/ 0.0° (*intermediate principal stress*)

σ_3 : 0.0°/ 90° (*min. principal stress*)

Shortening Direction

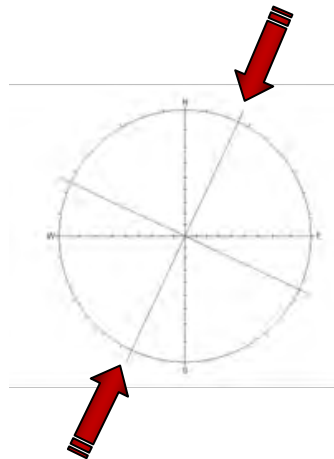


Figure 4.6.16. The direction of σ_1 / Shortening at Salman Farsi dam site.

4.7. Petrographical Analysis of the Asmari Formation at five Dam Sites

The petrographic examinations of about 250 thin sections are presented in detail in Appendix 1 to 5. The classification proposed by Dunham (1962) and Folk (1962) have proved to be the most practical. Modifications suggested by Embry and Klovan (1971), Wright (1992) and Strohmenger and Wirsing (1991) are also useful.

The most widely used classifications are those of Dunham (1962) and Folk (1962). Dunham (1962) classification can equally well be applied in the field, in investigations of cores, and in laboratories.

The porosity types are defined based on Choquette and Pray (1970) which represents the percentage of the bulk volume of a rock that is occupied by interstices, whether isolated or connected. This definition describes the total porosity which must be separated from the

effective porosity. The later is the percentage of the total rock volume that consists of interconnected pores.

The petrographical analyses according to the above methods are summarized in Table 4.7.1. In general, the Asmari carbonate rocks in the study area are classified into *Intrabiomicrite* to *Biodolomicrite*, *Wackestone* to *Packstone*, except at Salman Farsi that indicates locally *Biointrasparite* and *Grainstone*. *Dolomitization* is locally well developed in the middle parts of the Asmari Formation at Salman Farsi and Seymareh dam projects.

The bioclast elements (biota) consist of *Foraminifera*, *Bivalve* (mainly *Rudists*), *Echinoid* shells, *Serpolide* shell, *Calcisponges*, *Bryozoan* fragments and calcareous *Red Algae*. The identifiable Foraminifers that constitute the main bioclasts elements are generally as follow:

Peneroplis sp., *Archaias sp.*, *Borelis sp.*, *Ditrupa sp.*, *Rotalia sp.*, *Operculina sp.*, *Nummulites sp.*, *Meandropsina sp.*, *Heterostegina sp.*, *Miogipsina sp.*, *Elphidium sp.*, *Asterigerina sp.*, *Dendritina sp.*, *Lepidocyclina sp.*, *Haplophragmium sp.*, *Austrotrillina sp.*, *Miliolides* such as *Biloculina*, *Triloculina*, *Quinqueloculina*, and *Planktonic Foraminifera* such as *Globigerina sp.* and *Globorotalia sp.*,

The basic porosity types were defined by the Choquette and Pray (1970) chart which classify porosity into three main types, particularly; fabric-selective, non fabric-selective and fabric-selective or not.

The minimum and maximum porosity are estimated between 0.3% to 15.7% which relate to the Middle Asmari at Salman Farsi and the Lower Asmari at the Karun-3 projects respectively. However, an abnormal porosity value (19.4%) was related to the upper most part of the Upper Asmari at Salman Farsi, due to the *Darreh Siah* fault zone.

The percentage of total porosity has been measured by microscopic quantitative method/point-counting (Punktfeld-Method after Sander 1951). This method was developed by Glagolew (1933) and improved by Chayes (1956). The results of porosity values are presented in Table 4.7.1 and Figure 4.7.1.

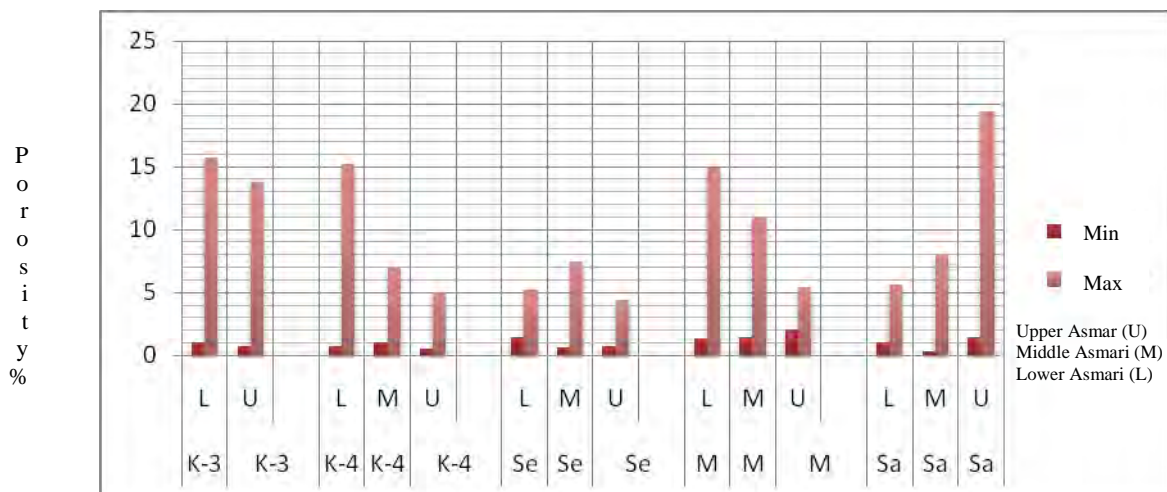


Figure 4.7.1. The minimum/maximum porosity values based on petrographical analysis of rock foundations at Karun-3 (K-3), Karun-4 (K-4), Seymareh (Se), Marun (M) and Salman Farsi (Sa) dam projects. L (lower), M (middle), U (upper).

Table 4.7.1. Summary of the petrographical analysis of five dam foundation rocks.

Dam site	Unit	Petrography	Porosity%	Porosity type	Karst features
Karun-3	U.Asmani	Marly limestone and marlstone, Biointramicrite, wackestone, porosities locally filled by microsparry calcite,	0.75-13.8	Vuggy: 46% Fracture/channel: 34% Others: 20%	Vuggy zones Solution cavities
	L.Asmani	Limestone, marly limestone, locally dolomitic limestone, Intrabiomicrite, wackestone to packstone, porosities partly filled by sparry calcite cement, Dolomitization locally developed	1- 15.7		Vuggy zones Solution cavities 1-2 m
Karun-4	U.Asmani	Limestone, marlylimestone, marlstone Intrabiomicrite, mudstone to wackestone, porosities are filled partly by sparry calcite.	0.5- 5	Vuggy: 42% Fracture/channel: 36% Others: 22%	Non to slightly karstified
	M.Asmani	Limestone, dolomitic limestone, marlstone Intrabiomicrite, dolomicrosparite, wackestone, dolomitization locally well developed, porosities partly filled by sparry calcite	1- 7		Slightly karstified
	L.Asmani	Limestone, marlylimestone, calcareous marls Intrabiomicrite, wackestone to packstone, porosities are filled partly by sparry calcite cement.	0.75- 15.2		Highly karstified
Seymareh	U.Asmani	Crystalline bioclastic limestone, marlylimestone Intrabiomicrite, wackestone to packstone Porosities are filled partly by sparry calcite cement	0.75- 4.4	Vuggy: 74% Fracture/channel: 17% Others: 9%	Karstified, dissolution cavities
	M.Asmani	Crystalline limestone, dolomitic limestone, marlylimestone Biodolointramicrite, wackestone to packstone, dolomitization widespread, karstification well developed, cavities partly filled by calcite cement.	0.6- 7.5		Karstified Caves 100s m ³
	L.Asmani	Microcrystalline limestone, marlylimestone Intrabiomicrite, wackestone to packstone, cavities are filled by coarse blocky/granular calcite cement.	1.4- 5.2		Karstified
Marun	U.Asmani	Limestone, marlstone interbeds Intrabiomicrite, wackestone, cavities are partly filled by coarse sparry calcite cement.	2.1- 5.4	Vuggy: 64% Fracture/channel: 11% Others: 25	Highly karstic
	M.Asmani	Crystalline limestone, marlylimestone, marlstone interbeds Biopelmicrite, wackestone to biolitic boundstone, Locally recrystallization of micrite to microsparry calcite cement	1.4- 11		Karstified
	L.Asmani	Microcrystalline limestone, marlylimestone Intrabiomicrite, wackestone to packstone, cavities are filed partly by coarse sparry calcite cement.	1.3- 14.9		Karstified
Salman Farsi	U.Asmani	Alternation of limestone, dolomitic limestone, marlylimestone, marlstone, porosities partly filled by microsparry calcite cement Biointrasparite, grainstone, locally dolomitization	1.5- 19.4	Vuggy: 68% Fracture/channel: 11% Others: 21%	Karstified dissolution cavities
	M.Asmani	Crystalline limestone, dolomitic limestone, marly limestone Biodolomicrite, wackestone to Intrabiosparite, grainstone Extensively Dolomitization.	0.3- 8		Chimney and caves 100s m ³
	L.Asmani	Alternation of fine grained limestone and marlstone Biomicrite, packstone to boundstone, Porosities partly filled by microsparry calcite cement.	1- 5.6		Isolated cavities

The porosity type results are plotted on a ternary diagram of pore types (Figure 4.7.2). The ternary porosity type plot provides information on the shapes and origin of pore systems. Two distinctive areas; namely groups 1 and 2 are indicated and related to Karun-3, Karun-4 and Seymareh, Marun, Salman Farsi cases respectively.

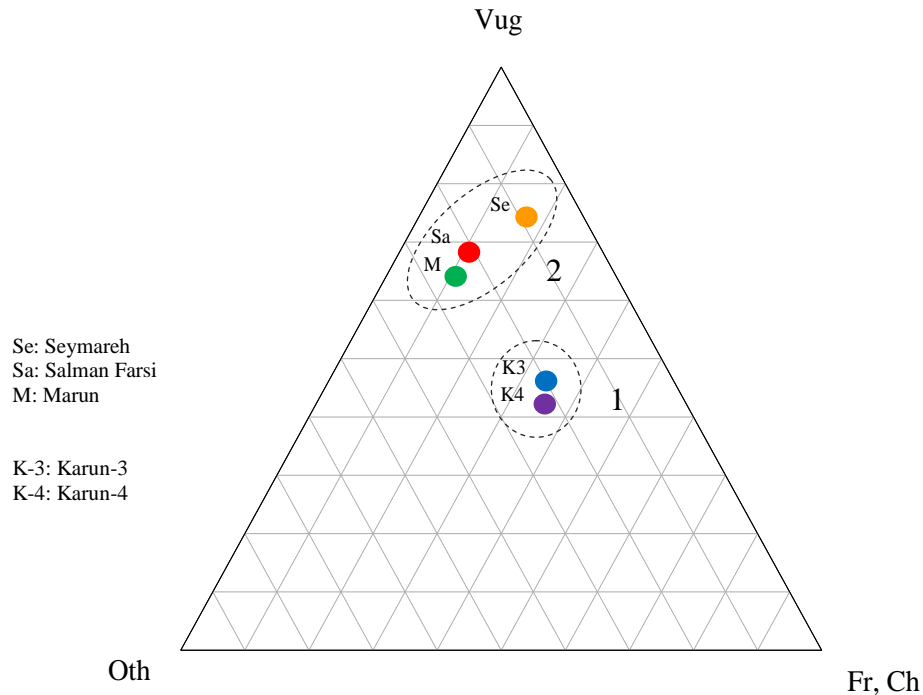


Figure 4.7.2. Ternary porosity type plot (ternary diagrams of carbonate pore types) provides information on the shapes and origin of pore systems. The plots are based on quantitative data derived from point counting of thin sections.

The percentage of Fracture/Channel porosity type for groups 1 and 2 are about 35% and 13% respectively. This can be explained by a higher fracture density due to more tilting or curvature of strata (70° - 90°) at the south-western flanks of anticlines resulting from tectonic movements. In general the porosity values based on the Cherenyshev and Dearman (1991) classification indicate *Medium to Extremely high porosity* for the Asmari limestones.

4.7.1. Standard Facies Zones and the Wilson Model

The succession of major facies belts on rimmed tropical carbonate platforms was used by Wilson (1975) to establish a Standard Facies Model depicted as a basin-to-shore transect and comprising Standard Facies Zones. The basis of the model is the recognition of consistently recurrent patterns of carbonate facies in the Phanerozoic records and the environmental interpretation of these patterns by using characteristics of Holocene sedimentation patterns (Flügel, 2004).

In this regard the analysis of samples resulted from petrographical studies (allochemical, orthochemical elements) generally indicate that the Asmari succession carbonates are mainly related to Facies Zones (FZ) 6, 7, and 8 of Wilson which refer to;

- 6- Platform-edge and platform sand shoals
- 7- Open-marine Platform
- 8- Restricted-marine platform

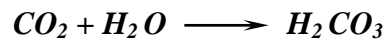
In addition at the Karun-3, Karun-4 sites the upper Asmari samples indicate planktonic foraminifera's assemblages which corresponds to Zone 1 of Wilson Facies, namely;

- 1- Basin and deep shelf- Deep sea

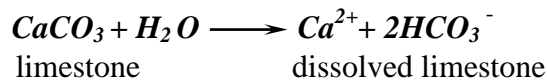
4.8. Hydrogeology

4.8.1. Weathering and Karst Features

Rock weathering is generally a near-surface feature but localized weathering was found at depth in some localities in dam abutments and beneath the riverbeds. Slight penetrative weathering into the rocks along discontinuities was observed in some drill core with iron oxide such as hematite, limonite staining and clay mineral fillings due to weathering widespread on discontinuities. The karstification of the Asmari limestone is the main characteristic of this formation. The dissolution of limestone involves three principal components: carbon dioxide, water, and calcium carbonate. Initially, atmospheric carbon dioxide diffuses into the moisture within the air or soil and simultaneously becomes hydrated to form carbonic acid (Blair, 2009):



In contact with limestone, carbonic acid dissolves the calcite. The reaction is often presented as:



The time required for aggressive water in karst regions to be neutralized or to reach saturation equilibrium varies considerably, depending on a number of factors such as temperature, turbulence, variations in the partial pressure of carbon dioxide, dilution, presence of other acids, and surface area of limestone (Blair, 2009). To achieve equilibrium may require several days. However, laboratory studies suggest that most of the limestone dissolution resulting from an influx of fresh aggressive water may occur within minutes to a few hours (Sweeting, 1950; Jakucs, 1977; Ritter, 1978). Additional acids, such as *organic acids* from soils and most recently sulphuric and nitric acids from acid rain, will contribute to the dissolution of carbonate rocks.

Three factors drive the development of karst; the lithology, distribution of rock type and the occurrence of discontinuities. In addition to the composition of limestone, the thickness of individual beds, the nature of interbeds, especially shaly beds, and lateral facies variations affect the style and degree of karstification (Dreybrodt et al., 2002; Blair, 2009). The main factors that influence rock permeability are the occurrence of fractures and fissures in the rock mass. From the lithological point of view, we have to distinguish the general tendency to strong dissolution of the porous, vuggy, micritic limestone from the more resistant, less porous, recrystallized, finely to medium-grained calcarenite, whereas marls and marly limestones are almost impervious (Blair, 2009).

Dolomitic limestones (or dolomites) are rocks which have undergone chemical changes resulting in the replacement of some of the calcium by magnesium. Magnesium carbonate (dolomite) has a different crystal structure to calcium carbonate and this creates additional *void space* in the rock which can increase the development of permeability and in some cases, karstification. The nature of the limestone strongly influences its susceptibility to karstification.

Pure limestones are more susceptible for dissolution than impure limestones. Another strong influence is the geological structure: folding of the limestone causes fracturing and the formation of a network of fissures along which water can penetrate and begin to dissolve the rock. In general, pure limestones tend to be brittle, allowing extensive open fractures, while impure limestones tend to deform more readily, sealing up the fractures and impeding water movement. The degree of karstification is significantly reduced where there are inter-bedded *shale layers* which restrict water movement and where very strong deformation causes re-sealing of fractures with crystalline calcite (Blair, 2009).

The observations indicate that the Asmari limestone cavities can be divided into two main groups;

- Cavities resulted by simultaneous diagenetic process
- Cavities resulted by karstification process

The first group is mainly circular to elliptical with maximum 20 cm in diameter, generally constituting 5% of the rock mass volume. These features apparently do not show any hydrogeological connection to each other.

The cavities resulted from karstification processes are partly filled by clay and silty materials with dimensions commonly about 1 to 2 m. The huge caves, caverns and chimnies tens of metres in dimension are recognized especially in the northern flank sites where the Seymareh, Marun, and Salman Farsi Dams are situated (Figure 4.8.1).

In general, highly karstic features due to solubility of the rock mass are observed in the Asmari Formation limestone. The karstifications are mainly well developed along discontinuity surfaces essentially on bedding planes. The fracture and joint systems constitute well developed patterns of water pathways in rock mass, and control infiltration of water in depth.

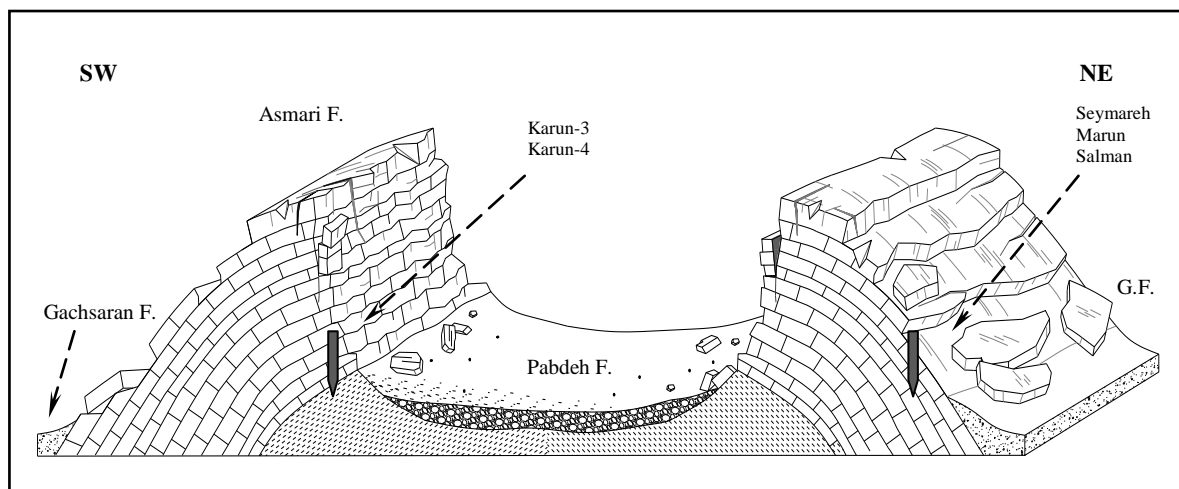


Figure 4.8.1. Block diagram showing three successive formations (Pabdeh, Asmari and Gachsaran) at the Zagros folded belt and relative dam site localities at the two flanks of anticlines.

The caves, stalagmites, stalactites, karstic channels (30-100 cm in diameter) and enlarged fissures resulting from water dissolution are common. The caves have almost longitudinal shapes parallel to the bedding planes and at the intersection of main discontinuities karstification is well developed. The sections of caves are circular to elliptical.

Field observations indicate many springs exist at the dam localities (12°- 25°) with some of them, especially at Salman Farsi, hot water springs with 35°- 42° C temperatures. This can explain the high solubility potential of the Asmari limestone due to active mineral water derived from depth (hydrothermal solutions).

Except for the lower part of the Asmari at Karun-4 with high karstification, the karst features at Karun-3 and Karun-4 dam localities are limited to slight to moderate karstification, solution cavities and vuggy zones, with maximum dimensions about 1 to 2 m. But the field observations in the reservoir areas indicated large to huge caves (50x30x20 m) in the Asmari succession.

Field investigations at the northern dam sites (Seymareh, Marun, Salman Farsi) also indicate various geological and karstification conditions. Karst development is common in this case with frequent, karst chimneys with apertures from a few centimetres to a few metres. In addition, large caves with a volume of thousands of cubic metres have been discovered on both sides and under river beds at dam localities. The volume of the largest one found on the right flank of the Salman Farsi project (*Golshani Cave*) is 150 000 m³. At the Seymareh and Marun projects some large caves have also been detected in both flanks and under the river bed in the downstream area.

Immediately after the excavation of tunnels in the Asmari limestone the surface springs dried up and hot water was discharging into the tunnels. A smell of H₂ S emanated from these waters.

Sulphide rich water (1-15 lit/min) and slightly bitter and brackish water mainly originate from the Gachsaran/Razak Formation and occur downstream from the Asmari limestones. The chemical compositions of spring water are calcium sulphate and sodium chloride and carbonate (MG. co., 1984, 2003). Springs with this composition indicate, hydraulic connections between the two Asmari and Gachsaran Formations as well.

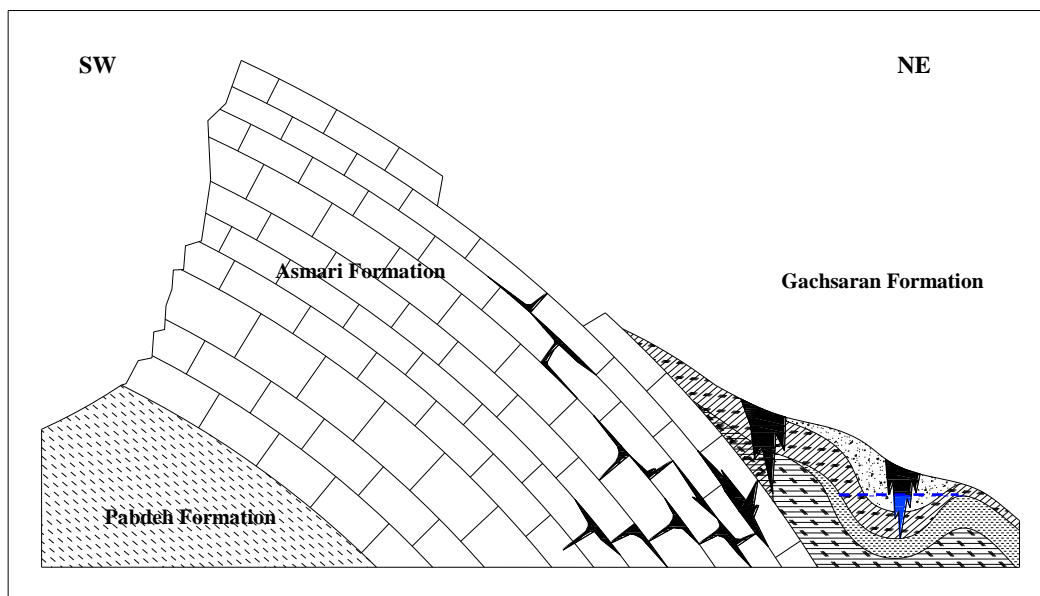


Figure 4.8.2. The karstification model at the northern flank of anticlines in the Zagros folded belt and the role of the Gachsaran/ Razak Formation evaporites on karstification of the Asmari limestone.

Closed depression caves, sinkholes and collapse sinks are well developed in the Gachsaran Formation due to chemical and physical dissolution of the evaporite rocks (Figure 4.8.2). The Asmari Formation limestones are influenced by active mineral solutions resulting from the Gachsaran Formation and this is the main factor for the extensive development of karst features in the Asmari limestones, especially in the upper and middle units. These units of the Asmari Formation are the main foundation rocks at the Seymareh, Marun and Salman Farsi dam sites. The dissolution mechanism of Gachsaran/Razak evaporites due to meteoric and underground waters in addition to the four stages of development of karst features in the Asmari limestones can be explained based on Figure 4.8.3. When gypsum is dissolved by underground water activities, the surrounding rocks collapse and then open space is then filled by collapsed rocks and create a funnel with karst breccia at the bottom of hole.

The Gachsaran/Razak Formations consist of hundreds of metres of alternating layers of gypsum, anhydrite, salt and coloured marls with high flexibility and solubility and have been extensively karstified to zones with various dimensions. These formations are widely distributed in the Zagros region and contain evidence of karst in most areas (Figures 4.8.3, 4.8.4 and 4.8.9).

The disruption of the Gachsaran/Razak evaporite sequence caused by tectonic movements is the main factor causing the infiltration of active mineral waters to develop karstification in depths. This phenomenon can be observed not only at the surface but also at depth (data from exploratory drillings). In some localities, due to impervious layers of marls, a perched water (perched aquifer) level can occur in the Gachsaran Formation (Figure 4.8.2). The dimensions of these sinkholes vary between 2 m to 15 m, based on field observations. One of the biggest sinkholes, with diameter 70 m and 10 m depth has been detected in the Seymareh dam site reservoir (Zam Zam Hole).

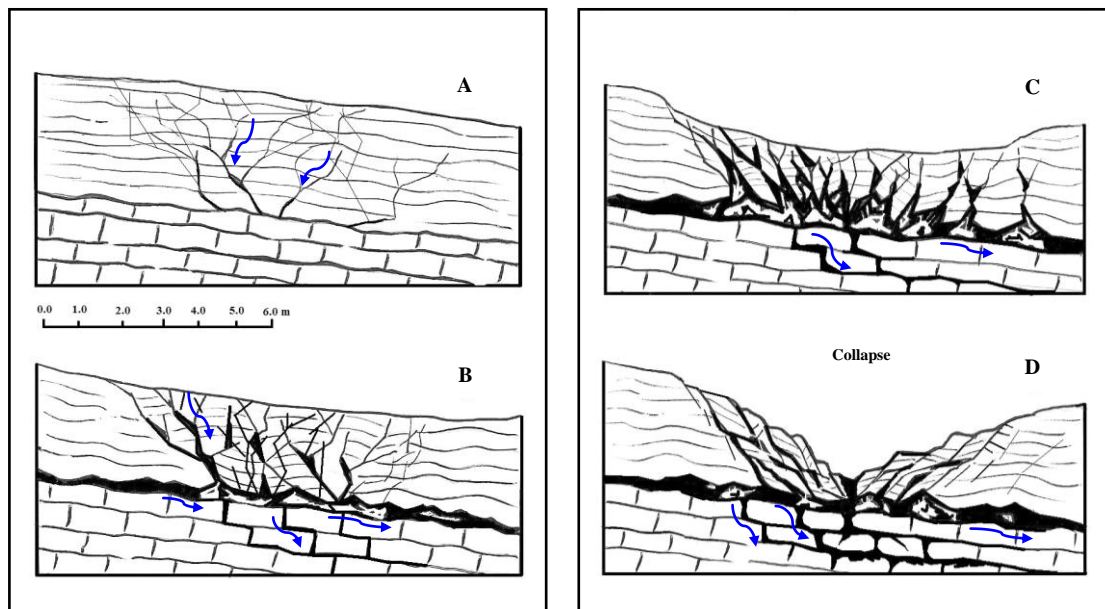


Figure 4.8.3. Schematic geological section through the Asmari-Gachsaran/Razak contact and evolution of karstic collapse feature. The dissolution of the Gachsaran/Razak evaporites (gypsum, anhydrite, salt, marl) due to high solubility of evaporites sequence (solution-collapse structures). The water bearing acid (H_2SO_4 solutions) will be the outcome of the process, which can dissolve the Asmari Formation limestone and accelerate the karstification process.

Gypsum is one of the most soluble of the common rock minerals; and it is readily dissolved to form caves, sinkholes, collapse columns, swallow holes, and other karst features that are typically found in limestones and dolomites. The principal difference is that gypsum-karst features can form rapidly in a matter of weeks or years, whereas carbonate-karst features typically take years, decades, or centuries to form. The four basic requirements for gypsum karst to develop are (Johnson, 1996a):

- A deposit of gypsum;
- Water unsaturated with CaSO_4
- An outlet for escape of dissolving water and
- Energy to cause water to flow through the system

When all four of these are met, dissolution of gypsum can be rapid in terms of geologic time (Johnson, 1996).

The solubility of $\text{CaSO}_4 \cdot 2\text{H}_2\text{O}$ ranges from about 2 200- 2 600 ppm in the temperature range of 0° - 10° C (Hardie, 1967; Blount and Dickson, 1973).

Evidence of gypsum karst includes surface and shallow-subsurface features, such as caves, sinkholes (dolines), karren, disappearing streams, shallow holes, springs, collapse structures, and result in the dropping of drill bits and /or loss of drilling fluids while drilling through gypsum beds.

All these karst features and many more, are identical in character and genesis to those found in carbonate rocks. In fact palaeokarst, brecciated zones, and other karst features found in some carbonates may have been initiated by earlier dissolution and karst development in gypsum that is interbedded with the carbonates (Sando, 1988; Friedman, 1997; and Palmer, 2000).

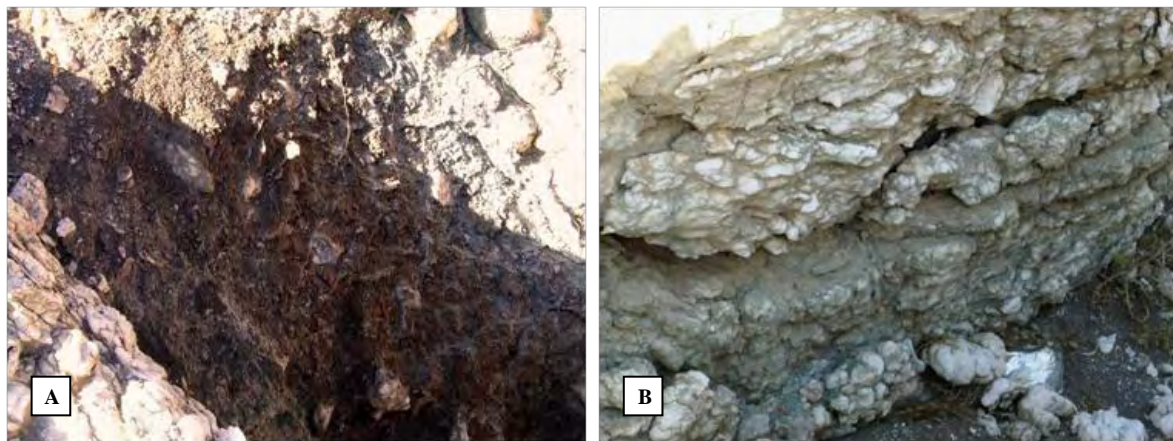


Figure 4.8.4. Closed depression in red marls bearing gypsum of Gachsaran Formation (A). Karst development in Razak evaporites formation at the Salman Farsi dam site. Dissolution is mostly pronounced along joints and bedding planes (B).

Gypsum karst can be accelerated by *human activities*. Gypsum-karst problems are caused by the same activities that cause problems in carbonate terranes such as;

- building structures that induce differential compaction of soils above an irregular gypsum-bedrock surface;
- building structures directly upon gypsum collapse features; and

- impounding water above, or directing water into a gypsum unit where soil piping can divert water (and soil) into underground gypsum cavities.

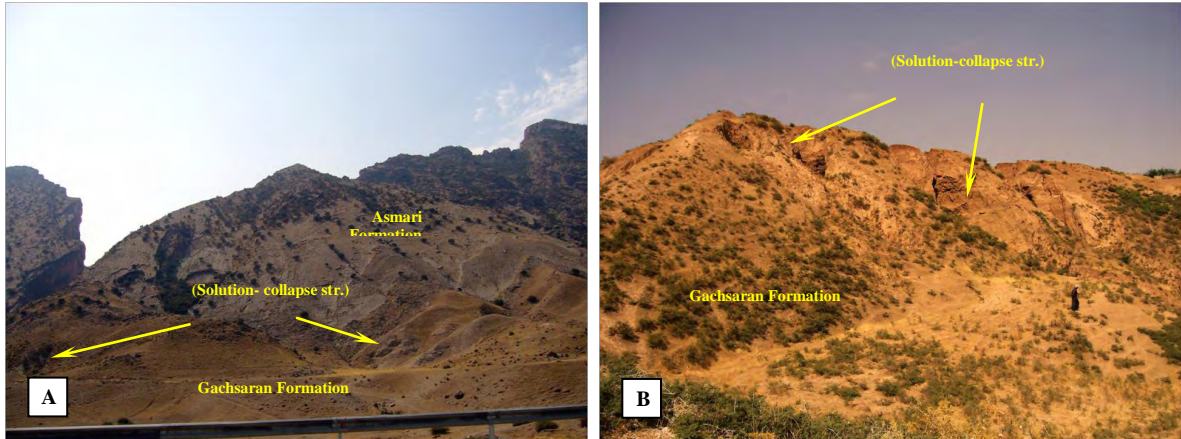
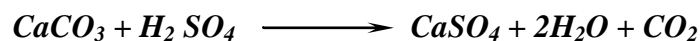


Figure 4.8.5. Some solution-collapse structures in Gachsaran Formation due to high solubility and erodible evaporite rocks. Gypsum-dissolution at the region generates sulphate-rich water then collapse of overlying rocks into cavities occurs.

These human activities can cause land subsidence or can cause new or concealed sinkholes and cave systems to open up; this can result in settling or catastrophic collapse of the ground (Johnson, 1996b). In evaporite rocks, cavity formation, collapse, and ground subsidence can developed within a few decades.

Some researchers reported that the dissolution of gypsum ($\text{CaSO}_4 \cdot 2\text{H}_2\text{O}$) in the presence of NaCl will be raised (e.g. Ford and Williams, 2007), so that a solution with 50 to 150 gr/l of NaCl can increase the solubility of gypsum up to 6 to 7 times (Figure 4.8.7). Therefore the high karstification of the Gachsaran Formation can be explained by this process.

In addition the Asmari succession limestones (CaCO_3) can be influenced by acidic solutions resulting from the deterioration of Gachsaran Formation evaporites as follows (Blair, 2009):



This evidence clearly explains the well developed karst features in the Asmari limestones in the northern flanks due to karstification processes in the Gachsaran Formation (Seymareh, Marun and Salman Farsi dam sites). In addition, the considerable areas of the reservoirs are also by the Asmari and Gachsaran Formations the two high karstified formations (Figure 4.8.6).



Figure 4.8.6. The distribution of the Gachsaran evaporites rocks (mainly gypsum) at reservoir area of the Marun dam site. The surface karstification and weathering features can be observed as well. The residential structures are constructed almost on karstified rocks of the Gachsaran Formation (2007).

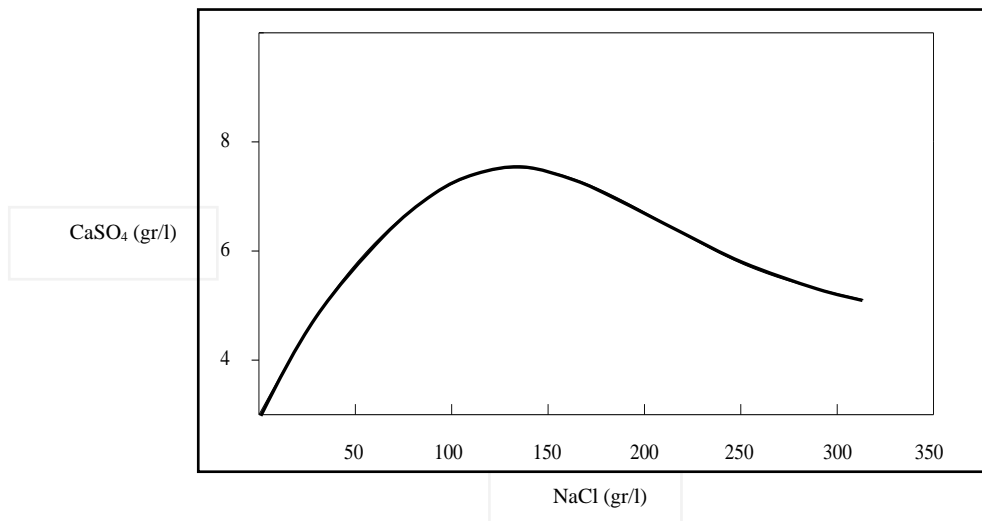


Figure 4.8.7. Illustrating common Ion, foreign Ion and Ionic strength effects. Increase of gypsum solubility with addition of NaCl (after Ford and Williams, 2007).